Mobile Brain and Body Imaging during Walking Motor Tasks

by

Grant M. Hanada

A dissertation submitted in partial fulfillment
of the requirements for the degree of
Doctor of Philosophy
(Biomedical Engineering)
in the University of Michigan
2018

Doctoral Committee:

Associate Professor Cindy K. Chestek, Co-Chair
Professor Daniel P. Ferris, Co-Chair
Assistant Professor Sean K. Meehan, University of Waterloo
Associate Professor William C. Stacey

Grant M. Hanada

ghanada@umich.edu

ORCID iD: 0000-0002-0878-6939

Acknowledgements

First and foremost, I would like to thank my committee for their gracious support. I would especially like to thank my advisor, Dan Ferris, for his constant encouragement and unending trust from the day he recruited me to work with him in his lab. This PhD took on a bigger scope and more time than we planned for, but the learning process was humbling and rewarding. I would like to thank all my lab mates for their continual support, even as many have come and gone. Finally, I would like to thank my family and friends that stuck by my side and cheered me on along the way.

Table of Contents

List of Tables

List of Figures

Abstract

Mobile brain and body imaging (MoBI) presents new and promising methods for moving traditional research studies out of a controlled laboratory and into the real world. Most current neuroimaging techniques require subjects to be stationary in laboratory settings because of both hardware and software limitations. Recent developments in mobile brain imaging have utilized Electroencephalography (EEG) in conjunction with advanced signal processing techniques such as Independent Component Analysis (ICA) to overcome these obstacles and study humans doing complex tasks in non-traditional environments. In my first study, I used high density EEG to examine the cortical dynamics of subjects walking on a split-belt treadmill with legs moving independently of each other at different speeds to investigate how humans adapt to novel perturbations. I found significantly increased low and high frequency spectral power across all sensorimotor and parietal neural sources during split-belt adaptation compared to normal walking, which provides insight into the brain areas and patterns used to accommodate locomotor adaptation. In my second study I combined multi-modal sensing and biometric devices including EEG, eye tracking, heart rate, accelerometers, and salivary cortisol into a portable setup that subjects wore indoors on a treadmill using virtual reality as well as outdoors in a public arboretum. Subjects walked for 1 hour each indoors and outdoors while completing a free viewing visual search oddball task in virtual reality and in real life. I reported on the methods for how to set this experiment up, synchronize all data, and standardize the data in order to make it usable as an open access dataset that has been made available to the public online. My third study used this data set to examine the P300 event-related potential response during both

indoors in virtual reality and outdoors in the arboretum. I found a significantly increased amplitude response between 250 to 400 ms across the centro-parietal electrodes that distinguished target flags from distractor flags during visual search for both indoor and outdoor environments. And finally, for my fourth study I used the same data set to look at the behavioral and neural correlates associated with gait dynamics when subjects walked indoors on a treadmill vs outdoors in variable terrain while also doing the visual search task. I found significant EEG power differences across multiple neural sources that showed increased spectral fluctuations throughout the gait cycle when subjects walked outdoors compared to indoors on a treadmill.

The collective studies in this dissertation present new ways of using mobile brain and body imaging devices to expand our knowledge of the neural dynamics involved in humans moving in complex ways and in variable environments outside of traditional laboratories.

Chapter 1 Introduction

Recent developments in human neuroimaging have made it possible to understand how the brain and body interact in ways that weren't possible before. Traditional neuroimaging has relied on expensive, heavy, and stationary scanners like functional magnetic resonance imaging (fMRI) and positron emission tomography (PET) that often require subjects to remain completely still. This poses limited options for tasks that can be studied as well as limited environments in which experiments can take place. Advances in neuroimaging technology and software has allowed for other technologies like functional near-infrared spectroscopy (fNIRS) (Meyerding and Risius 2018; Miyai et al. 2001; Suzuki et al. 2004) and electroencephalography (EEG) (Debener et al. 2012) to be used in mobile experiments that comprise a large range of opportunities for moving traditional neuroimaging into more real world situations. For instance, using cheaper and more affordable mobile technologies could form the foundation for brain-computer interface (BCI) devices which could help in applications like gait assistance or rehabilitation.

Currently, EEG is increasingly becoming more common in mobile research (Minguillon, Lopez-Gordo, and Pelayo 2017) as it has the advantage of maintaining a high temporal resolution for capturing the dynamics in locomotion. Many recent studies have used EEG combined with independent component analysis (ICA) to show how the brain functions during locomotion. The first study to demonstrate these techniques in locomotion showed anterior cingulate, posterior parietal, and sensorimotor electrocortical sources were involved and associated with significant intra-stride fluctuations in spectral power during normal treadmill walking (Gwin et al. 2011).

Since then, more studies have explored other ways to use EEG show gait dynamics in more complex locomotion tasks (Bradford, Lukos, and Ferris 2016; Bruijn, Van Dieën, and Daffertshofer 2015; Bulea et al. 2015; Castermans et al. 2012; Gramann et al. 2011; Gwin et al. 2011; Kline, Poggensee, and Ferris 2014a; Lau, Gwin, and Ferris 2014; Oliveira, Schlink, Hairston, et al. 2017; Petersen et al. 2012; Presacco et al. 2011; Seeber et al. 2015; Sipp et al. 2013; Wagner et al. 2016; Wieser et al. 2010). For instance, one study had subjects walk on an inclined treadmill and showed an increase in theta (4-7 Hz) power in anterior cingulate, posterior parietal, and sensorimotor areas compared to level walking (Bradford et al. 2016). Other gait studies are investigating the mechanism of balance and control. In a stabilized walking experiment, subjects walked on a treadmill connected to elastic cords and they found significant increases in high beta band (~17 Hz) power around contralateral push off in the left premotor area (Bruijn et al. 2015). Another group used a balance beam mounted on a treadmill to show increased theta (4-7 Hz) power in anterior cingulate, anterior parietal, superior dorsolateral-prefrontal, and medial sensorimotor areas compared to normal treadmill walking (Sipp et al. 2013). And left and right sensorimotor areas showed significantly less beta (12-30 Hz) power on the balance beam compared to walking. However, there are still many known and unknown variables that could negatively hinder our ability to capture clean EEG signal as things like line noise, eye movements, muscle, and motion related artifacts.

Another popular area of study for mobile brain and body imaging is in perception and navigation in the real world. For instance, searching a scene for an object of interest is a common occurrence in everyday life for humans (Eckstein 2011; Hopf et al. 2000). Scientists have studied this aspect of active perception for decades using tasks like visual search in the fields of

psychology and cognitive neuroscience (Braun and Julesz 1998; Luck, Fan, and Hillyard 1993; Luck and Ford 1998; Sutton et al. 1965; Treisman and Gelade 1980). EEG has been a useful tool in examining the brain in this capacity as it has been shown that attention to visual targets can elicit sensory invoked activity in the brain known as event-related potentials (ERPs) (Luck et al. 1993). The ERPs are best identified by looking at changes in electrocortical activity time-locked to presentation of a stimulus (Luck 2005).

The P3 (sometimes referred to as the P300) component is an robust, and well-studied electrocortical potential that occurs approximately 250-500 ms after a target or task-relevant stimulus has been presented (Patel and Azzam 2005; Ravden and Polich 1999). This particular component is quite useful for its wide-scale applications because it is relatively easy to detect, and the amplitude is dependent on voluntarily controlled attentional processes. This makes it a popular tool for analyzing changes in cognitive load (Debener et al. 2012; Polich 1987; Polich and Kok 1995), diagnosing neurological pathologies (Alonso-Prieto et al. 2002; Lagopoulos et al. 1998; Münte, Matzke, and Johannes 1997), and developing brain computer interfaces (BCI) (Brouwer et al. 2013; Farwell and Donchin 1988; Krusienski et al. 2006). However, most visual search implementations rely on using computer screens flashing predefined targets while the subject looks straight ahead, maintaining gaze fixating on the screen (Aziz-Zadeh, Liew, and Dandekar 2013; Brouwer et al. 2013; Katayama, Miyata, and Yagi 1987; Kazai and Yagi 1999; Thickbroom et al. 1991; Thickbroom and Mastaglia 1985).

Recently, a small number of research studies have begun to use visual search tasks with relatively natural scene conditions (Graupner et al. 2007; Kaunitz et al. 2014; Ossandon et al.

2010). Kaunitz and colleagues were combined EEG and eye tracking to examine and compare the cognitive components of visual search in a traditional oddball task to a free viewing search of complex, natural images. They relied on using eye tracking to determine fixation event-related potentials (fERPs) in which stimulus onset was synchronized to the onset of eye gaze fixation. Their findings showed that fERP responses to target detection in free viewing search could elicit P3 components that behave similarly to ERP components with unconstrained exploration of natural scenes. But even these studies using natural scenes still take place in controlled laboratories indoors using computer screens. It is unknown how those findings would translate to natural experiences in real world environments outside of a lab.

In order to relate traditional research from laboratory experiments to outdoor, real world settings, virtual environments are being used a way to simulate the outdoor experience (Cruz-Neira et al. 1992; Diemer et al. 2015; Holden 2005; Livingston et al. 2009; McCall and Blascovich 2009; Mine, Brooks, and Sequin 1997; Sandstrom, Kaufman, and A. Huettel 1998). Virtual reality is becoming more accessible and feasible in research and it provides a naturalistic context in feature rich scenarios while still being able to work in controlled laboratory conditions. One of the areas that EEG and virtual reality is becoming more popular is in research on the cognitive neuroscience of driving. One study (Chin-Teng Lin et al. 2007) recorded EEG during virtual reality automobile driving simulations and was able to demonstrate the effectiveness of single trial (ERP) analysis. Other studies (Mager et al. 2000; Pugnetti, Meehan, and Mendozzi 2001) have reported on the success of using EEG and ERPs to study attention and presence in virtual reality. Based on the findings of these previous EEG and virtual reality studies, virtual reality

could be a useful tool in exploring the cognitive neuroscience involved in visual search tasks and how ERP components change in more natural environments.

The primary goals for this dissertation were to 1) explore new methods for using mobile EEG in complex motor tasks to better understand gait dynamics in locomotion and 2) advance the field of mobile brain and body imaging (MoBI) systems and test the feasibility of using them in more complex real world environments. In chapter 2, I used high density EEG to examine young, healthy adults walking on a split-belt treadmill with legs moving independently of each other at different speeds to understand the neural dynamics of how humans adapt to complex perturbations. In chapter 3, I documented the design of a novel brain and body imaging system that combined multi-modal sensing and biometric devices including EEG, eye tracking, heart rate, accelerometers, and salivary cortisol into a portable setup. I collected data from 49 healthy adults as they used this system while walking indoors in virtual reality completing a free viewing visual search task as well as completing an analogous version of that same visual search task in the real world outside in a public arboretum. I then showed that the data could be synchronized and aligned to the EEG recordings and standardized in a way that would be made freely available to the public as an open access data set stored online. In chapter 4, I used that data set to analyze the EEG activity to see if I could capture the P300 event-related potential response both indoors and outdoors during the visual search task. In chapter 5, I used the same data set to explore the neural and behavioral patterns associated with gait dynamics when subjects walked indoors on a treadmill and outdoors in variable terrain while also doing the visual search task. The goals of these studies were to explore new ways of using mobile brain and body imaging devices to expand our knowledge of the neural dynamics involved as humans move in complex ways and in

variable real world situation. The following chapters (2-5) contain complete manuscripts that can be read as independent studies. The first three chapters have been submitted for publication and are under peer-review. The fourth chapter will be submitted for publication shortly.

Chapter 2 Electrocortical activity of locomotor adaptation during split-belt treadmill walking

Abstract

Split-belt treadmill walking is a highly studied walking task that has been used to better understand the principles of locomotion adaptation. The goal of this study was to use scalp electroencephalography (EEG) to determine if there are detectable changes in electrocortical activity between normal treadmill walking and split-belt treadmill walking. We had 20 young, healthy adults walk for 5 minutes on a normal treadmill (0.5 m/s) both before and after 10 minutes of asymmetric split-belt walking (one foot at 0.5 m/s, the other at 1.5 m/s) to observe changes in locomotor adaptation. We recorded high-density EEG combined with independent component analysis (ICA) to find the maximally independent brain sources active during both tasks. We clustered similar components into left sensorimotor, right sensorimotor, anterior cingulate, and posterior parietal areas, and analyzed their spectral power changes across each task as well as their event-related spectral fluctuations synchronized to gait events. We found significantly increased theta (4-7 Hz) and gamma (31-80 Hz) band power across all clusters during split-belt adaptation compared to normal walking. In addition, there was increased theta fluctuation desynchronizations during swing phase of the faster moving foot followed by increased theta and alpha (8-12 Hz) synchronizations in double support phase. These fluctuation patterns were consistent in most clusters except the right sensorimotor area which suggest that

both event-related synchronizations and desynchronizations in theta and alpha power are involved and relevant for gait adaptation. The differences between spectral power patterns in left and right sensorimotor areas are congruent with previous studies indicating that the two sides take on different roles in control of walking. These findings provide new insights into the neural correlates of locomotor adaptation and indicate the high-density EEG could be used to study cortical correlates to gait adaptation in patient populations.

Introduction

Motor adaptation is an important mechanism underlying gait biomechanics. It is defined as the process of modifying a previously learned movement due to an environmental or contextual perturbation on the basis of error feedback such that a new movement pattern is temporarily learned to respond to new task demands (Reisman, McLean, and Bastian 2010). If the perturbation is removed after the new movement pattern is adapted, the movements will again be erroneous in the opposite manner because the adapted pattern still remains. These initial errors are termed aftereffects. Motor adaptation to a perturbation happens relatively quickly after practiced motor movements and then requires active de-adaptation, rather than passively adjusted over time (Roemmich, Long, and Bastian 2016).

Split-belt treadmills have become popular for locomotion adaptation because of the ability to control each foot independently. Reisman et al. (Reisman 2005) first demonstrated that healthy adults were able adapt their gait in order to walk on a treadmill with one leg moving faster than the other. Intra-limb parameters from each individual leg showed a rapid change in order to adapt to split-belt walking, but there was no aftereffect present. However, walking parameters

associated with interlimb relationships showed slow changes during adaptation and displayed an aftereffect during post-adaptation. To understand how this affects sensory perception, one split-belt study found people had altered perception of leg speed during walking after motor adaptation, but that adaptation did not alter the perception of leg position or stepping force (Vazquez et al. 2015). Because recalibration of sensory perception occurred in the same domain of the applied perturbation during walking (i.e., speed but not position or force), this showed that both motor and sensory changes from locomotor adaptation may be linked and there might be overlapping mechanisms driving these changes in both domains.

These split-belt studies have led to questions about the neural mechanisms and control during locomotor adaptation. Decerebrate cats were able to achieve stable locomotion on a split-belt treadmill by slightly shortening step cycle durations and by adjusting durations of bisupport phases asymmetrically in the left and right forelimbs (Yanagihara et al. 1993). More recently, humans with cerebellar stroke damage were also able make reactive motor adaptations to walking on a split-belt treadmill, but they did not display an aftereffect which suggests the cerebellum may be essential for predictive, but not reactive locomotor adjustments (Morton 2006). That same group (Reisman et al. 2007) hypothesized that if cerebellar-cerebral motor connections are important in adaptation then cerebral motor damage should also impair adaptation. They showed stroke patients with various cerebral damage (not to the cerebellum) were still able to make both reactive and adaptive abilities (retained aftereffect) from split-belt walking adaptation. This suggests that it may be cerebellar interactions with the brainstem (rather than cerebral structures) that are responsible for the neural mechanism underlying this type of interlimb control.

In order to further investigate the sensorimotor neural mechanism involved in locomotor adaptation, there is a need for neuroimaging studies in this field. Recently, it has become possible to study human brain function during locomotion using electroencephalography (EEG) combined with independent component analysis (ICA) (Bradford et al. 2016; Bruijn et al. 2015; Brunner et al. 2016; Bulea et al. 2015; Castermans et al. 2012; Gramann et al. 2011; Gwin et al. 2011; Haefeli et al. 2011; Kline et al. 2014a; Lau et al. 2014; Petersen et al. 2012; Presacco et al. 2011; Sipp et al. 2013; Wagner et al. 2012). It was first shown that anterior cingulate, posterior parietal, and sensorimotor electrocortical sources were present and exhibited significant intra-stride fluctuations in spectral power during normal treadmill walking (Gwin et al. 2011). Since then, many other studies have compared normal treadmill walking to different gait patterns. Compared to normal walking, walking on an incline showed an increase in theta (4-7 Hz) power in anterior cingulate, posterior parietal, and sensorimotor areas (Bradford et al. 2016). However, there was greater gamma (30-70 Hz) power during level walking for the left sensorimotor and anterior cingulate areas. To investigate walking with more natural control, one study used a treadmill in which speeds of belts were constantly adjusted based on the pelvis position and swing foot velocity and found that the left and right sensorimotor areas showed increased desynchronizations in mu (8-13 Hz) and beta (14-30 Hz) frequency (Bulea et al. 2015). In addition, the prefrontal and posterior parietal cortices showed phasic low gamma (30-50 Hz) power increases during double support and early swing phases of the gait cycle. More gait studies are further investigating the mechanism of balance and control. In a stabilized walking experiment, subjects walked on a treadmill connected to elastic cords and that showed significant increases in high beta band (~17 Hz) power around contralateral push off in the left premotor

area (Bruijn et al. 2015). Using a balance beam, one group showed more theta (4-7 Hz) power in anterior cingulate, anterior parietal, superior dorsolateral-prefrontal, and medial sensorimotor area than treadmill walking (Sipp et al. 2013). While left and right sensorimotor areas had significantly less beta (12-30 Hz) power on the balance beam compared to treadmill.

The purpose of this study is to locate the neural sources involved in locomotor adaptation and to determine the dynamics of these sources during the different phases of the gait cycle. We expect increased theta fluctuations in the left and right sensorimotor areas during split-belt walking compared to normal walking, but their patterns would be different due to lateralized specializations. This is based on previous studies that show left hemisphere is dominant for motor skills across both sides of the body, whereas the right hemisphere may be more specialized in goal-directed behavior for motor control (Serrien, Ivry, and Swinnen 2006). Previous studies from our lab showed similar lateralized differences in left and right sensorimotor areas during both walking and balance (Bradford et al., 2016; Joseph T. Gwin et al., 2011; Sipp et al., 2013). We also believe the motor areas along with anterior cingulate and posterior parietal areas will exhibit greater spectral fluctuations in alpha, beta, and gamma bands during asymmetric adaptation walking as compared to normal walking due to demands of increased balance, coordination, and motor planning.

Material and methods

Participants

Twenty healthy volunteers with no neurological or locomotor deficits participated in this study. All subjects reported themselves as right hand and right foot dominant (15 males; age 24 ± 5.5

years). Prior to testing, all subjects signed an informed consent document approved by the human subject Institutional Review Board of the University of Michigan. One subject was not able to complete the entire protocol due to technical problems during data collection and was excluded from data analysis.

Experimental Setup

EEG. We recorded EEG with a 256-channel active electrode cap (ActiveTwo, Biosemi, Amsterdam, The Netherlands, 512 Hz sampling rate). We placed 8 additional sensors on the neck of the subject to record neck muscle activity. All electrode locations were recorded relative to the subject's head with a digitizer (Zebris, Isny, Germany). Before data collection, we applied electrode gel underneath each sensor and kept all offsets below 20 mV as is recommended by Biosemi user manual for optimal data quality. Subjects then put on a small backpack that contained the EEG amplifier and battery such that only a fiber optic cable connected the EEG system to the data collection computer (Figure 2-1).

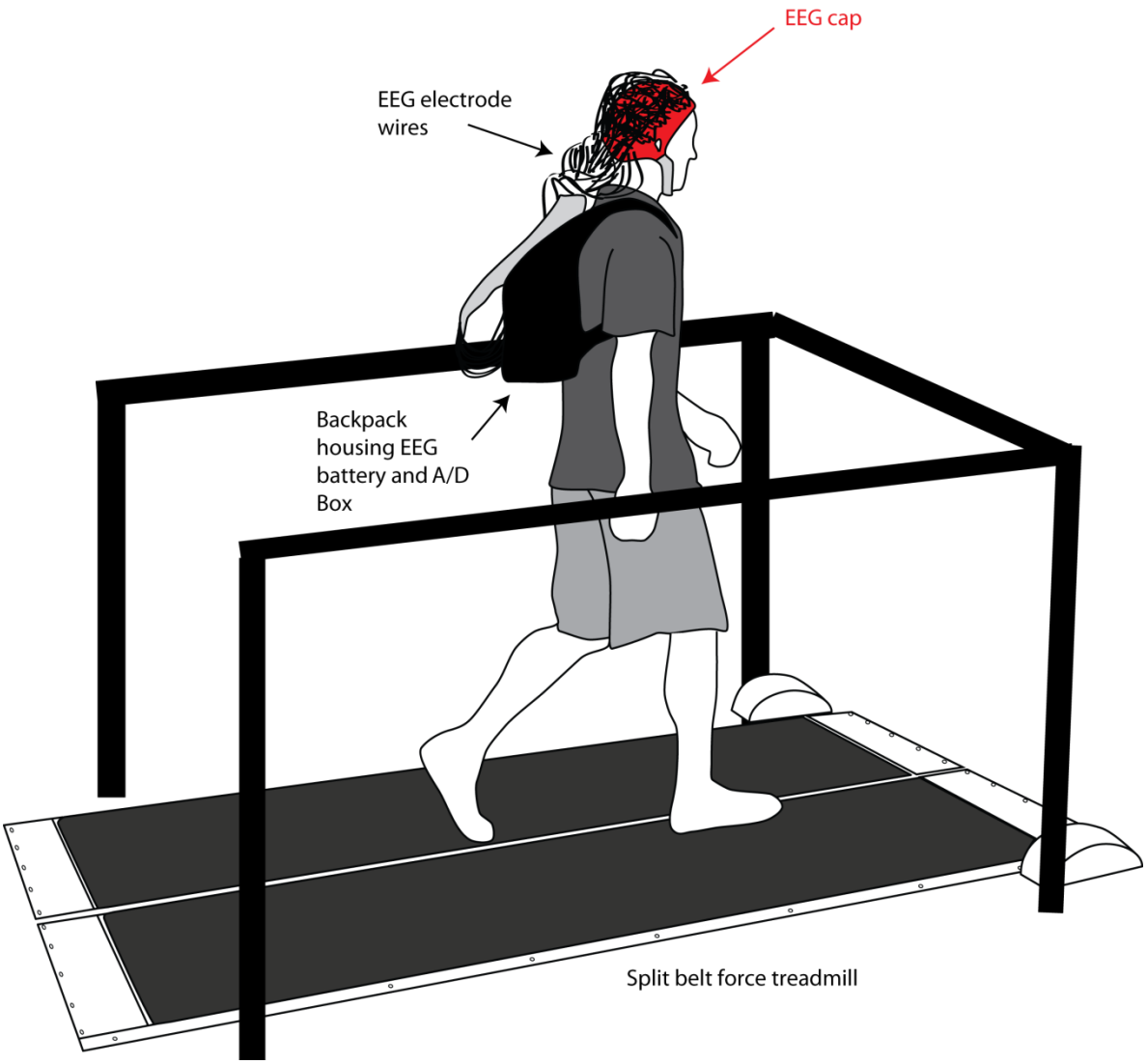

Figure 2-1. Experimental Setup. Subject wore a backpack holding the EEG battery and analog to digital converter. Instrumented split-belt treadmill required subjects to keep each foot on each separate belt while walking. Safety bars surrounded the subject at all times.

Instrumented treadmill. Subjects walked on an instrumented, split-belt treadmill (1000 Hz; Bertec, Columbus, OH) which has separate belts, each with its own motor, for the left and right side of the walking surface. Separate force transducers under each belt were used for the collection of 6 degree of freedom ground reaction forces from the left and right foot separately.

Protocol

Subjects walked for a total of 1 hour within different testing periods in which the two belts each moved at the same speed ('tied' configuration) or different speeds ('split-belt' configuration) according to Table 1. Testing periods were ordered in three blocks, each with the following pattern: *Pre-adaptation* 5 minutes (tied), *Adaptation* 10 minutes (split), and *Post-adaptation* 5 minutes (tied). Standing breaks were given between each walking trial. In addition, blocks 1 and 3 were identical in order to determine if increased training affected outcomes. Event-related spectral perturbations (ERSPs) comparing blocks 1 and 3 showed minimal to no changes (Supplemental Figures 2-1 and 2-2). To minimize muscle and movement artifact in the EEG data, we instructed subjects to restrain from unnecessary movements (e.g. jaw clenching, eye blinking) and to fixate their gaze straight ahead on a white projector screen placed in from of them. While there were safety hand rails installed on both sides of the treadmill, subjects were not allowed to hold onto them during walking unless they were needed for safety.

Table 2-1 Belt speeds for each condition within each block.

	First 5 Minutes		**Middle 10 Minutes**		**Last 5 Minutes**	
	Left Belt	**Right Belt**	**Left Belt**	**Right Belt**	**Left Belt**	**Right Belt**
Block 1	0.5 m/s	0.5 m/s	0.5 m/s	1.5 m/s	0.5 m/s	0.5 m/s
Block 2	0.5 m/s	0.5 m/s	1/5 m/s	0.5 m/s	1.5 m/s	1.5 m/s
Block 3	0.5 m/s	0.5 m/s	0.5 m/s	1.5 m/s	0.5 m/s	0.5 m/s

Data Processing

We synchronized force plates measurements and EEG by sending a 2 Hz square wave signal to both systems simultaneously. We verified data alignment offline after each participant and downsampled force plate data to 512 Hz to match EEG sampling rate.

Gait Cycle Events. We used the vertical ground reaction forces obtained from the instrumented treadmill to determine gait cycle events. When force exceeded or dropped below a 15 N threshold (Kersting 2011; Sinclair et al. 2013; Zeni, Richards, and Higginson 2008), we marked heel strike or toe off, respectively, for each foot separately. This determined four distinct gait events: right heel strike (RHS), right toe off (RTO), left heel strike (LHS), and left toe off (LTO). All gait cycle events greater than 3 standard deviations from the mean time of their cycle periods were removed as outliers and not included in further analyses.

Gait parameters were measured using the double support time as a percentage of stride time. This refers to the time in which both feet were on the treadmill (as measured by the treadmill's force plate ground reaction forces) expressed as a percentage of the stride time for each leg. For one complete gait cycle, there are two periods of double support designated as *slow double support*—time from fast leg heel strike to slow leg toe off, and *fast double support*—time from slow leg heel strike to fast leg toe off.

EEG cortical source localization. We performed all EEG analyses in MATLAB (The MathWorks, Natick, MA) using custom scripts based on EEGLAB (Delorme and Makeig 2004). First, all EEG was downsampled to 256 Hz and high pass filtered at 1 Hz to remove drift. All blocks were concatenated together for all downstream processing. Channel data was re-referenced to the common average reference and the EEGLAB plug-in, Cleanline (https://www.nitrc.org/projects/cleanline/), was used to remove 60 Hz line noise. In order to minimize gait-related movement artifact from the EEG data, we first removed EEG channels

with activity highly correlated with the gait cycle as described by Anderson and colleagues in a previous study (Oliveira, Schlink, David Hairston, et al. 2017). Briefly, individual channel activations were first smoothed with a 128 point moving average filter and then epoched into complete gait cycles (RHS to RHS). The mean amplitude of each time point across all gait cycles was used to create an average waveform template per channel. Every individual gait cycle for each channel was cross-correlated against the average template for that channel. Individual channels with highly correlated ($r > 0.4$) gait cycles for more than 75% of the total number of gait cycles were discarded. We then removed bad EEG channels as described previously by Gwin et al. (Gwin et al. 2010, 2011). Briefly, we removed bad channels using standard statistical thresholds (i.e., range, SD, kurtosis). Next, we applied Artifact Subspace Reconstruction (ASR) (Mullen et al. 2013) with a standard deviation threshold of 20 to correct for time segments induced with high variable noise and ungrounding. We then used the EMDLAB toolbox (Al-Subari et al. 2015) to apply Ensemble Empirical Mode Decomposition (EEMD) (WU and HUANG 2009), which performs selective low-pass filtering to target high frequency activity associated with muscle and noise. We isolated the first intrinsic mode function (IMF1) of each channel, which contained high frequencies over 40 Hz and ran Canonical Correlation Analysis (CCA) (Hotelling 1936) on IMF1 and a copy of IMF1 time-lagged by one data point (Friman et al. 2004). CCA components were removed from IMF1 based on interquartile range to target high-frequency data that is well-clustered by CCA (Safieddine et al. 2012). Next, we used CCA to find and remove low frequency components correlated with motion-related artifact. CCA was run on clean channel data that was high-pass filtered at 4 Hz to isolate the first low frequency component and then subsequently subtracted from the channels. After data cleaning, channels that were removed in the initial pre-processing steps were re-interpolated to full rank and then

common average referenced. Adaptive mixture independent component analysis (AMICA) (J A Palmer et al. 2008; Palmer, Kreutz-Delgado, and Makeig 2006) was applied to the cleaned channel time series using Principal Component Analysis to parse the data into 100 spatially fixed, maximally temporally independent component (IC) signals (Makeig et al. 1996) per subject. The DIPFIT function in EEGLAB (Oostenveld and Oostendorp 2002) modeled each independent component as an equivalent current dipole within a boundary element head model based on the Montreal Neurological Institute standard brain (Quebec). We removed independent components from further analysis if their best-fit equivalent current dipole accounted for less than 85% of the variance seen at the scalp (Gwin et al. 2011), or if their scalp map or spectra were indicative of an eye or muscle artifact (T. P. Jung et al. 2000; T.-P. Jung, Makeig, Humphries, et al. 2000).

EEG group analyses. We used a k-means clustering algorithm across all independent components from all 19 subjects on vectors jointly coding similarities in dipole location, scalp topography, and frequency spectra (Gramann, Onton, et al. 2010; Jung et al. 2001) and set the number of clusters to 13 to agree with previous studies from our lab(Bradford et al. 2016; Gwin et al. 2010, 2011; Sipp et al. 2013). Four of the 13 clusters (Figure 2-2) were located in cortical areas that were the most relevant for the locomotor task and were similar to those found in previous studies (Bradford et al. 2016; Gwin et al. 2011; Sipp et al. 2013): Left Sensorimotor (22 sources, 12 subjects), Right Sensorimotor (20 sources, 9 subjects), Anterior Cingulate (19 sources, 10 subjects), and Posterior Parietal (21 sources, 10 subjects). All further analyses were performed only on these four clusters of interest. Localization of all independent components and associated clusters used for analysis are displayed in Figure 2. We computed log power spectra

for each cluster for four conditions: (1) *Pre-adaptation*, all blocks combined, (2) *post-adaptation*, blocks 1 and 3 combined, (3) split-belt with *left foot faster adaptation*, block 2, and (4) split-belt with *right foot faster adaptation*, blocks 1 and 3 combined. Blocks 1 and 3 were combined for group analyses due to similar patterns shows in event-related spectral perturbations (ERSPs) (Supplemental Figures 2-1 and 2-2). Due to large amounts of noise artifact in the fastest *post-adaptation* walking trial in block 2 (1.5 m/s), that trial was excluded from further data analyses for all subjects. A repeated measures ANOVA test was used to evaluate mean spectral power differences among conditions ($\alpha = 0.05$).

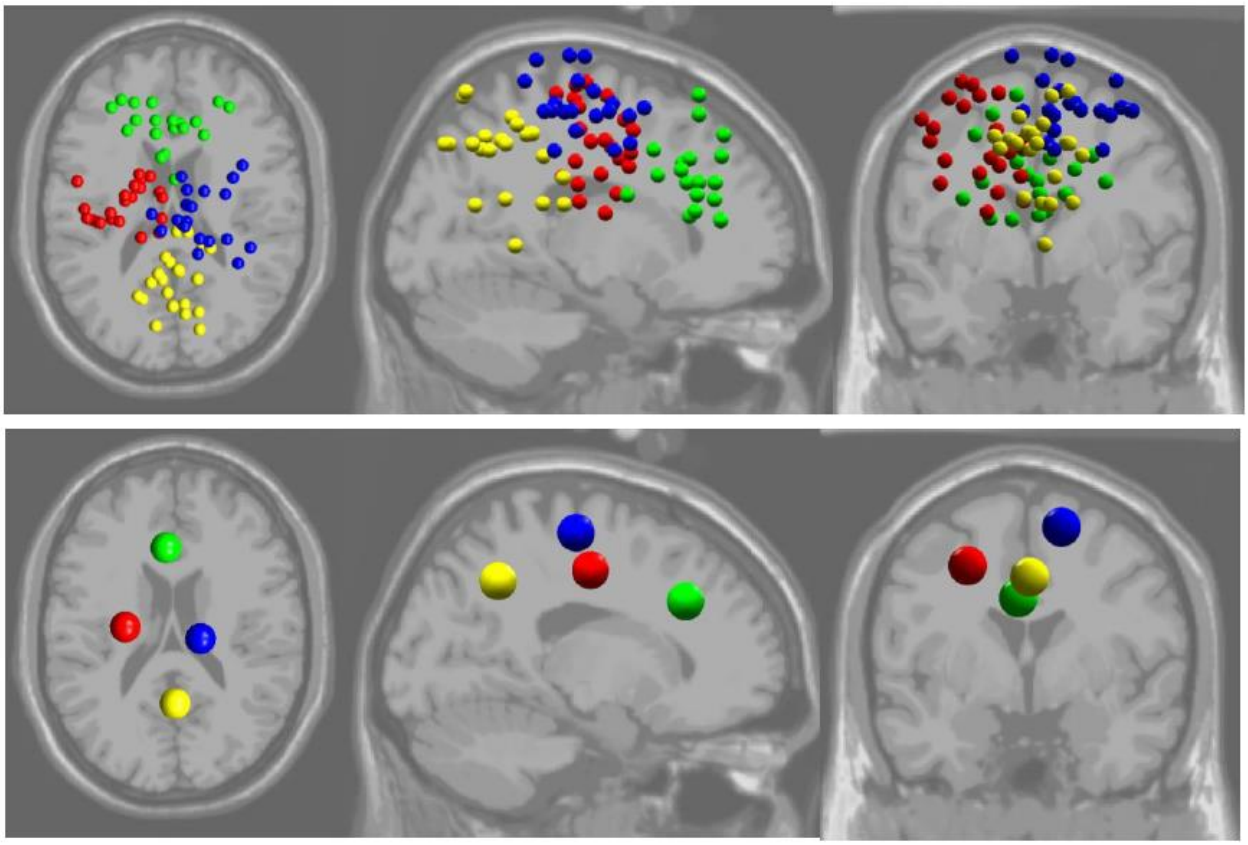

Figure 2-2. Clusters of independent component (IC) EEG sources. Clusters are plotted on the Montreal Neurological Institute brain. Left sensorimotor (red), right sensorimotor (blue), anterior cingulate (green), and posterior parietal (yellow). Top: small spheres indicate the equivalent current dipole locations of each clustered IC source. Bottom: larger spheres show the locations of the cluster centroids.

For time-frequency analyses, we examined the same four conditions. All conditions for each subject were epoched at each RHS to produce discrete gait cycle trials across the experiment. For each gait cycle, we computed a single trial time-frequency log spectrogram for each independent component source activity using three-cycle Morlet wavelets. To allow us to examine time-sensitive cortical activity changes related to gait events, the spectrograms were time-locked to the subsequent gait events (i.e., LHS, RTO, LTO) and linearly time warped so each gait event occurred at the same latency in every trial (Gwin et al. 2011; Makeig 1993a). For visualizing spectral changes across gait cycles, we subtracted a baseline (calculated as the average log spectrum across all gait cycles within each condition) from the log spectrum for each individual gait cycle within each condition. Thus, these analyses show spectral change from baseline and are referred to as event-related spectral perturbations (ERSPs) (Gwin et al. 2011; Onton et al. 2006). We averaged the ERSP plots across each independent component in each cluster to make a grand mean ERSP for each cluster for all conditions (Figure 2-3). Statistically significant differences from baseline frequency power across the gait cycle ($p < 0.01$) were determined using a 200-iteration bootstrapping method available in EEGLAB (Delorme and Makeig 2004) separately for each condition. ERSP data were significance masked, such that all nonsignificant regions were set to zero.

Results

Gait analysis showed that the percentage of time spent in double support for both legs were significantly different in the split-belt adaptation periods than in the pre and post-adaptation conditions. The left foot forward during pre-adaptation was in double support on average 18.3%

(S.D. = 1.6%) of the gait cycle and the right foot forward was at 17.6% (S.D. = 1.5%), while during split-belt walking the *slow double support* foot was only 12.3% (S.D. = 0.9%) of the gait cycle and the *fast double support* foot at 11.6% (S.D. = 0.8%). However, for post-adaptation the double support percentages increased again to 17.6% (S.D. = 1.3%) when the left foot was forward and 17.7% (S.D. = 1.7%) when the right foot was forward.

There were many significant EEG spectral power interactions (Table 2-2, Figure 2-3) across multiple frequency bands in all cortical areas among the four conditions (*pre-adaptation, post-adaptation, left foot faster adaptation,* and *right foot faster adaptation*). The left sensorimotor area showed both *left* and *right foot faster adaptation* had significantly greater theta band (4-7 Hz) power than both *pre* and *post-adaptation.* Alpha band (8-12 Hz) didn't show significant changes from *pre* or *post-adaptation* compared to either foot faster adaptation, but *post-adaptation* was significantly greater than *pre-adaptation* in alpha power. *Left foot faster adaptation* showed significantly greater gamma power (31-80 Hz) than *post-adaptation*. Similarly, right sensorimotor area showed both *left and right foot faster adaptation* had significantly greater theta power than both *pre* and *post-adaptation*. *Post-adaptation* showed significantly greater alpha power than *pre-adaptation,* and also *left foot faster adaptation* was greater than *pre-adaptation*. Both *left* and *right foot faster adaptation* showed greater gamma band power compared to *post-adaptation*. Anterior cingulate showed both *left* and *right foot faster adaptation* had significant power increase across theta power compared to *post-adaptation,* as well as *left foot faster adaptation* was greater than *pre-adaptation*. Both alpha and beta (13-30 Hz) bands showed increased power in both *left* and *right foot faster adaptation* compared to *pre-adaptation*. Gamma band was significantly greater power for *left foot faster*

adaptation than *post-adaptation*. Posterior Parietal area showed significantly greater theta, beta, and gamma powers for *right foot faster adaptation* compared to *pre-adaptation*. And both *left* and *right foot faster adaptation* also showed greater gamma power than *post-adaptation*.

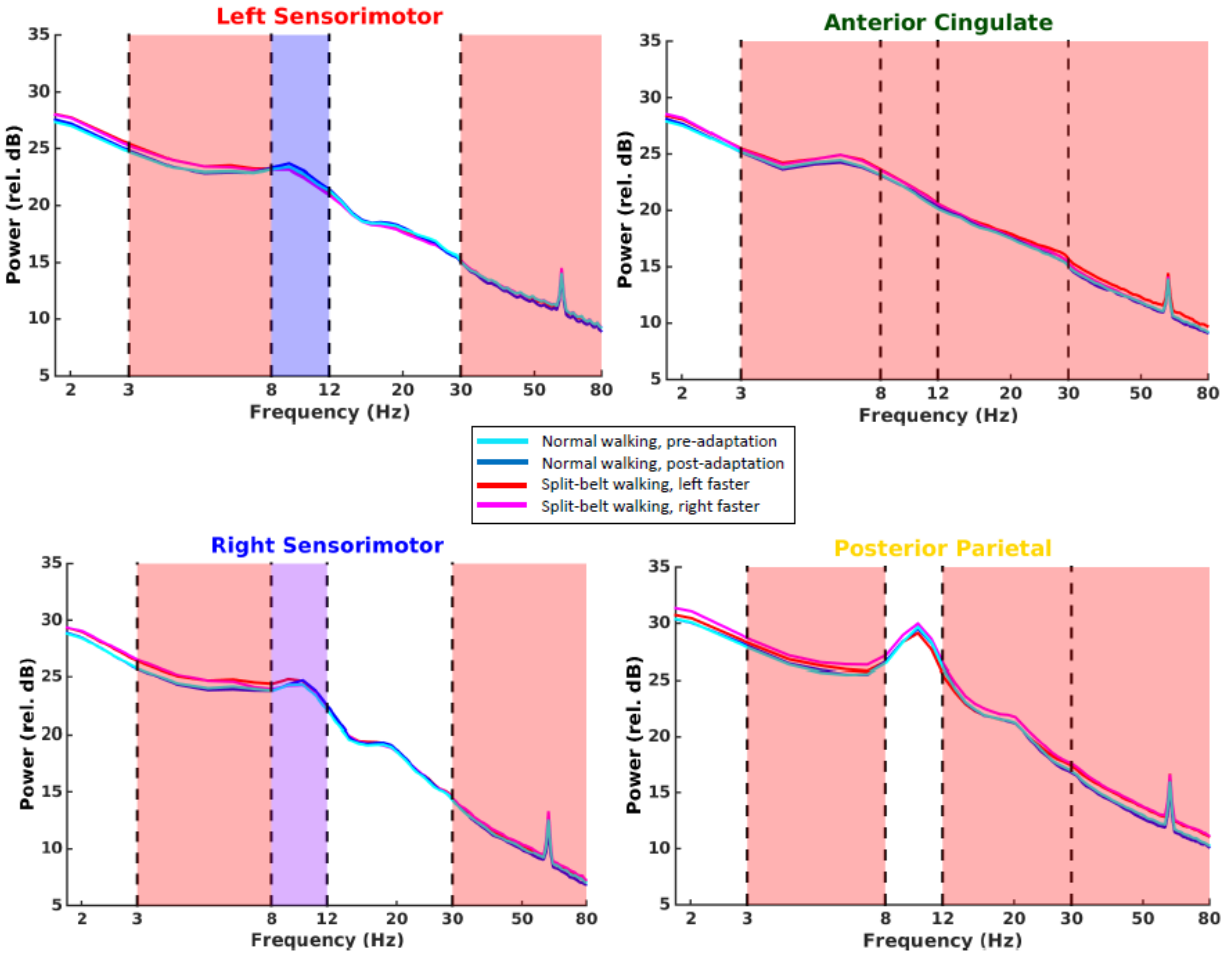

Figure 2-3. Grand average spectral power for each electrocortical cluster during normal walking. Conditions are *pre-adaptation* (light blue), normal walking, *post-adaptation* (dark blue), split-belt walking, *left foot faster adaptation* (red), and split-belt walking, *right foot faster adaptation* (pink). The dashed lines mark boundaries of frequency bands—theta (3-7 Hz), alpha (8-12 Hz), beta (13-30 Hz), and gamma (31-80 Hz). Red shaded regions indicate at least one or both split-belt walking conditions are significantly greater than at least one or both normal walking conditions. Blue shaded region indicates normal walking, *post-adaptation* is significantly greater than *pre-adaptation*. Purple shaded region indicates normal walking, *post-adaptation* is significantly greater than *pre-adaptation* and split-belt walking, *left foot faster adaptation* is greater than *pre-adaptation*. For specific pairwise statistics see Table 2-2.

Table 2-2. Significant spectral differences between pairs of conditions.

	Theta (4-7 Hz)	Alpha (8-12 Hz)	Beta (13-30 Hz)	Gamma (31-80 Hz)
Left Sensorimotor Cortex	Spl (L) > Pre (p=0.006) Spl (L) > Post (p=0.002) Spl (R) > Pre (p=0.034) Spl (R) > Post (p=0.017)	Post > Pre (p=0.011)		Spl (L) > Post (p=0.022)
Right Sensorimotor Cortex	Spl (L) > Pre (p=0.002) Spl (L) > Post (p<0.001) Spl (R) > Pre (p=0.001) Spl (R) > Post (p<0.001)	Spl (L) > Pre (p=0.03) Post > Pre (p=0.028)		Spl (L) > Post (p=0.05) Spl (R) > Post (p=0.014)
Anterior Cingulate	Spl (L) > Pre (p=0.037) Spl (L) > Post (p=0.002) Spl (R) > Post (p<0.001)	Spl (L) > Pre (p=0.041) Spl (R) > Pre (p=0.006)	Spl (L) > Pre (p=0.014) Spl (R) > Pre (p=0.009)	Spl (L) > Post (p=0.011)
Posterior Parietal	Spl (R) > Pre (p<0.001)		Spl (R) > Pre (p=0.006)	Spl (L) > Post (p=0.001) Spl (R) > Pre (p=0.001) Spl (R) > Post (p=0.037)

Spl (L) = Left foot faster adaptation, Spl (R) = Right foot faster adaptation, Pre = Pre-adaptation, Post = Post-adaptation

Fluctuations of spectral power during the gait cycle

All four brain areas showed significant spectral power fluctuations in theta, alpha, beta, and gamma bands across the gait cycle during *pre-adaptation, post-adaptation, left foot faster adaptation,* and *right foot faster adaptation* (Figure 2-4). Left sensorimotor area showed significant alpha and beta power synchronizations during late left foot swing phase between left toe off (LTO) and left heel strike (LHS) and the following double support phase between left heel strike (LHS) and right toe off (RTO) for *pre-adaptation* as well as theta synchronization right before and after RTO. However, during *post-adaptation* both the theta and beta power synchronizations were significantly reduced. For both *left and right foot faster adaptation* there was a lateralized result such that there was significant beta and gamma power during double support (slow foot leading) followed by theta power desynchronizations during late swing phase

of the faster moving foot and then theta and alpha synchronization as the faster foot came down for double support.

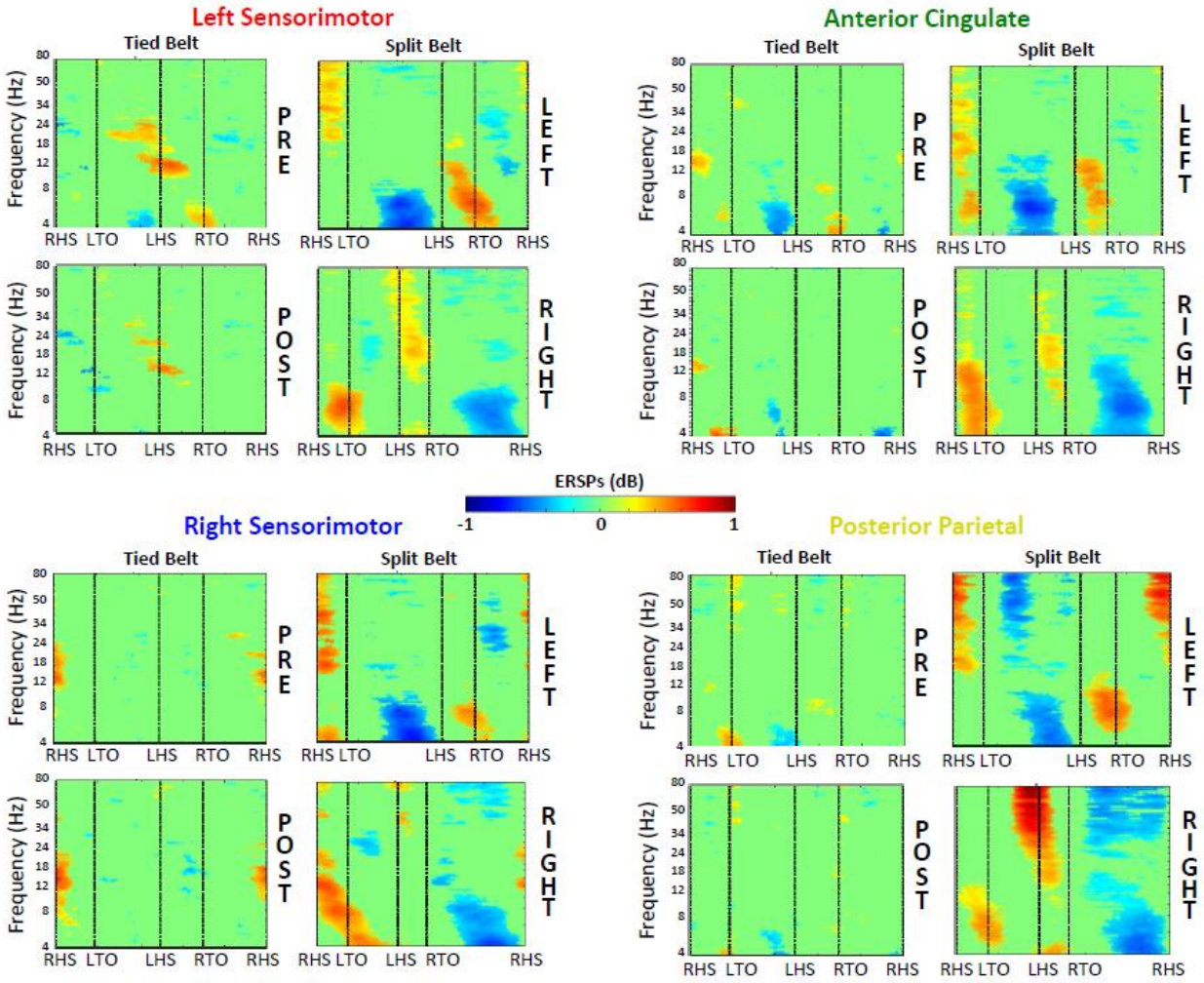

Figure 2-4. Grand average normalized spectrograms. Significance masked ($p < 0.01$) for left sensorimotor, right sensorimotor, anterior cingulate, and posterior parietal clusters during *pre-adaptation* ("PRE"), *post-adaptation* ("POST"), *left foot faster adaptation* ("LEFT"), and *right foot faster adaptation* ("RIGHT"). All plots represent one gait cycle from right heel strike (RHS) to RHS, with left toe off (LTO), right toe off (RTO), and left heel strike (LHS) designated by dashed vertical lines. Nonsignificant values were set to zero (green).

Right sensorimotor area also showed significant alpha and beta synchronizations during late right foot swing phase and the following double support phase during both *pre* and *post-adaptation*.

However, there was no significant fluctuation differences between the two tied belt conditions. Unlike the left sensorimotor ERSPs, right sensorimotor fluctuations *during left and right foot faster adaptation* were not completely lateralized. During *left foot faster adaptation*, there was significant beta and gamma power during double support (slow foot leading) followed by theta power desynchronizations during late swing phase of the faster moving foot and then theta synchronization as the faster foot came down for double support. There was also beta desynchronization during right foot swing phase. For *right foot faster adaptation* there the fast foot leading double support phase contained theta, alpha, and beta synchronizations that extended through slow foot swing phase. There were no fluctuations during double support before the faster foot (right) swing phase, which showed both theta and alpha desynchronizations.

The anterior cingulate cluster showed a significant reduction of theta desynchronization during left foot swing phase from *pre* to *post-adaptation*. But there were no large fluctuations across alpha or beta band as the sensorimotor areas showed. However, there were lateralized fluctuations for both *left and right foot faster adaptation* with alpha, beta, and gamma power synchronizations during double support (slow foot leading) followed by theta and alpha power desynchronizations during faster foot swing phase and then theta and alpha synchronizations during the following double support (fast foot leading).

Posterior parietal area did not show any large fluctuations during *pre* and *post-adaptation*. But there were lateralized fluctuations for both *left and right foot faster adaptation* with beta and gamma power synchronizations during double support (slow foot leading) followed by theta.

Alpha, and gamma power desynchronizations during faster foot swing phase and then theta and alpha synchronizations during the following double support (fast foot leading). There was also beta and gamma synchronizations present during the end of swing phase of the slow foot.

Discussion

The results of this study showed many significant differences in electrocortical activity during a locomotor adaptation task in young, healthy adults walking on a split-belt treadmill. There was always greater spectral power in theta (4-7 Hz) and gamma (31-80 Hz) bands during split-belt adaptation compared to normal walking in the left sensorimotor, right sensorimotor, anterior cingulate, and posterior parietal clusters.

Theta Band Power Differences Among Conditions

Theta band consistently showed greater spectral power in split-belt *adaptation* walking compared with *pre* and *post-adaptation* tied belt walking conditions for all clusters as we predicted in our hypothesis. Similarly, the ERSPs for all clusters showed strong theta synchronizations in one or both double support phases across the gait cycle during both *left foot and right foot faster adaptation* conditions while strong theta desynchronizations happened during swing phase of the faster moving foot in the *adaptation* conditions. This might suggest that theta fluctuations are necessary for asymmetric walking but not present for normal walking. Since the faster moving foot takes a quicker and longer step than the slower foot, foot placement is critical and stabilization afterwards is more challenging. This suggests that the increased theta band power synchronizations during double support might be important for balance and stabilization while the theta desynchronizations during swing phase of the faster moving foot is

needed to facilitate planning foot placement when more control is necessary compared to normal walking. Previous studies have also found increased theta power in similar brain areas for locomotor tasks that involve more motor control than normal walking (Bradford et al. 2016; Bulea et al. 2015; Sipp et al. 2013; Slobounov et al. 2009). Incline treadmill walking was shown to have increased theta band power across the entire gait cycle compared to flat treadmill walking (Bradford et al. 2016) in left sensorimotor, medial sensorimotor, anterior cingulate, and posterior parietal areas. It was also shown that the largest differences occurred at heel strike and toe off which suggests the transition between single and double support may be a critical time period for the control of foot adjustments. Theta power was also shown to significantly increase for active, speed-adjusted treadmill walking vs normal, passive treadmill walking in prefrontal, left premotor, and right motor cortices (Bulea et al. 2015). Balance beam treadmill walking increased theta power compared to normal treadmill walking in the anterior cingulate, anterior parietal, right sensorimotor, medial sensorimotor, and dorsolateral prefrontal cortices (Sipp et al. 2013). That study also showed increased theta synchronizations during the moment of balance loss before falling off the beam. Similarly, theta power increased when participants stood on an unstable vs stable surface (Hülsdünker et al. 2015; Slobounov et al. 2009). Another study showed similar increased theta desynchronizations during single support with subject walking with eyes closed compared to open (Oliveira, Schlink, Hairston, et al. 2017). Our results support the theory that theta power modulation increases during more demanding motor tasks compared to normal walking.

Alpha Power Differences During Split-Belt Adaptation

Significant alpha band (8-12 Hz) power fluctuations appeared throughout all clusters during *split-belt adaptation walking*. Left sensorimotor area showed a significant alpha synchronization during double support after LHS during left foot faster adaptation but not after RHS during right foot faster adaptation. Conversely right sensorimotor area showed a significant alpha synchronization during double support after RHS during right foot faster adaptation but not after LHS during left foot faster adaptation. Similarly, both anterior cingulate and posterior parietal showed increased alpha desynchronizations during swing phase of the faster foot for both left and right foot faster adaptation conditions along with increased alpha synchronizations during both double support phases while none of these patterns were seen in any of the pre or post-adaptation conditions. This suggests an important role for alpha power across both swing and stance phases of the gait cycle, which was most prevalent during asymmetric walking. Other studies support this by also showing similar patterns of increased alpha (mu) desynchronizations during tasks that require increased cortical involvement (Bulea et al. 2015; Wagner et al. 2012; Wieser et al. 2010). Stepping movements showed sustained alpha power depression over the primary sensory motor regions when changing direction between flexion and extension phase (Wieser et al. 2010). Robot assisted treadmill walking showed suppression of mu rhythms over the right primary motor cortex during active vs passive mode (Wagner et al. 2012). Another study showed sustained mu band desynchronization in the left premotor, left motor, right motor, and posterior parietal cortices during walking compared to rest as well as consistent mu desynchronizations in all cluster except prefrontal cortex for active vs passive treadmill walking (Bulea et al. 2015). Oliveira et al. (Oliveira, Schlink, Hairston, et al. 2017) also showed increased alpha synchronizations in left and right somatosensory cortex during double support (ipsilateral foot ahead) when subjects walked with eyes closed compared to with eyes open. Our results

confirm our hypothesis that alpha power fluctuations are used in complex walking patterns compared to normal walking.

Left and Right Sensorimotor Lateralization Differences

While left and right sensorimotor areas showed similar ERSP patterns, there were clear lateralized differences in beta band (13-30 Hz) fluctuations. Beta synchronizations were present in both left and right sensorimotor areas at the end of ipsilateral swing phase into double support during tied walking *pre-adaptation*, but beta power synchronization was significantly reduced in the left sensorimotor area during *post-adaptation* while it was sustained in right sensorimotor area. Left sensorimotor also showed beta synchronization during double support before the fast leg swing phase for both *left and right foot faster adaptation* while right sensorimotor only showed this pattern for *left foot faster adaptation* but not *right foot faster adaptation*. One study (Bruijn et al. 2015) also found significant increases in beta power when subjects walked on a treadmill while being laterally stabilized by elastic cords compared to normal walking. The lateralized differences between left and right sensorimotor areas has also been shown in previous studies (Bradford et al. 2016; Bruijn et al. 2015; Sipp et al. 2013). Balance beam walking showed no significant changes in spectral power for the right sensorimotor area during balance loss that was found in left sensorimotor area. They conclude that the left compared to right sensorimotor cortex plays a larger role in sensing loss of balance during walking, which was also demonstrated in another study (Serrien et al. 2006) that the left hemisphere plays a more dominant role in skilled complex movements. Bruijin et al. (Bruijn et al. 2015) initially found sources in the left and right premotor areas when comparing normal vs stabilized walking, but subsequent source level analysis revealed only significant differences in the left premotor area and not the right

side. The theory that left sensorimotor may be more involved in coordination and balance is reflected in our results showing a significant reduction of beta synchronizations in swing phase from *pre* to *post-adaptation* as well as increased beta synchronizations during double support before the faster foot swing phase in both *left and right foot faster adaptation* conditions that were not present in the right sensorimotor area.

Posterior Parietal Beta and Gamma Increases During Split-Belt Adaptation

We found many large gait-related synchronizations and desynchronizations during split-belt adaptation walking in the posterior parietal cortex that were not present in the other neural sources. Particularly, both *left and right foot faster adaptation* conditions showed beta and gamma (31-80 Hz) synchronizations during double support phase with the slow foot forward and primarily only theta and alpha synchronizations in the double support phase with fast foot forward. Similarly, there were also theta, alpha, and gamma desynchronizations in *adaptation* conditions during the swing phase of the faster foot. These results suggest that theta, alpha, and gamma desynchronizations are used during the swing phase for planning critical foot placement when walking asymmetrically. Previous research has shown that the parietal area in cats may be directly involved in interlimb coordination during locomotion (Beloozerova and Sirota 1993; Drew, Kalaska, and Krouchev 2008; Drew, Prentice, and Schepens 2004; Lajoie et al. 2010; Widajewicz, Kably, and Drew 1994). Other studies (Bulea et al. 2015) further support this idea and found low gamma band in posterior parietal cortex was increased in double stance and early swing phase when comparing active to passive treadmill walking. They also showed increased low gamma synchronizations when participants tracked a target speed using the active treadmill which lead them to conclude that parietal gamma band activity may demonstrate increased

attention to foot velocity in order to track a target walking speed. Another study (Sipp et al. 2013) also showed that successful balance beam walking was associated with sustained theta band power synchronizations compared to off-beam treadmill walking. They concluded that parietal lobe might be important for sensory information integration and decision related activity (de Lafuente 2013) while also contributing to the anterior cingulate processing regarding error trend detection. Together, these findings show support for the role of posterior parietal cortex in motor planning and error correction during more challenging walking conditions.

Limitations

Mechanical and movement related artifacts are always a concern with human locomotion EEG studies. It has been shown using passive electrodes and faster treadmill speeds that walking-related artifacts exist, especially in delta bands (0-3 Hz) and subsequent harmonics (Castermans et al. 2014). Therefore, due to the nature of increased movement related artifact with fast walking speeds in EEG (Kline et al. 2015), we chose to only analyze slow treadmill speeds where at least one leg was moving at 0.5 m/s. We also used active, wet electrodes processed with independent component analysis (ICA) to present results in neural source components rather than scalp channels. We also employed a series of novel cleaning methods including template gait-related channel rejection to remove channels most correlated with the gait cycle, Ensemble Empirical Mode Decomposition (EEMD) to remove high frequency components associated with muscle electromyography (EMG), and Canonical Correlation Analysis (CCA) to remove low frequency cyclic components most closely aligned with stepping frequency. We also used a computationally intensive ICA method, Adaptive Mixture ICA (AMICA) (Delorme et al. 2012) to provide the best component source separation with maximum independence. However, better

methods for cleaning movement-related artifact and muscle-related (EMG) artifact are continually being updated as well as better hardware that incorporates noise data for extraction would help to further improve the detail of EEG results and allow for more complicated and challenging locomotor tasks.

Conclusions

We found significant differences in both cortical spectral power and event-related fluctuations between normal treadmill walking and split-belt motor adaptation in the left sensorimotor, right sensorimotor, anterior cingulate, and posterior parietal areas. This builds upon previous studies that showed similar brain areas are involved in demanding walking tasks and examines the relationship between theta synchronizations and desynchronizations in balance and postural control. We confirmed previous findings that alpha power plays an important role with more challenging motor task. We also found lateralized differences between left and right sensorimotor areas that suggest different roles for each hemisphere in asymmetric walking. Finally, we show support for posterior parietal area being more active during motor planning and foot placement in motor adaptation compared to normal walking. These results further show that it is possible to use EEG to study locomotor adaptation, which is important for future understandings of neurological rehabilitation in gait asymmetries.

Supplementary Figures

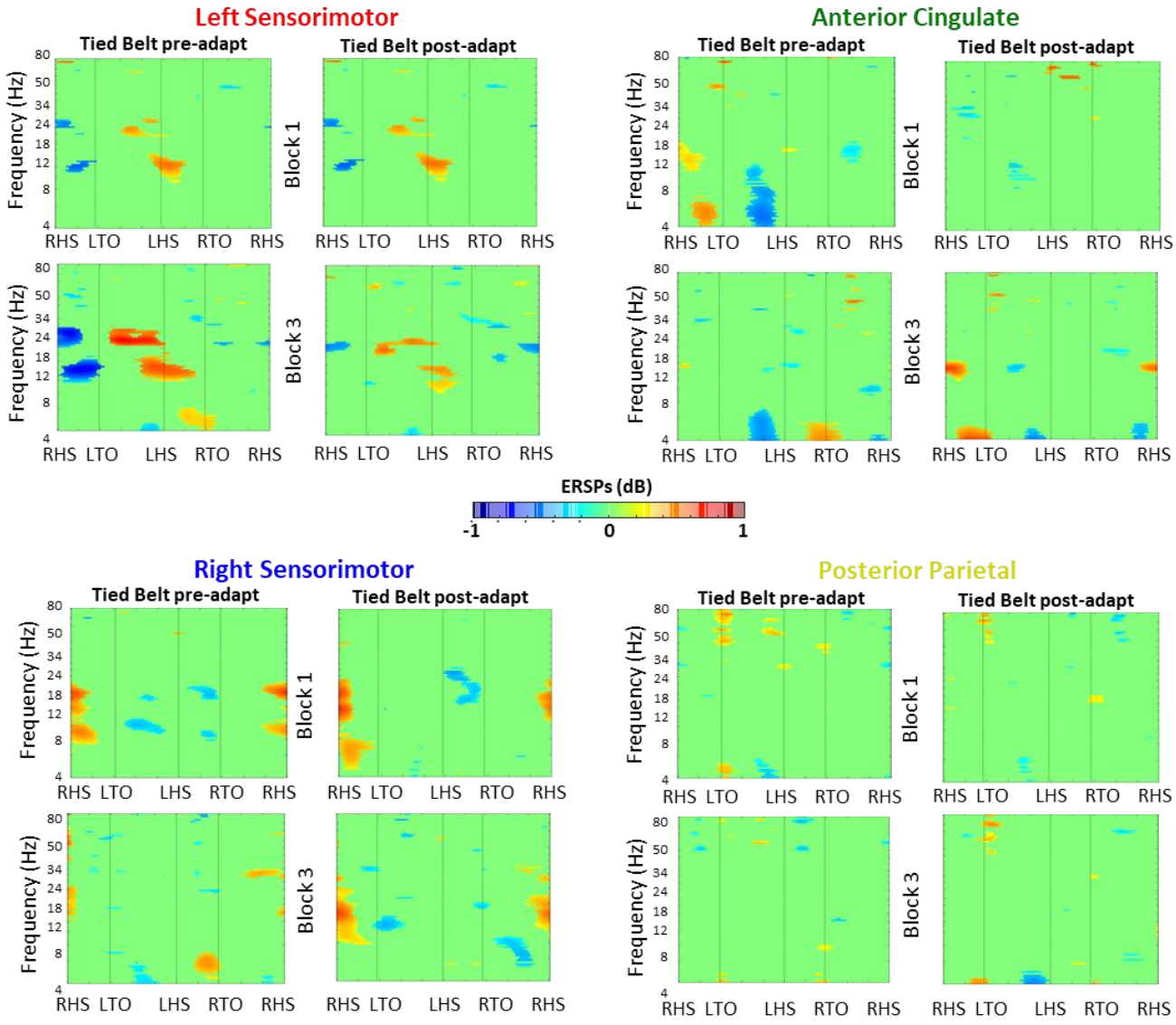

Supplementary Figure 2-1. Grand average normalized spectrograms. Comparison of pre and post-adaption for Block 1 (top plots) vs Block 3 (bottom plots) showing minimal to no differences. Significance masked ($p < 0.01$) for left sensorimotor, right sensorimotor, anterior cingulate, and posterior parietal clusters. All plots represent one gait cycle from right heel strike (RHS) to RHS, with left toe off (LTO), right toe off (RTO), and left heel strike (LHS) designated by dashed vertical lines. Nonsignificant values were set to zero (green).

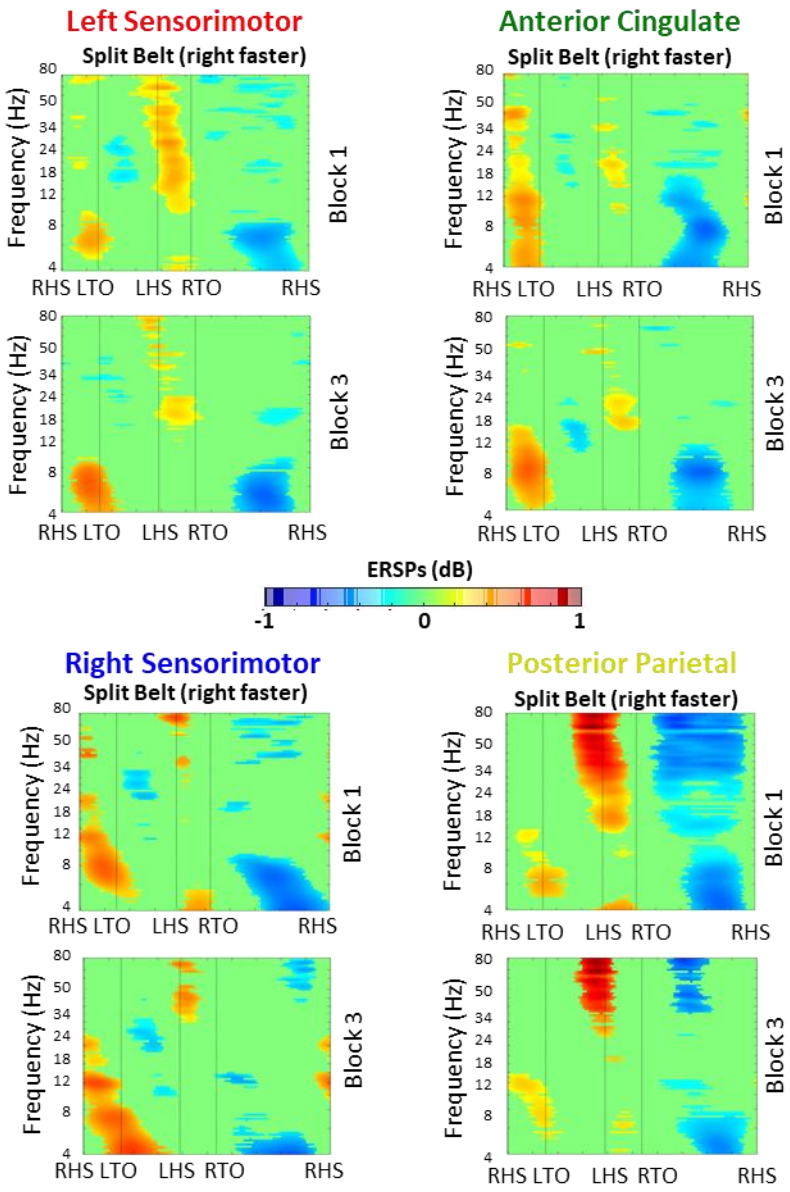

Supplementary Figure 2-2. Grand average normalized spectrograms. Comparison of split-belt walking for Block 1 (top plots) vs Block 3 (bottom plots) showing minimal to no differences. Significance masked ($p < 0.01$) for left sensorimotor, right sensorimotor, anterior cingulate, and posterior parietal clusters. All plots represent one gait cycle from right heel strike (RHS) to RHS, with left toe off (LTO), right toe off (RTO), and left heel strike (LHS) designated by dashed vertical lines. Nonsignificant values were set to zero (green).

Chapter 3 Mobile brain-body imaging of indoor treadmill walking and outdoor walking during a visual search task

Abstract

To fully understand brain processes in the real world, it is necessary to record and study brain processes during human locomotion across varying terrain. Advances in electroencephalography (EEG) and signal processing techniques provide new opportunities for studying mobile subjects outside of the laboratory. Previous research has shown success in using these techniques to identify neural correlates and spectral power fluctuations during various human walking studies on treadmills. The purpose of this study was to document the current viability of using high density EEG for mobile brain imaging both indoors and outdoors. The data set includes 49 young, healthy subjects walking on an outdoor arboretum path while completing a visual search task. Subjects also completed a laboratory version of the same task on a treadmill using virtual reality. The data provide a valuable research tool for scientists interested in electrocortical brain processes, mobile brain imaging, and brain-computer interfaces based on EEG.

Background and Summary

Identifying neural correlates and their dynamics in ambulatory tasks have presented many challenges in research. Previously, neuroimaging studies of human locomotion have been confined to laboratory environments that use large and expensive scanners like positron emission tomography (PET) and functional magnetic resonance imaging (fMRI). Both have shown that

during movement preparation and anticipation frontal and association areas are activated (Christensen et al. 2001; Dobkin et al. 2004; Heuninckx et al. 2005; Luft et al. 2002; Sahyoun et al. 2004). These findings have also been confirmed in electroencephalogram (EEG) studies using similar tasks that show lower limb movement related electrocortical potentials (Liv Hansen and Bo Nielsen 2004; Raethjen et al. 2008).

Currently, EEG is the only non-invasive brain imaging modality that is portable enough to wear during ambulation in the real world while measuring cortical dynamics in the brain with high enough temporal resolution to record intra-stride changes (Makeig et al. 2009). EEG has long been considered to be too noise prone to allow such recordings (Gwin et al. 2010). Mechanical artifacts such as head movements can have amplitudes orders of magnitudes larger than the underlying EEG brain signals. The use of advanced signal processing techniques, such as Independent Component Analysis (ICA), however, allows for filtering out electromyographic (EMG), electroocular, movement artifact, and line noise contamination of EEG signals (Delorme et al. 2012; Jung et al. 2001; Makeig et al. 2004, 1996; Onton and Makeig 2006). Gwin and colleagues have demonstrated that it is possible to directly measure cortical activity using these methods and showed significant increases in alpha (8-13 Hz) and beta (13-30 Hz) band power in the sensorimotor and anterior cingulate cortices when both feet are on the ground during normal walking on a treadmill (Gramann, Onton, et al. 2010; Gwin et al. 2011).

While previous studies (Gramann et al. 2011; Gramann, Onton, et al. 2010; Gwin et al. 2011) have shown that using EEG during ambulation is possible with the use of treadmills indoors, few studies have examined EEG in natural outdoor settings over ground. A couple of recent studies

(Debener et al. 2012; Roe et al. 2013) have measured EEG outdoors, but these use a limited set of electrodes (<15 channels). Using less than 64 EEG channels enables limited separation of mixed signals when using blind source separation techniques to identify neural components (Lau, Gwin, and Ferris 2012). A high density EEG system provides a much richer dataset to analyze neural dynamics of human locomotion.

The overall goal of this project was to document the possibility of high-density electroencephalography (EEG) to provide insight into human brain function during ambulatory tasks in real world environments. The current study examined young, healthy subjects walking in a natural arboretum environment while they wore a high-density (256 channel) EEG. Subjects completed a visual search task where they had to identify colored flags in their environment. Subjects also completed an indoor virtual reality version of the task on a treadmill. By completing similar tasks indoors in a laboratory on a treadmill, and outdoors in an arboretum on natural terrain, the data set can reveal differences between traditional laboratory experiments and real world experiments. A secondary goal was to provide a potentially stressful intervention on the task, where subjects gained and lost monetary rewards based on their performance.

Methods

Subjects

Forty-nine healthy adults (20 males, 29 females) between the ages of 18-45 (average age 22.7) participated in the study. None of the subjects had any history of neurological or physical impairments and were in good shape, such that they could walk on a treadmill and on outdoor terrain for one hour while carrying a fifteen-pound load without issue. The University of

Michigan Internal Review Board approved all study procedures and all subjects provided signed consent prior to participating in the study.

Equipment

EEG acquisition

Subjects were fitted with a high density, pre-amplified 256-channel EEG cap (sampling rate: 512 Hz; Biosemi Activetwo, Amsterdam, Netherlands). We placed 8 additional sensors on the neck of the subject to record neck muscle activity. The position of each electrode relative to the subject's head was recorded using a 3D digitizer (Zebris, Germany). Before data collection, we applied electrode gel underneath each sensor and kept all offsets below 20 mV as recommended by Biosemi user manual for optimal data quality.

Inertial measurement units

Subjects wore 6 inertial measurement units (IMUs) (sampling rate: 128 Hz; APDM Opal, Portland, OR) attached to both feet, both ankles, waist, and chest. Each IMU monitored limb movements using 3D accelerometers, gyroscopes, and magnetometers.

Instrumented treadmill

Subjects walked on an instrumented, split-belt treadmill (sampling rate: 1000 Hz; Bertec, Columbus, OH) which has separate belts, each with its own motor, for the left and right side of the walking surface. Separate force transducers under each belt were used for the collection of 6 degrees of freedom ground reaction forces from the left and right foot separately.

Cortisol

The SalivaBio Oral Swab saliva collection method was used to obtain participant salivary cortisol samples (Salimetrics, Newmarket, UK). Subjects were previously informed not to consume any food or beverages (other than water) one hour prior to testing. Subjects were not allowed to eat during the duration of testing. A total of 8 saliva samples (4 indoors, 4 outdoors) were collected during testing as follows: before the start of each experiment, between the first and second conditions, between the second and third conditions, and after the third condition for both indoor and outdoor sessions. Collections were done by placing an oral swab under the subject's tongue for two minutes. Swabs were then removed and placed in storage tubes and held in an ice chest at below 4°C during testing after which they were frozen at below -20 °C until analysis.

Heart Rate

Heart rate was measured using photoplethysmogram (PPG) recordings obtained from a Pulse Sensor heart rate monitor (sampling rate: 500 Hz; World Famous Electronics LLC, New York, NY) attached to the subject's right earlobe and controlled through an external Arduino.

Eye Tracker

Each subject had visual gaze recorded with Mobile Eye XG eye tracking glasses (sampling rate: 30 Hz; Applied Science Laboratory, Boston, MA) with 0.5 to 1 degree accuracy.

Video

High definition video recordings of the experiment were done using a high definition camcorder

(sampling rate: 30 Hz; Canon USA) handheld by an experimenter. Subjects wore a backpack that contained the EEG amplifier, battery, eye tracker acquisition logger, and connectors such that a line of cables connected the multiple systems to the data collection laptop placed in a carrying tray held by an experimenter following behind the subject approximately 10 feet away (Figure 3-1A and 3-1B).

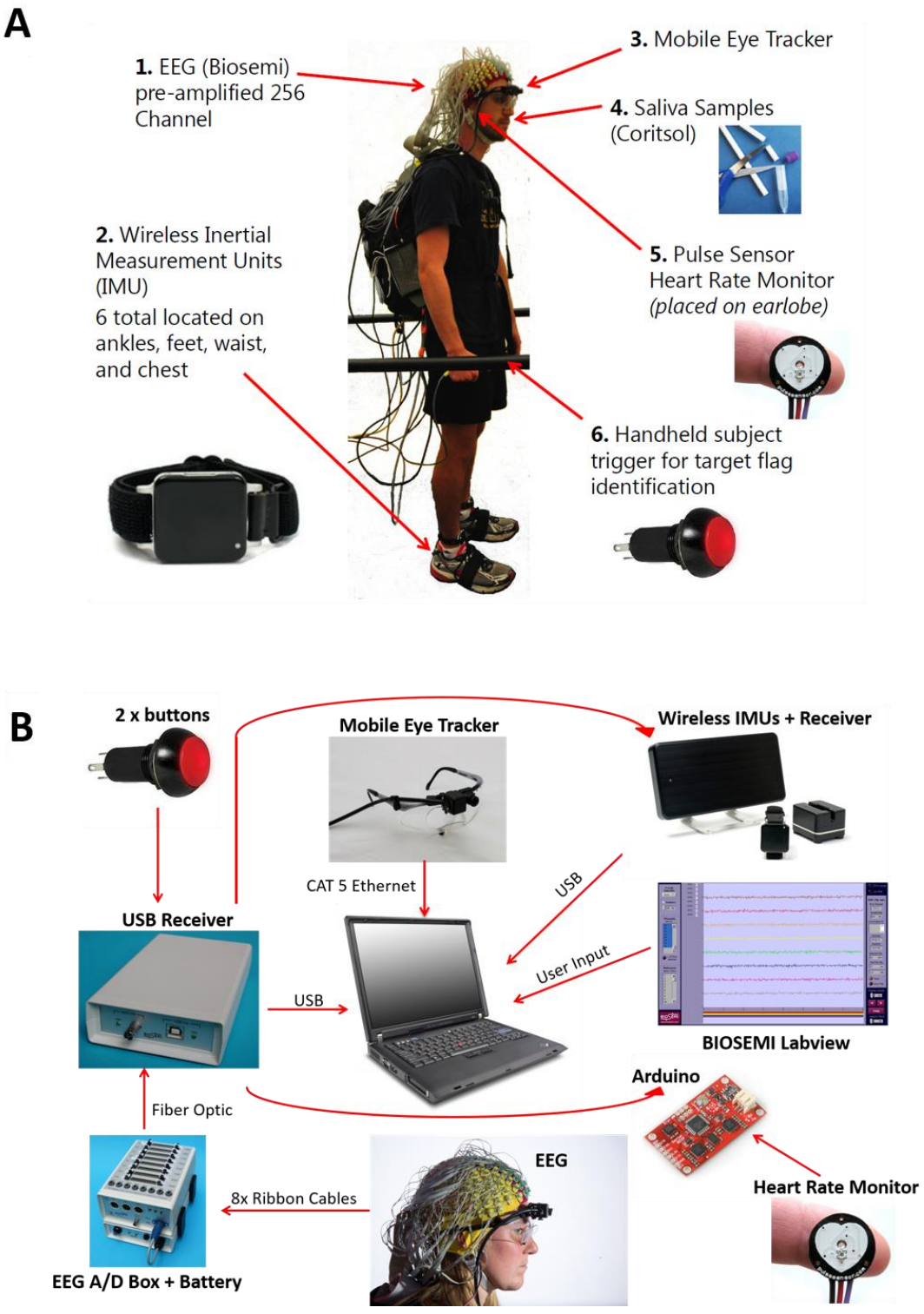

Figure 3-1. Experimental Design. (A) Diagram of measurement devices placed on an example subject (B) Layout of recording devices and how they were connected to each other for synchronization.

Testing Environments

Virtual reality environment

A 3D animated environment (designed in Google SketchUp) of a virtual park was displayed as a video on a projector screen directly in front of the treadmill (Figure 3-2) set at 0.7 m/s moving at the same pace as the video. Within the virtual landscape, there were a total of 50 animated target flags (bright green) and 150 animated non-target flags (dark green) split evenly between the non-stress and stress conditions. There were no flags displayed during the baseline condition. The difficulty of the target flag detection level varied based on position relative to environmental objects as well as distance from path.

Real world environment

Subjects walked outdoors on a marked trail path (Figure 3-2) at an arboretum (Nichols Arboretum, Ann Arbor, MI). The path was accessible to the public during testing. The marked path was approximately 2 miles long in total (Figure 3-3). There was a total of 50 target flags (bright green) and 150 non-target flags (dark green) split evenly between the non-stress and stress conditions. Flags were 2” x 3” trail marking flags attached to a 15” pole. There were no flags in place during baseline walking. Subjects were instructed to walk straight along the path at a slow to moderate pace without stopping. Auditory cues to speed up or slow down were given if necessary. Flags were placed within 10 feet off the path and not higher than 10 feet off the ground. They were placed in such a manner that they were visible from the path without having to step off of it.

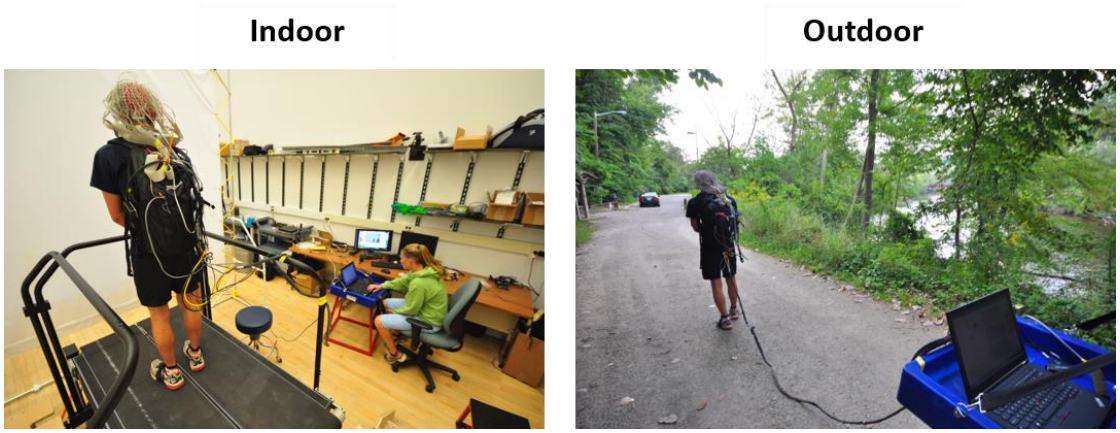

Figure 3-2. **Indoor and outdoor environments.** Left panel shows an example subject standing on the instrumented, split-belt treadmill in front of the projector screen displaying the indoor, virtual environment. Right panel shows an example subject walking along the outdoor path tethered to an experimenter by cables from measurements devices connected to a laptop on a tray.

Protocol

Subjects walked for approximately one hour continuously in each environment while performing a visual search task. First, subjects started with a 20 minute baseline condition of normal walking in which no flags were present in the environment. After baseline walking was complete the visual search task began. The goal of the task was to search and identify bright green flags (targets) within the environment and to ignore dark green flags (non-targets). Subjects were to press the button on a joystick they were holding when they saw a target flag and to not press anything when they saw a non-target flag. There were 2 conditions, 20 minutes each, during the visual search task: 1) "Non-stress" – subjects were told each correct flag identified earned an extra $0.25 toward their compensation for the study and 2) "Induced Stress" - in addition to earning $0.25 per correctly identified target flag subjects were also told they would be penalized $1.00 for every unidentified target flag and a loud siren was played immediately after the subject walked passed the unidentified target flag. To further induce stress, subjects were given false negative siren noises indicating a missed target flag randomly (approximately once every 2

minutes, 10 times total). Subjects were naïve to the random penalties during the task, but were debriefed after the conclusion of the experiments. Baseline walking was always first, but the order of the 2 visual search conditions was randomized.

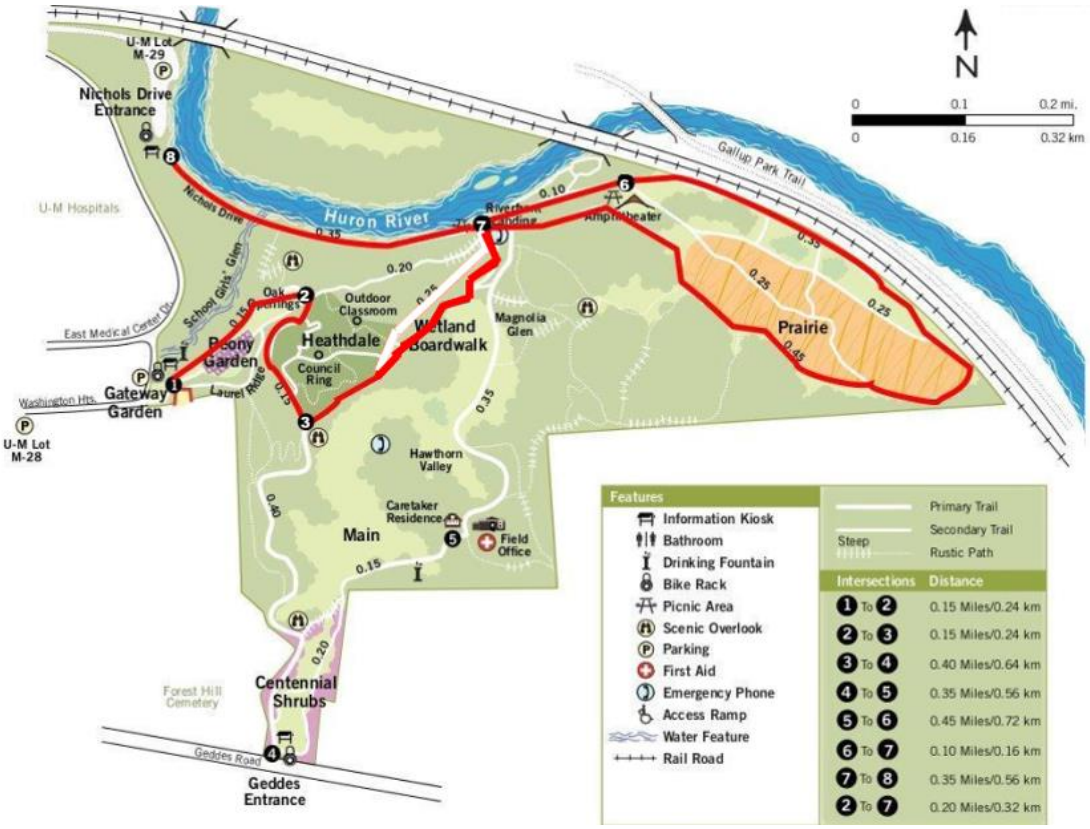

Figure 3-3. Map of the arboretum. Walking path highlighted in red. Subjects started at maker 1, and at marker 7 continued northwest toward marker 6. After looping back to marker 7 subject proceeded west to the finish at marker 8.

Code availability

Code for importing data measures from all sources into Matlab and EEGLAB is provided.

Data Records

Data storage

All data measures used in this study are stored in IEEE Dataport (https://ieee-dataport.org/open-access/mobile-brain-body-imaging-during-indoor-treadmill-walking-and-outdoor-overground-walking; DOI: 10.21227/H24T0V) as an open-access data set. The data is stored as a single compressed .zip file (778 GB) and archived into individual folders by subject ID. A second copy archived as 49 individual .zip files by subject is also made available in Figshare (https://doi.org/10.6084/m9.figshare.6741734; DOI: 10.6084/m9.figshare.6741734).

Data organization

This study is an EEG Study Schema (ESS) Standard Data Level 1 container. This means that it contains raw, unprocessed EEG data arranged in a standard manner. Data is in a container folder and ready to be used with MATLAB to automate access and processing. All other data measures other than EEG are in .mat (MATLAB) format. For more information please visit eegstudy.org.

There is one folder for every subject that includes the following files when available:

(1) Indoor EEG session (<ID number_Indoor.set>)

EEG files have been imported into EEGLAB and are stored as unprocessed raw .set format in standard EEGLAB Data Structures.

(https://sccn.ucsd.edu/wiki/A05:_Data_Structures)

(2) Outdoor EEG session (<ID number_Outdoor.set>)

Same as Indoor EEG session (above)

(3) Indoor IMU session (<ID number_Indoor_imu.mat>)

The IMU .mat file contains a structure with 6 fields (variable name: IMU)

IMU.dataLabel: string including ID number, environment, and sensor type

IMU.dataArray: 10xNx6 matrix. Third dimension refers to each of 6 IMU sensors (left foot, right foot, left ankle, right ankle, chest, and waist). Columns are frame numbers. Rows are:

- x, y, and z direction of accelerations, in m/s^2
- x, y, and z direction of gyroscopes, in rad/s
- x, y, and z direction of magnetometers, in microteslas
- Temperature, in degrees Celsius

IMU.axisLabel: String headings for ‘dataType’ and ‘frame’ and ‘sensorNumber’

IMU.axisValue: 1x10 cell array of string headings for each row of data type, and 1x6 cell array of string headings for each IMU sensor

IMU.samplingRate: Sampling rate

IMU.dateTime: String of date and time information of recording

(4) Outdoor IMU session (<ID number_Outdoor_imu.mat>)

Same as Indoor IMU session (above).

(5) Indoor eye tracking session (<ID number_Indoor_eye_tracker.mat>)

The eye tracker .mat file contains a structure with 6 fields (variable name: Eye_tracker)

Eye_tracker.dataLabel: string including ID number, environment, and sensor type

Eye_tracker.dataArray: 7xN matrix. Columns are frame numbers. Rows are:

- x and y coordinates of the master spot, in eye image pixels
- x and y coordinates of the pupil center, in eye image pixels
- Pupil radius, in eye image pixels
- Eye direction with respect to the scene image, in scene image pixels

The eye and scene images are displayed and recorded with resolution of 640 x 480 pixels. The origin is the top left of the image with the X-axis positive to the right and the Y-axis positive downwards. Unavailable data is shown by the number –2000.

Eye_tracker.axisLabel: String headings for ‘dataType’ and ‘frame’

Eye_tracker.axisValue: 1x7 cell array of string headings for each row of data type

Eye_tracker.samplingRate: Sampling rate

Eye_tracker.dateTime: String of date and time information of recording

(6) Outdoor eye tracking session (<ID number_Outdoor_eye_tracker.mat>)

Same as Indoor eye tracking session (above).

(7) Indoor heart rate from pulse sensor session (<ID number_Indoor_pulse_sensor.mat>)

The pulse sensor .mat file contains a structure with 6 fields (variable name: Pulse_sensor)

Pulse_sensor.dataLabel: string including ID number, environment, and sensor type

Pulse_sensor.dataArray: 3xN matrix. Columns are frame numbers. Rows are:

- pulse (normalized wave), in volts
- Inter-beat Interval (IBI), in milliseconds
- heart rate, in beats per minute (BPM)

Pulse_sensor.axisLabel: String headings for ‘dataType’ and ‘frame’

Pulse_sensor.axisValue: 1x3 cell array of string headings for each row of data type

Pulse_sensor.samplingRate: Sampling rate

Pulse_sensor.dateTime: String of date and time information of recording

(8) Outdoor heart rate from pulse sensor session

(<ID number_Outdoor_pulse_sensor.mat>)

Same as Indoor pulse sensor session (above).

(9) Indoor heart rate from EEG session (<ID number_Indoor_pulse_from_eeg.mat>)

If pulse rate was recovered from EEG ECG a corresponding file is available. The pulse from EEG .mat file contains a structure with 6 fields (variable name: Pulse_from_EEG)

Pulse_from_EEG.dataLabel: string including ID number, environment, and sensor type

Pulse_from_EEG.dataArray: 3xN matrix. Columns are frame numbers. Rows are:

- pulse (normalized wave), in volts
- Inter-beat Interval (IBI), in milliseconds

• heart rate, in beats per minute (BPM)

Pulse_from_EEG.axisLabel: String headings for ‘dataType’ and ‘frame’

Pulse_from_EEG.axisValue: 1x3 cell array of string headings for each row of data type

Pulse_from_EEG.samplingRate: Sampling rate

Pulse_from_EEG.dateTime: String of date and time information of recording

(10) Outdoor heart rate from EEG session (<ID number_Outdoor_pulse_from_eeg.mat>)

Same as Indoor pulse from EEG session (above).

(11) Indoor treadmill force plate session (<ID number_Indoor_force_plate.mat>)

The force plate .mat file contains a structure with 6 fields (variable name: Force_plate)

Force_plate.dataLabel: string including ID number, environment, and sensor type

Force_plate.dataArray: 3xNx2 matrix. Third dimension is for left and right force plates, respectively. Columns are frame numbers. Rows are:

• x, y, and z direction of force, in newtons

Force_plate.axisLabel: String headings for ‘dataType’ and ‘frame’ and ‘sensorNumber’

Force_plate.axisValue: 1x3 cell array of string headings for each row of data type

Force_plate.samplingRate: Sampling rate

Force_plate.dateTime: String of date and time information of recording

(12) EEG digitized head map (<ID number.sfp>)

Besa coordinates of all electrode positions.

(13) Indoor eye tracking video (<ID number_Indoor_eye_tracker.avi>)

The eye tracker .avi file is a video from the subject's perspective (640x480 resolution, 30 frames/sec)

(14) Outdoor eye tracking video (<ID number_Outdoor_eye_tracker.avi>)

The eye tracker .avi file is a video from the subject's perspective (640x480 resolution, 30 frames/sec)

(15) Indoor video camera (<ID number_Indoor_video_camera(#).avi>)

The camcorder .avi file is a video from the experimenter's perspective (704x384 resolution, 30 frames/sec). If there are multiple parts the (#) appended indicates the order.

(16) Outdoor video camera (<ID number_Outdoor_video_camera(#).avi>)

The camcorder .avi file is a video from the experimenter's perspective (704x384 resolution, 30 frames/sec). If there are multiple parts the (#) appended indicates the order.

Cortisol (Cortisol_all_subjects.xlsx)

Salivary cortisol data is provided as a single spreadsheet 'Cortisol_all_subjects.xlsx'. It contains the following variables:

- subid: ID number
- sex: 1 = male, 2 = female

- age: in years
- height: in inches
- weight: in pounds
- environment: 1 = outdoors, 2 = indoors
- ordererenvironment: 1 = outdoor first, 2 = indoor first
- orderstress: 1 = stress first, 2 = non-stress first
- condition: 1 = Initial sample taken before walking started, 2 = Baseline sample after baseline walking, 3 = Non-stress sample taken after non-stress condition, 4 = Stress sample taken after stress condition
- concentration: cortisol levels in µg/L
- cond_ordered = order of conditions by environment

Technical Validation

Data synchronization

All data collection devices (EEG, mobile eye tracker, IMUs, force plates, and heart rate monitor) were synchronized with custom software written in Labview to link with Biosemi (Figure 1b). Synchronization triggers from each device were marked in Biosemi in order to align each device in time with EEG.

HED Tagging

Hierarchical event descriptor (HED) tags are EEG semi-structured annotations used to provide categorized and detailed descriptors of events during an experiment (Bigdely-Shamlo et al, 2017). These events that are logged with a predefined, structured, and common annotated language across studies that use the HED system. Some of these events like button presses are tagged automatically in real-time during the experiment. But most other events were marked manually by an experimenter.

In order to recover events we relied on both videos and timestamps using the subject eye tracker and the handheld HD camcorder. To ensure accuracy a trained member would visually inspect

both video types for each subject and each environment watching frame by frame in order to obtain the most precise timing possible. Events were encoded in a spreadsheet correctly categorized and labelled with corresponding timestamps. Every session was reviewed a second time by a different staff member to ensure agreement of both event label and timing. If any disagreements occurred, a third, senior staff member would resolve the issue.

Once all events were recovered and reviewed, the timestamps of each event were encoded into the corresponding EEG file and stored in the 'EEG.event' struct to indicate the event name, category, and timing.

Generally, events to be tagged were categorized by priority as follows:

1) Critical

1A: Conditions (Baseline, Non-stress, Stress)

1B: Button presses (The HED tags differentiate correct from incorrect button presses)

1C: Flag looks (If a subject looked at a flag multiple times, each look was tagged)

1D: Audible feedback (e.g. siren to indicate missed flag)

1E: Voluntary subject actions related to the experimental procedure (e.g. subject opens mouth to receive the swab for the saliva sample)

1F: Technical errors (e.g. video projector playback skips during indoor trial)

2) Likely to be useful for analyses

2A: Terrain changes (e.g. downhill/uphill/flat, dirt, grass, rock, wood chips, boardwalk)

2B: Experimenter instructions (sound played to instruct subject to slow down or speed up their pace)

2C: Involuntary subject actions related to walking (e.g. subject stumbles over a tree root)

2D: Voluntary subject actions that are incidental, related to walking (e.g. subject walks around a mud puddle)

3) Not as likely to be useful for analyses

3A: Distractors (e.g., pedestrian runs down the trail, construction noise is heard)

3B: Involuntary subject actions not related to walking (e.g. subject sneezes)

3C: Voluntary subject actions that are incidental, not related to walking (e.g. subject lifts arm, subject scratches face, subject reads a road sign, subject drinks water, subject whistles)

Events hierarchy used primary and secondary categories shown in Table 3-1.

Table 3-1. Commonly used primary and secondary category types in HED tagging along with the most specific examples for each.

Primary Categories	**Secondary Category**	**Event**
1) Environmental Event	a) distracter	● Pedestrian passes ● Helicopter overhead ● Truck passes ● Animal crosses path
	b) terrain	● Downhill/uphill portion ● Puddle in path ● Subject trips on branch

2) Scenario Event	a) verbal cue	● Condition change [baseline/stress/non-stress] ● Directions ● Instructions ● Slow down/ speed up
	b) non-verbal cue	● Horn (stressor) ● Slow down/speed up ● Saliva swab
3) Behavioral Event	a) purposeful	● Saliva swab ● Subject speaks
	b) accidental	● Subject trips on branch ● Sneeze ● Cough
4) Technical Error	a) distracter	● Eye-tracker slipping ● Experimenter next to subject ● Video skips
	b) non-distracter	● Heart rate monitor falls off ear ● Trigger cord disconnects ● EEG software stops recording

EEG data

EEG was constantly monitored in real-time throughout the duration of the experiment. Any technical problems with individual channels were noted in a log. If a channel appeared noisy during testing an experimenter applied more gel without interrupting the subject when possible. Figure 3-4A (left=indoors, right=outdoors) shows an example of 5 seconds of EEG data from a

single representative subject during baseline walking for 7 common EEG channels across the head (FPz, Fz, Cz, Pz, Oz, C3, and C4).

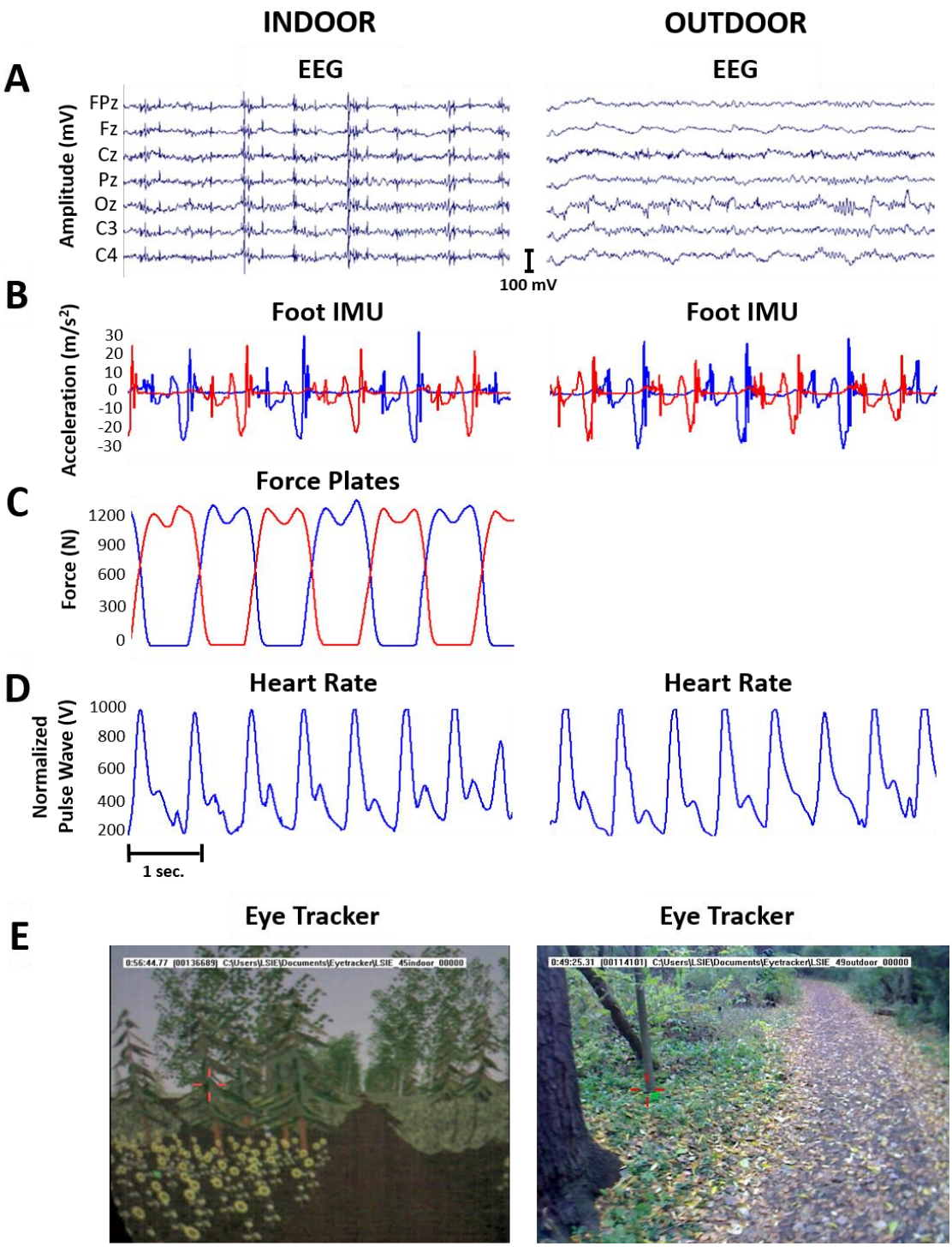

Figure 3-4: Example data from a single representative subject. Left column shows example indoor data and right column shows example outdoor data (5 seconds each) for (A) EEG, (B) both feet IMU z-axis accelerations (blue = left foot, red = right foot), (C) ground reaction forces of both force plates (blue = left foot, red = right foot), (D) pulse sensor heart rate, and (E) screenshot of subject's eye tracker video with crosshair in red indicating eye gaze.

Inertial Measurements Units (IMUs) and Ground Reaction Forces (GRF)

IMUs were placed in 6 locations (one on the top of the toe box of each foot, one around the ankle of each foot, one around the chest, and one around the waist). We found that the IMU on the top of the toe box provided the most reliable data for recovering gait events. In order to validate this we matched corresponding peaks in acceleration with known heel-strikes and toe-offs from the ground reaction forces of each force plate. Figure 3-4B shows the accelerations of the foot IMUs in the vertical direction (z-axis) aligned with force plate measurements (Figure 3-4C).

Cortisol

All samples were sent to a lab on campus using Salimetrics Assay kits. Results were given in concentration (µg/L).

Eye Tracking

Eye tracking videos were time synchronized with EEG data and aligned accordingly. Timestamps of eye tracking events were converted to match EEG sampling rate and encoded in the EEG.event struct as described in HED Tagging section.

Heart Rate

Pulse Sensor was linked to an Arduino logging data in real-time. The pulse sensor uses Pulse Transit Time (PTT), which is a measurement of the time it takes for the heart pulse wave to travel throughout your body. In application this measures the time between the R wave of an Electrocardiogram (ECG) against the pulse wave recorded with a Photoplethysmogram (PPG). The Pulse Sensor Amped software amplifies the raw signal of the previous Pulse Sensor, and

normalizes the pulse wave around V/2 (midpoint in voltage). The Pulse Sensor responds to relative changes in light intensity. If the amount of light incident on the sensor remains constant, the signal value will remain at (or close to) 512, the midpoint of Arduino's range.

For some subjects the Pulse Sensor data was not reliable and didn't provide reliable peak detection or showed clipping. In those cases, we recovered ECG heart rate peaks from EEG electrodes attached to the back of the neck.

Chapter 4 Fixation event-related potentials during free visual search while walking indoors on a treadmill and outdoors in the natural world

Abstract

Detecting targets with a visual search is an important, daily task relevant to the normal behavior of humans and other animals. In controlled laboratory studies on humans with scalp electroencephalography (EEG), there is a positive event-related potential (ERP) over the centro-parietal region occurring ~300 ms following the presentation of a target. As the laboratory studies have relied on stationary subjects in very controlled settings, it is less clear if the stereotypical event-related potential occurs in mobile, real world scenarios during visual search. We recorded mobile EEG and eye tracking on 34 healthy adults during walking while they performed a free viewing visual search task under two conditions: treadmill walking indoors with a virtual reality (VR) screen, and overground walking outdoors in a real world setting. Subjects were to press a button when they identified bright green flags (targets) and ignore dark green distractor flags (non-targets), both planted along their path. Using eye gaze fixations synchronized with EEG, we observed a significant fixation-event related potential (fERP) response across the centro-parietal brain areas when discriminating targets vs. non-targets in both indoor and outdoor environments. Our results provide an important step in extending cognitive neuroscience methods and insights on brain dynamics from past laboratory studies to real world applications.

Introduction

Searching a scene for an object of interest is a common occurrence in everyday life for humans and other animals (Eckstein 2011; Hopf et al. 2000). To provide insight into how the brain handles this aspect of active perception, scientists have studied visual search tasks for decades in the fields of psychology and cognitive neuroscience (Braun and Julesz 1998; Luck et al. 1993; Luck and Ford 1998; Sutton et al. 1965; Treisman and Gelade 1980). Past studies using electroencephalography (EEG) have shown that attention to visual targets can elicit sensory invoked activity in the brain known as event-related potentials (ERPs) (Luck et al. 1993). The ERPs are best identified by looking at changes in electrocortical activity time-locked to presentation of a stimulus (Luck 2005).

The P3 (sometimes referred to as the P300) component is an evoked electrocortical potential that occurs approximately 250-500 ms after a target or task-relevant stimulus has been presented (Patel and Azzam 2005; Ravden and Polich 1999). This P3 is of particular interest for wide-scale applications because it is relatively easy to detect and the amplitude is dependent on voluntarily controlled attentional processes. This makes it popular for analyzing changes in cognitive load (Debener et al. 2012; Polich 1987; Polich and Kok 1995) diagnosing neurological pathologies (Alonso-Prieto et al. 2002; Lagopoulos et al. 1998; Münte et al. 1997), and developing brain computer interfaces (BCI) (Brouwer et al. 2013; Farwell and Donchin 1988; Krusienski et al. 2006). However, most visual search implementations use computer screens flashing predefined targets while the subject looks straight ahead, fixating on the screen (Aziz-Zadeh et al. 2013; Brouwer et al. 2013; Katayama et al. 1987; Kazai and Yagi 1999; Thickbroom et al. 1991; Thickbroom and Mastaglia 1985).

Only recently have research studies employed visual search tasks using relatively natural scene conditions (Graupner et al. 2007; Kaunitz et al. 2014; Ossandon et al. 2010). Kaunitz and colleagues were able to combine EEG and eye tracking to compare the cognitive components of visual search in a traditional oddball task to a free viewing search of complex, natural images. They used fixation event-related potentials (fERPs) in which stimulus onset was synchronized to eye gaze fixation. Their findings indicate that fERP responses to target detection showed P3 components that behave similarly to ERP components across spatially unconstrained exploration of natural scenes. Up to this point these types of studies have all taken place in controlled laboratories indoors using computer screens. Little is known how those findings would translate to natural experiences in real world environments outside.

Advances in mobile EEG have recently enabled its use for functional brain imaging during human walking and running. The large size and high cost of devices for functional brain imaging scanners like positron emission tomography (PET), magnetoencephalography (MEG), and functional magnetic resonance imaging (fMRI) have limited their use for to studying subjects in laboratories in stationary positions. Technology for functional near-infrared spectroscopy (fNIRS) allows for quantification of mobile brain activity but its temporal and spatial capabilities limit its use (Meyerding and Risius 2018; Miyai et al. 2001; Suzuki et al. 2004) EEG has become the most commonly used imaging modality in mobile studies (Minguillon et al. 2017) as it has the advantage of maintaining a high temporal resolution for capturing events like ERP components. A few recent studies have demonstrated that an auditory oddball task can elicit a P3 component while walking or cycling outdoors (Debener et al. 2012; Scanlon et al. 2017; Zink et

al. 2016). However, using an auditory task still provides a very clean experimental paradigm as the stimulus timing is very clear relative to changes in electrocortical dynamics. The first studies to show that it was possible to quantify a P3 component with a visual oddball task during walking and running were published in 2010 (Gramann, Gwin, et al. 2010). They found using high density EEG with independent component analysis (ICA) and spatial filtering could clean EEG signals sufficiently to recover the negative ERP component at ~100 ms (called the N1) and the P3 component during a visual oddball task. A more recent study (De Sanctis et al. 2014) similarly used mobile EEG to quantify amplitude differences in the ERP components related to a Go/NoGo response-inhibition task while walking. These findings suggest that ERP components are robust enough to be captured in mobile situations in real world environments.

To bridge the gap between indoor, laboratory experiments and outdoor, real world settings previous studies have used virtual environments to simulate the outdoor experience (Cruz-Neira et al. 1992; Diemer et al. 2015; Holden 2005; Livingston et al. 2009; McCall and Blascovich 2009; Mine et al. 1997; Sandstrom et al. 1998). Virtual reality provides a naturalistic context in feature rich scenarios while still being able to work in controlled laboratory conditions. The combination of EEG and virtual reality is becoming more popular in research on the cognitive neuroscience of driving. One study (Chin-Teng Lin et al. 2007) recorded EEG during virtual reality automobile driving simulations and was able to demonstrate the effectiveness of single trial ERP analysis. Other studies (Mager et al. 2000; Pugnetti et al. 2001) have reported on the success of using EEG and ERPs to study attention and presence in virtual reality. Recently, EEG and virtual reality was used to show reliable ERP components in a language study (Tromp et al. 2018) with participants placed in a virtual restaurant. Based on the successful use of EEG and

virtual reality in these past studies, virtual reality could be a useful tool in exploring the cognitive neuroscience involved in visual search tasks and how ERP components are modified in more natural environments.

The goal of this study was to determine if mobile EEG and eye tracking could allow study of a similar P3 ERP component during free viewing visual search in both an indoor virtual reality environment and an outdoor real world environment. Based on previous evidence of fERP components eliciting P3 responses with free view visual search using natural images (Kaunitz et al. 2014) and P3 responses during a traditional visual oddball search while walking on a treadmill (Gramann, Gwin, et al. 2010), we hypothesized that we could resolve a fERP component near 300 ms in target discrimination for both the indoors and outdoors conditions. However, due to eye tracking sampling rate (30 Hz) limitations causing variable fixation onsets we believe there will be uncertainty in the exact time range at which a positive waveform occurs. An important aspect of the work is extending the mobile brain imaging methodologies to more naturalistic settings to determine how they have to be modified to work in the real world. The study also provides new insight into the brain dynamics while exploring natural, visual scenes.

Methods

Participants

We recruited forty-nine healthy adults (20 males, 29 females) between the ages of 18-45 (average age 22.7) to participate in this study. None of the participants had any history of neurological or physical impairments and were healthy enough such that they could walk on a treadmill and on outdoor terrain for at least one hour while carrying a fifteen-pound load without

issue. The University of Michigan Internal Review Board and the U.S. Army Institutional Review Board approved all study procedures and all participants provided signed consent before the start of the study. Due to the complex challenges involved with recording multiple data streams, synching, and calibration in mobile settings, 15 of the 49 participants were missing relevant data (e.g. eye tracker malfunction, inertial measurement units losing synch, etc.) for the full analyses proposed in this study. The results presented here are from 34 participants that had complete data sets.

Virtual reality (VR) environment

A large scale video of a 3D animated environment (designed in Google SketchUp) of a virtual park was displayed on a projector screen in a dark room directly in front of the treadmill (Figure 4-1A) set at 0.7 m/s while subjects walked at the same pace as the video. A total of 50 animated target flags (bright green) and 150 animated distractor, non-target flags (dark green) were displayed during the visual search task (Figure 4-1B). Target flag detection varied in difficulty based on the position relative to environmental objects as well as distance from path.

Real world environment

Subjects walked outdoors (Figure 4-1B) on a marked trail path at an arboretum (Nichols Arboretum, Ann Arbor, MI). The park and walking trail (Figure 4-2) was accessible to the public during testing. The path was approximately 2 miles long in distance and terrain varied between gravel, grass, and wooden planks. A total of 50 target flags (bright green) and 150 distractor, non-target flags (dark green) were placed along the trail path placed within 10 feet off the path and not higher than 10 feet off the ground. The flags were 2” x 3” trail marking flags attached to

a 15” pole (Figure 4-1B). They were placed in a way to be visible from the path without having to step outside the marked trail. Subjects were instructed to walk straight along the set path at a slow to moderate pace that matched the 0.7 m/s speed used on the treadmill. Subject were not allowed to stop walking at any point during the experiment. Auditory cues to speed up or slow down were given if necessary.

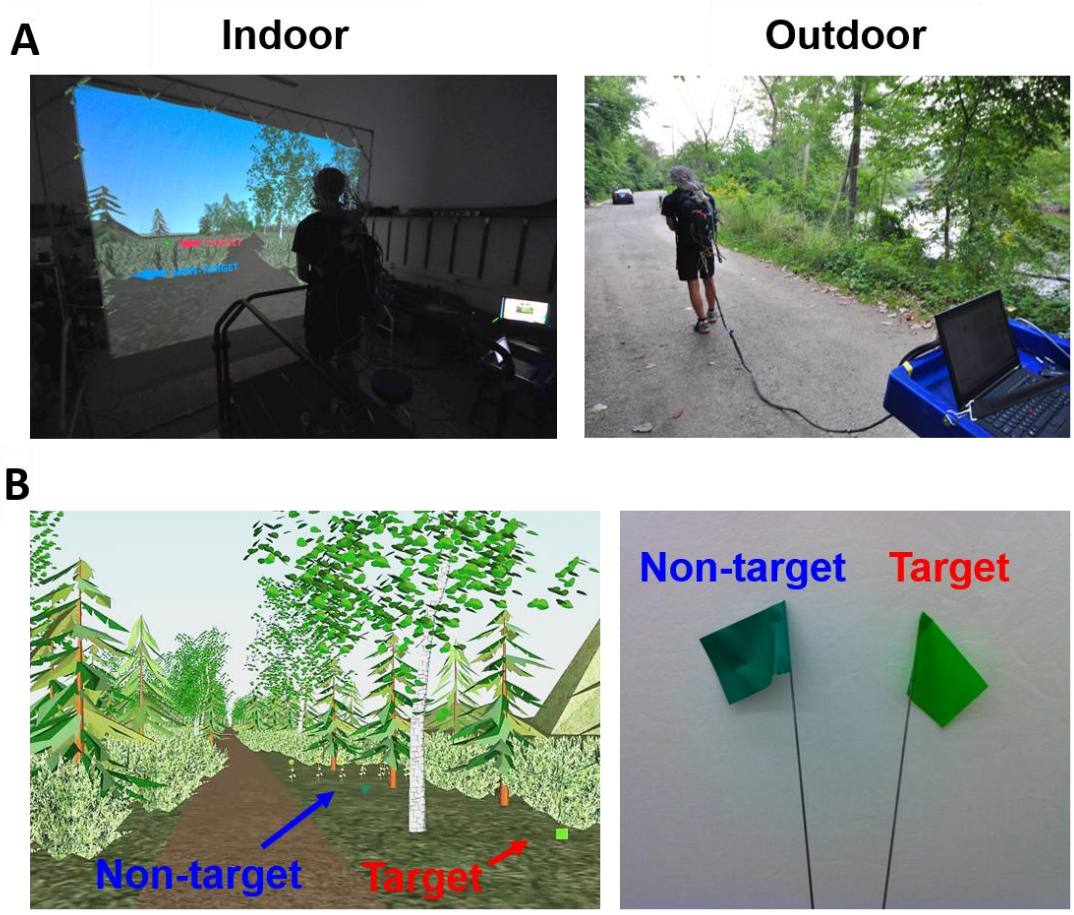

Figure 4-1. Indoor and outdoor environments with example flags. (A) Left panel shows an example subject standing on the instrumented, split-belt treadmill in front of the projector screen. Right panel shows an example subject walking along the outdoor path tethered to an experimenter by cables from measurements devices connected to a laptop on a tray. (B) Left panel shows a screenshot from the virtual environment with a non-target (dark green) and target (bright green) flag placed to the right of the walking path. Right panel shows a real non-target (dark green) and target (bright green) flag that were used for the outdoor environment.

Figure 4-2. Trail map for Nichols Arboretum, Ann Arbor, MI. Thick red line indicates walking path used for experiment. The trail started at point 1 and continued through points 2 and 3. Once subjects arrived near the river at point 7 they walked to the right toward point 6 and looped back around until continuing past point 7 until the end position at point 8. Total distance walked was approximately 2 miles.

Protocol

Subjects walked continuously for approximately one hour in each environment. The testing began with subjects normally walking for a 20 minute baseline condition in which no flags were present in the environment. The visual search task began immediately following the baseline condition. The goal of the task was to search and identify bright green flags (targets) and to ignore dark green flags (non-targets). Once target flags were identified subjects were instructed to press the button on a joystick they were holding. They were instructed to not press anything when they saw a non-target flag. We also asked subjects to fixate their gaze on all flags for at least 1 second when possible. The visual search task was completed in two conditions, 20

minutes each: 1) "*Non-stress*" - each correct flag identified earned an extra $0.25 toward compensation for the study and 2) "*Induced Stress*" - in addition to earning $0.25 per correctly identified target flag subjects were told they would be penalized $1.00 for every missed target flag and a loud siren was played immediately after the subject walked passed the unidentified target flag. Subjects were also given false negative siren noises indicating a missed target flag at random times (approximately once every 2 minutes, 10 times total). Subjects were naïve to the random penalties during the task, but were debriefed after the conclusion of all the experiments and were not penalized in compensations. The order of the two visual search conditions was randomized for each subject, but order remained constant for both indoor and outdoor environments.

Equipment and Data Processing

Instrumented treadmill

Subjects walked on an instrumented, split-belt treadmill (sampling rate: 1000 Hz; Bertec, Columbus, OH) with separate force transducers under each belt. Ground reaction forces using 6 degrees of freedom could be obtained from the left and right foot separately to determine gait events. Vertical ground reaction forces above 30 Newtons were marked as a heel strike and vertical ground reaction forces under 30 Newtons were marked as a toe-off for each foot.

Inertial measurement units

For both indoors and outdoors subjects wore 6 inertial measurement units (sampling rate: 128 Hz; APDM Opal, Portland, OR) attached to both feet, both ankles, waist, and chest. Each inertial measurement unit was used to monitor lower limb movements using 3D accelerometers,

gyroscopes, and magnetometers. We found that the inertial measurement units on the top of the toe box provided the most reliable data for recovering gait events and was validated by matching corresponding peaks in anterior-posterior acceleration with known heel-strikes and toe-offs from the ground reaction forces of each force plate. The gait events from the inertial measurement units were synced to the EEG data (Figure 4-3) and used in pre-processing for artifact detection removal.

Eye Tracker and stimuli detection

Each subject was fitted with Mobile Eye XG eye tracking glasses (sampling rate: 30 Hz; Applied Science Laboratory, Boston, MA) accurate within 0.5 to 1 degree (Figure 4-3). Before testing, eye tracker was calibrated indoors to ensure proper alignment. All eye tracking videos were examined off-line by reviewers trained to mark eye gaze fixation events to stimulus flags. All timestamps were confirmed by at least two different reviewers for consistency. Fixation events were determined when subjects held gaze for at least 0.5 seconds on a flag. Timestamps of eye tracking events were upsampled to match EEG sampling rate and labelled accordingly in the EEG data.

Statistical analysis of flag detection

Both indoor and outdoor environments had 50 bright green target flags and 150 dark green distractor flags (non-targets). A two-way repeated measures ANOVA was used to assess target identification accuracy with factors of environment (indoor vs outdoor) and stress condition (*non-stress* vs *induced stress*) using the order of environment and the order of stress condition as covariates.

EEG recordings

Subjects wore a high density, pre-amplified 256-channel EEG cap (sampling rate: 512 Hz; Biosemi Activetwo, Amsterdam, Netherlands) (Figure 4-3). Eight additional external sensors were placed on the neck of the subject to record neck muscle activity. Electrode positions relative to the subject's head were recorded using a 3D digitizer (Zebris, Germany). Electrode gel was placed underneath each sensor and all offsets were kept below 20 mV as recommended by Biosemi for optimal data quality. Offsets were checked between indoor and outdoor sessions and more electrode gel was applied if sensors went above 20 mV.

EEG Pre-processing

All EEG analyses were performed in MATLAB (The MathWorks, Natick, MA) using custom scripts based on EEGLAB (Delorme and Makeig 2004). EEG was first downsampled to 256 Hz and a high pass filter at 1 Hz was applied to remove drift. We re-referenced to the common average reference and the EEGLAB plug-in, Cleanline (https://www.nitrc.org/projects/cleanline/), was applied to remove 60 Hz line noise. To minimize the effects of gait-related movement artifact from the EEG data, we first removed EEG channels with activity highly correlated with the gait cycle as described by Anderson and colleagues (Oliveira, Schlink, David Hairston, et al. 2017). Briefly, individual channel activations were smoothed with a 128 point moving average filter and then epoched into individual gait cycles from right heel strike to right heel strike. The mean amplitude for each channel at each time point across all gait cycles was used to create an average waveform template. Then every individual gait cycle for each channel was cross-correlated against the average waveform template.

Individual channels which were highly correlated ($r > 0.4$) to the gait cycles for more than 75% of the total number of gait cycles were discarded. Further bad channels were identified and rejected using standard statistical thresholds (i.e., range, SD, kurtosis). For the remaining clean channels we applied adaptive mixture independent component analysis (AMICA 15) (J A Palmer et al. 2008; Palmer et al. 2006) using Principal Component Analysis to parse the data into 150 spatially fixed, maximally temporally independent component (IC) signals (Makeig et al. 1996) per subject. The DIPFIT function in EEGLAB (Oostenveld and Oostendorp 2002) was used to model each independent component as an equivalent current dipole within a boundary element head model based on the Montreal Neurological Institute standard brain (Quebec). We identified all sources indicative of eye blinks, eye movements, or muscle artifact (T.-P. Jung, Makeig, Humphries, et al. 2000) and marked them for removal. The remaining sources were back projected to the channel domain and clean EEG was re-interpolated to full rank.

Statistical analysis of event-related waveforms

Cleaned EEG data was analyzed using custom scripts based on ERPLAB and the Mass Univariate ERP Toolbox (Groppe, Urbach, and Kutas 2011). Continuous EEG data was split into indoor and outdoor environment conditions, low-pass filtered at 30 Hz, and epoched from -300 ms to 1000 ms around the onset of eye gaze fixation on a non-target or target flag as determined by the eye tracker. Any epochs with amplitude outside of +-75 uV were removed. To avoid potential eye movements before fixation, we chose a non-standard period from 0 to 100 ms after fixation onset as baseline and subtracted that activity for all epochs. Previous studies using eye gaze fixation as stimulus onset also used post-onset baseline activity (Hutzler et al. 2007; Rämä and Baccino 2010) for this purpose. Fixations to targets only included trials in which a correct

button response was given and did not include misses. Fixations to non-targets only included trials that were correctly ignored (correct rejections) and did not include trials in which the button was pressed (false alarms). All epochs were averaged for each subject and across all subjects for a grand average. To detect differences in waveform amplitudes between targets and non-targets we used a repeated measures, two-tailed t-tests at the average of time points between 250 and 400 ms at 6 scalp electrode sites (Fz, Cz, Pz, CP1, CP2, and Oz). We used the Benjamini & Yekutieli (Benjamini and Yekutieli 2001) procedure for the control of the false discovery rate (FDR) to assess statistical significance of each test using an FDR adjusted p-value level of 5%.

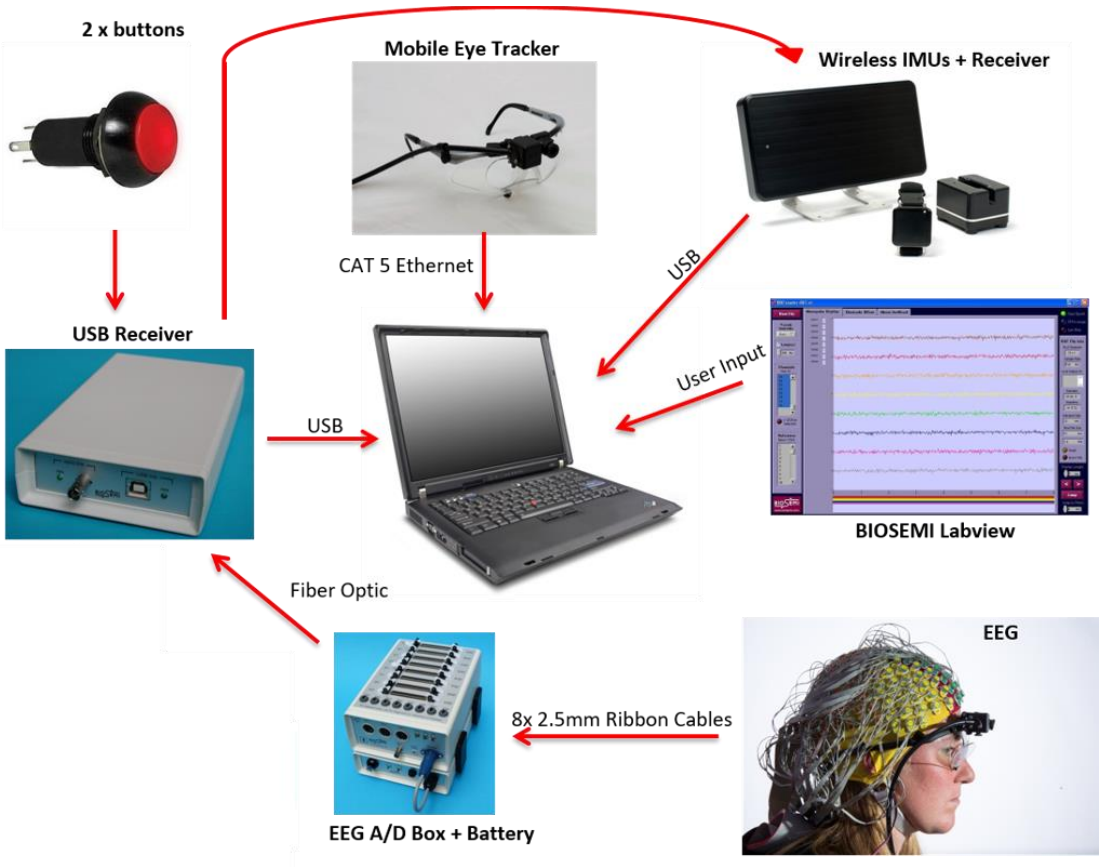

Figure 4-3. Layout of recording devices. Diagram shows how all devices were connected to each other for synchronization. EEG amplifier, battery, and USB receiver were placed in a backpack worn by the participant. Laptop and wireless inertial measurement unit (IMU) receiver were carried externally by an experimenter following the participant.

Results

Flag identification accuracy

There were no significant differences in the accuracy of the subject responses to the flags between stress conditions. There was a significant difference ($F = 8.59$, $p = 0.005$) between indoor accuracy (mean = 90.5% SD = 8.2%) and outdoor accuracy (mean = 84.2%, SD = 13.3%). Since the stress condition did not produce significant behavioral differences the proceeding statistical analyses combined trials from both *non-stress* and *induced stress* conditions together within each environment.

Analysis of fixation-event related potentials during visual search

After removing fixation events that did not fit within criterion, for 34 subjects the average number of target fixations indoors was 36.0 (SD = 11.0) and non-target fixations indoors was 93.0 (SD = 20.4). For outdoors, the number of average target fixations was 34.8 (SD = 11.7) and non-target fixations was 90.5 (SD = 29.1).

Fixation-event related potentials (fERPs) during indoor visual search showed a significant amplitude increase around 250 ms to 400 ms after fixation onset (Figure 4-4) for targets vs non-targets in both left (FDR adjusted p-value = 0.02) and right [False Discovery Rate (FDR) adjusted p-value = 0.001] centro-parietal areas, CP1 and CP2 (Figure 4-5). There were no significant amplitude differences in the midline frontal, central, or occipital areas. Similarly,

outdoor visual search showed a significant left centro-parietal (CP1) amplitude increase (FDR adjusted p-value = 0.04) for targets vs non-targets 250 to 400 ms after fixation onset. There were no significant fERP differences in frontal, central, centro-parietal (right), or occipital areas during outdoors. The average scalp topography (Figure 5) during the 250 to 400 ms period for both indoor and outdoor environments showed the activation patterns of amplitude increases originating in the central to parietal areas with low activation in the frontal region across targets and non-targets in both environments.

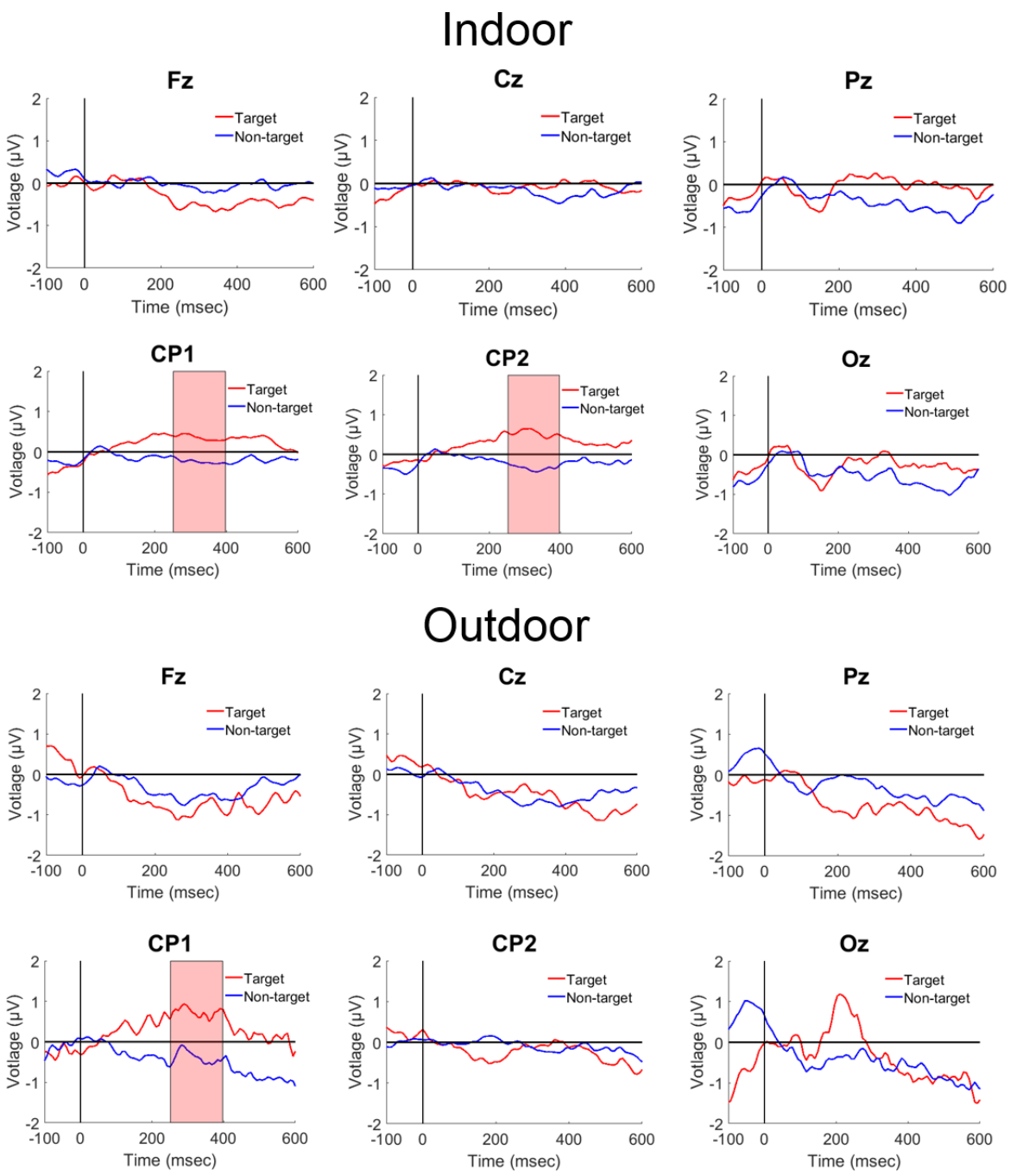

Figure 4-4. Grand average fixation-event related potentials (fERPs). Targets and Non-target flags shown for frontal (Fz), central (Cz), parietal (Pz), centro-parietal (CP1, CP2), and occipital (Oz) EEG channels during indoor (top) and outdoor (bottom) visual search. Stimulus onset represents eye gaze fixation on Target or Non-target flags. Shaded red boxes around 250-400 ms represents time periods of significant (FDR adjusted p-values < 0.05) increases in amplitude for Target vs Non-target trials.

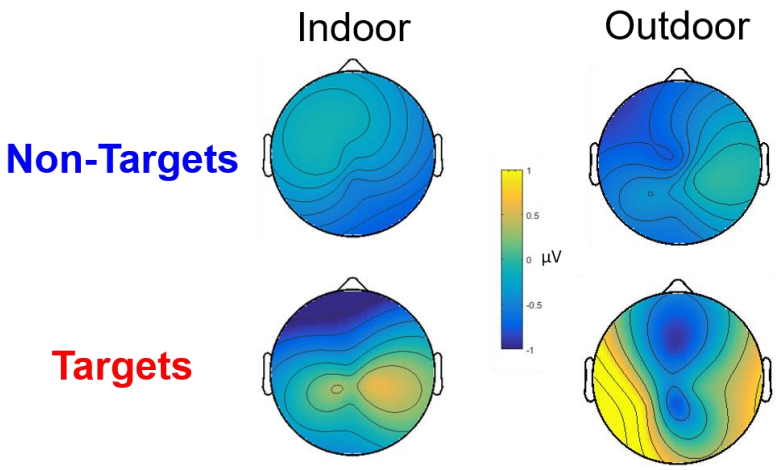

Figure 4-5. Grand average fixation-event related potentials (fERPs) between 250-400 ms scalp topographies. Centro-parietal cortical activations during indoor (left) and outdoor (right) visual search. Non-targets (top) showed little activation across the entire scalp while Targets (bottom) showed significant amplitude increases across the central and parietal regions.

Discussion

We were able to identify fixation based amplitude increases in walking human subjects performing a free viewing visual search task both indoors in a virtual reality environment and outdoors in a real world environment (Gramann, Gwin, et al. 2010). A previous study (Kaunitz et al. 2014) of stationary subjects found that fixation-event related potentials (fERPs) can be recovered during free viewing visual search of natural scenes. That study was done with a computer based test and subjects were sitting, not moving through their environment. Gramann and colleagues (Gramann, Gwin, et al. 2010) were able to recover P3 ERP components using a visual oddball task while walking on a treadmill across different speeds. However, they did not use eye tracking and instead relied on a stimulus presentation on a computer screen that subjects were fixated on. To the best of our knowledge, no other study has attempted to measure EEG ERPs in a free viewing visual search with natural scenes walking on a treadmill and fully mobile outdoors in an uncontrolled public space. Our results demonstrate that using mobile EEG in

combination with a mobile eye tracker could be successful in identifying target vs. distractor event-related components across centro-parietal regions in fERPs during a free viewing visual search task. These amplitude increases around 300 ms were present when subjects walked inside a laboratory on a treadmill in a virtual environment as well as in an uncontrolled, real world environment.

The primary goal of this study was to determine if ERP components could be detected in free viewing visual search as it is a robust electrocortical response used for many purposes in basic, applied, and clinical research. Many previous EEG studies have used various discrimination tasks such as serial visual presentation, attentional blink, or oddball paradigms to demonstrate that targets and distractors are best separated by the P3 component evoked potential (Hillyard et al. 1973; Kranczioch, Debener, and Engel 2003; Polich and Kok 1995). We chose to focus on this later fixation-event related component to minimize contamination by eye movements in earlier periods. Our recording equipment was not able to account for microsaccades, which have been suggested to be correlated to ongoing brain activity (Martinez-Conde, Otero-Millan, and Macknik 2013). Another study (Brouwer et al. 2013) also looked at P300 fixation-related potentials (FRPs) in a visual target search task and demonstrated that the P300 component was reliably distinguished between target and nontarget fixations. To rule out the possibility of eye movement contamination they used machine learning on both EEG and electrooculogram (EOG) and found that EEG classification performance was significantly higher for discriminating target vs nontargets than EOG performance. Another challenge related to our device limitations was the relatively low sampling rate of our eye tracker (30 Hz). Due to the low sampling rate, there may be deviations in precise time locked fixations which could account for our waveform results not

showing stereotyped positive/negative fluctuations as is common in traditional ERP studies. The loss of precision in time-locked fixations might have smeared the waveform patterns that were expected. However, the significantly increased amplitudes we found after 250 ms were in agreement with the stereotyped amplitude increases found in typical P3 waveforms from ERP studies.

Using a free viewing task also made this challenging to compare our results using earlier ERP components such as P1 (positive peak at 100 ms), N1 (negative peak at 150 ms), and P2 (positive peak at 200 ms). We chose to align our fixation events to saccade offset knowing that earlier components influenced by presaccadic spike, premotor negativity, and premotor positivity (Jagla and Riecansky 2007; Thickbroom et al. 1991; Thickbroom and Mastaglia 1985) would be washed out. One study (Kaunitz et al. 2014) that directly compared free viewing fERPs to traditional oddball ERPs found that the first 250 ms were equivalent in latency and amplitude for targets and distractors. They also found that only the P3 response was robust enough for target detection, which occurred after ~300 ms. In their study, they showed that the P3 component had a maximum amplitude over the parieto-central areas in the free viewing condition, which was in line with our findings in CP1 and CP2 electrodes. However, we were not able to find similar midline frontal (Fz), central (Cz), or occipital (Oz) P3 differences that they and other studies (Brouwer et al. 2013; Kamienkowski et al. 2012; Kaunitz et al. 2014) have found in free viewing visual search. This could be due to our EEG cleaning methods and removal of source components determined to be eye movements and muscle artifacts, which are often located in the frontal and occipital areas, respectively (Gramann, Gwin, et al. 2010).

Another challenge of experimenting in uncontrolled environments is that we can't account for the outside sources that might affect temporal modulation of attention during free viewing. Some studies (Corbetta et al. 1998; Melcher and Colby 2008) have shown that high attentional engagement is naturally present in free viewing from fixation onset or earlier. This may account for the differences we found between our indoor and outdoor experiments. The indoor experiment showed much more consistent fERP waveforms across the scalp with less variability. The indoor environment was in a dark room in which the subjects were not able to view anything in the room other than the projection screen ahead. The outdoor environment took place in a public park with lots of external stimuli that may have split attentional resources and lowered engagement to the visual search task. Previous studies have shown that the level of temporal attention affects both the amplitude and the latencies of N2 (Correa et al. 2006) and P3 components (Miniussi et al. 1999). It is possible that our P3 findings outdoors were just more variable due to the completely novel nature of conducting this experiment in public. We acknowledge the need for more work comparing attentional differences in public settings when conducting goal-directed tasks like visual search.

One of the most difficult aspects with using EEG in mobile situations is potential contamination from noise sources. Several previous studies have reported on spectral and time-frequency analyses during locomotion (Artoni et al. 2017; Bradford et al. 2016; Bruijn et al. 2015; Bulea et al. 2015; Castermans et al. 2012; Gwin et al. 2011; Kline et al. 2014a; Severens et al. 2012; Sipp et al. 2013). One study (Castermans et al. 2014) examined the harmonics present in EEG electrodes and accelerometer spectra and determined that stepping frequency may pollute EEG signals depending on walking speed. Another study (Kline et al. 2015) designed a study using a

nonconductive cap over a simulated electrically conductive scalp (e.g. wig) in locomotion in order to characterize movement related artifacts recorded by EEG electrodes. The findings from these studies have suggested that EEG can be affected by movement related artifact that shows up in time-frequency analyses and varies across different walking speeds and affects individual subjects differently that must be taken into consideration when designing mobile EEG experiments. However, both of these studies concluded that artifact caused by locomotion was tied directly to stepping frequency, particularly at higher walking speeds. The conclusions from these studies suggest that analyzing EEG synchronized to cognitive tasks rather than the gait cycle is much less likely to have substantive motion artifacts affecting the results. In order to minimize the potential for noise artifacts, the present study used slow walking speeds (0.7 m/s) and careful pre-processing methods were applied to remove EEG channels that were most highly correlated with the gait cycle (Oliveira, Schlink, David Hairston, et al. 2017). As in many previous studies, we also used ICA decompositions to remove non-neural sources from the EEG channel data before ERP analysis. Because we analyzed electrocortical data synchronized to a visual search cognitive task and not synchronized to the gait cycle, it greatly attenuated the motion artifact effects. Gramann and colleagues (Gramann, Gwin, et al. 2010) studied P3 responses during treadmill locomotion in walking speeds up to 1.25 m/s with a similar approach. The variability in our EEG results for the outdoor condition might be related to gait differences when navigating complex terrain outdoors rather than smooth, flat terrain on a treadmill. Further work should investigate the differences in walking patterns used indoors on a treadmill compared to outdoors over ground while using neuroimaging devices like EEG.

Conclusions

As mobile brain imaging technology has become more portable and affordable, researchers have expanded their use of functional brain imaging during walking and running. Taking the studies into the real world is inevitable as the technology continues to progress. The P3 event-related potential component is one of the most studied brain electrocortical responses in cognitive neuroscience, but there is little understanding of how natural environments affect the P3 and brain dynamics in general. In order to provide additional insight into how the brain functions in real world situations, it is necessary to extend research study paradigms from traditional stationary computer tasks in a laboratory to ecologically valid tasks such as visual searches in more natural settings. We were able to use mobile EEG with simultaneous eye tracking to detect a similar amplitude increase around 250 to 400 ms after fixation for discriminating target stimuli that was consistent in virtual reality as well as outdoors. These methods and results provide a step forward to realizing the future of mobile brain imaging in the real world (Gramann et al. 2011, 2014).

Chapter 5 Mobile brain-body locomotion dynamics of indoor treadmill walking in a virtual environment vs outdoor walking in real world during visual search

Abstract

To understand brain and body dynamics in the real world, it is necessary to move research studies outside of traditional laboratory environments. Advances in mobile brain and body imaging (MoBI) using electroencephalography (EEG) and signal processing techniques have provided new opportunities for studying mobile subjects in real world situations. We recorded EEG, eye tracking, heart rate, salivary cortisol, and gait kinematics in healthy adults walking both indoors using virtual reality on a treadmill and outdoors in an arboretum while completing a visual search task. Heart rate, cortisol concentration, and gait kinematics showed significant behavioral differences between normal walking and visual search walking. We used independent component analysis and source localization to identify four neural sources in left and right sensorimotor cortices, anterior cingulate, and posterior parietal area. All clusters showed significant increases in theta (4-7 Hz) power during visual search walking compared to normal walking as well as increases in alpha (8-12 Hz) and beta (13-30 Hz) power synchronizations and desynchronizations in outdoor walking compared to indoors for all conditions. These findings suggest that mobile brain and body imaging is a feasible tool for studying locomotion and there are many differences in both behavioral and neural measures between controlled settings indoors in a laboratory and outside in a natural environment.

Introduction

Everyday life often requires walking in varying terrains and environments while searching a scene for an object of interest (Eckstein 2011; Hopf et al. 2000). However, understanding how the brain and body coordinate those efforts is not well understood due to limitations in technology (Minguillon et al. 2017). Recently, a new field of mobile brain and body imaging (MoBI) has emerged with promising results showing ways to study these complex motor tasks (Gramann et al. 2011; Kranczioch et al. 2014; Malcolm et al. 2015; Ojeda, Bigdely-Shamlo, and Makeig 2014; De Sanctis et al. 2014). By combining portable, multi-modal biometric devices we can now do research studies outside of traditional laboratory settings and start to understand the ways in which the brain and body function in real world situations.

One of the recent developments for making mobile neuroimaging possible has been the combination of better hardware systems with advanced signal processing methods. Traditionally, neuroimaging has been confined to indoor studies due to the large size and high cost of scanners like positron emission tomography (PET), magnetoencephalography (MEG), and functional magnetic resonance imaging (fMRI) that require subjects to be in stationary positions. Recently, other neuroimaging technologies have been proposed as useful tools to examine brain activity in mobile settings using portable devices like functional near-infrared spectroscopy (fNIRS) (Meyerding and Risius 2018), and EEG (Debener et al. 2012). EEG is increasingly becoming more common in mobile research (Minguillon et al. 2017) as it has the advantage of maintaining a high temporal resolution for capturing the dynamics in locomotion. Many recent studies have shown that EEG combined with independent component analysis (ICA) can be used to understand how the brain functions during locomotion (Bradford et al. 2016; Bruijn et al. 2015;

Bulea et al. 2015; Castermans et al. 2012; Gramann et al. 2011; Gwin et al. 2011; Kline et al. 2014a; Lau et al. 2014; Oliveira, Schlink, Hairston, et al. 2017; Petersen et al. 2012; Presacco et al. 2011; Seeber et al. 2015; Sipp et al. 2013; Wagner et al. 2016; Wieser et al. 2010). One of the first studies using these techniques showed anterior cingulate, posterior parietal, and sensorimotor electrocortical sources were involved in locomotion by creating significant intra-stride fluctuations in spectral power during normal treadmill walking (Gwin et al. 2011). Since then, more studies have emerged to show gait dynamics in other complex locomotion tasks using EEG. Walking on an inclined treadmill showed an increase in theta (4-7 Hz) power compared to normal walking in anterior cingulate, posterior parietal, and sensorimotor areas (Bradford et al. 2016). Level walking showed there was greater gamma (30-70 Hz) power for the left sensorimotor and anterior cingulate areas. One study looked at EEG of active treadmill walking in which the speeds of the belts were constantly adjusted based on the pelvis position and swing foot velocity and found that the left and right sensorimotor areas showed increased desynchronizations in mu (8-13 Hz) and beta (14-30 Hz) frequency (Bulea et al. 2015). The prefrontal and posterior parietal cortices also showed phasic low gamma (30-50 Hz) power increases during double support and early swing phases of the gait cycle. Other studies are investigating the mechanism of balance and control. One study showed that subjects walking on a treadmill connected to elastic cords displayed significant increases in high beta band (~17 Hz) power around contralateral push off in the left premotor area (Bruijn et al. 2015). Another group used a balance beam on a treadmill to show an increase in theta (4-7 Hz) power in anterior cingulate, anterior parietal, superior dorsolateral-prefrontal, and medial sensorimotor area compared to normal treadmill walking (Sipp et al. 2013), while left and right sensorimotor areas had significantly less beta (12-30 Hz) power on the balance beam compared to normal walking.

These previous mobile locomotion studies have taken place in a controlled laboratory using treadmills, and little is known how the neural dynamics of gait relates to the experiences outdoors in the real world. More recently some groups have started using virtual reality as a way to simulate outdoor, real world situations within a traditional laboratory (Cruz-Neira et al. 1992; Diemer et al. 2015; Holden 2005; Livingston et al. 2009; McCall and Blascovich 2009; Mine et al. 1997; Sandstrom et al. 1998). Virtual reality can provide a naturalistic context in feature rich scenarios while maintaining control within a laboratory environment. Some researchers are exploring the usefulness of virtual reality in the context of gait rehabilitation. One study used stroke patients to show that virtual reality can be used for gait training to augment walking speed and community ambulation compared to a control group that received only normal treadmill training (Yang et al. n.d.). Another study used a virtual reality based soccer scenario to provide interactive elements for engaging patients during robot assisted treadmill training which produced motor output effects similar to the outcome effects using verbal instructions from a therapist (Brütsch et al. 2010). Treadmill training and virtual reality was also used in another study with Parkinson's patients to show improvements in walking speeds (Mirelman et al. 2011). One study incorporated EEG and virtual reality with a balance beam to show that while virtual reality does provide a realistic experience it can also impair physical and cognitive performance during balance (Peterson, Furuichi, and Ferris 2018). Another study incorporated both EEG and virtual reality in the context of navigation to show theta power oscillations (4-8 Hz) are linked to spatial navigation while moving through a virtual maze (Bischof and Boulanger 2003). While there are many studies trying to use virtual reality and locomotion to provide applications in rehabilitation, none have directly examined the neural correlates of gait within this context.

The primary aim of this study was to use virtual reality and EEG to investigate the electrocortical dynamics related to gait as well as further explore how those findings relate to locomotion outdoors in a natural setting. One recent study showed that using mobile EEG outdoors is possible and conducted a dual-task experiment with subjects walking outdoors while either talking or texting to see how cortical gait dynamics changed compared to normal walking (Pizzamiglio et al. 2017). They found that walking while talking showed an increase in theta (4-7 Hz) and beta (15-30 Hz) power across left-frontal and right parietal regions and that walking while texting showed a decrease in beta power across frontal-premotor and sensorimotor cortices compared to the walking and talking condition. However, while this study was conducted outdoors it did not compare results to an indoor control condition or use source localization to investigate the neural sources for locomotor control. To the best of our knowledge this current study is the first to use high density EEG both indoors in virtual reality and outdoors in the real world.

A secondary aim of this study was to examine the stress response using EEG along with multi-modal measurement devices in both the indoor and outdoor environments. Stress is a challenging component to quantify and many approaches have been used in the past. Behavioral response to stress is known to increase production of the cortisol hormone by the hypothalamus-pituitary-adrenal axis (Tsigos and Chrousos 2002). Blood or urine can be used to measure cortisol levels but those methods are invasive. Cortisol concentrations can also be done through saliva excretion in subjects. Salivary cortisol has been known to be a reliable indicator of levels of free cortisol in the body (Hellhammer, Wüst, and Kudielka 2009). Many past studies have effectively elicited an

increase in salivary cortisol in laboratory testing (Dickerson and Kemeny 2004). They reviewed common categories of stress-inducing tasks which include social-evaluative threats, motivated performances and uncontrollability (Dickerson & Kemeny, 2004). One drawback to the salivary cortisol approach is its variability between individuals in its onset after a stressor (Hellhammer et al. 2009). It has been shown that individual cortisol trajectories can vary and that some individuals can experience an elevated cortisol level up to 100 minutes after an acute stressor in laboratory (Admon et al. 2017). Also, many of these studies focus on mental stress in stationary settings. Little is known about mobile subjects engaged in physical and mental tasks, and the relationship between exercise and cortisol is unclear (Hill et al. 2008).

Heart rate variability (HRV) has also been used in laboratory as an indicator of acute stress in subjects (Thayer et al. 2012). Studies have shown that reduced variability in inter-beat intervals is an indicator of a disturbance of the autonomic nervous system and thus a potential sign of mental stress (Clays et al. 2011; Taelman et al. 2008). Power spectral analysis of these inter-beat intervals helps us understand the mechanism of the autonomic nervous system during a stress response. Low frequency bands are associated with the sympathetic nervous system, the system that is activated during a stressor, while high frequencies are associated with the parasympathetic nervous system activity, which tends to be suppressed during stress (Taelman et al. 2008). However, heart rate variability measures can be conflicting and can vary depending on the type of paradigm being used (Schlink et al. 2017).

The overall goals of this study were to use brain and body imaging to determine the neural correlates of gait as well as the stress response and how they change in a laboratory indoors and

an arboretum outdoors. In order to mimic daily life challenges we chose to use a visual search task while walking. Visual search is a common paradigm used across the fields of psychology and cognitive neuroscience (Braun and Julesz 1998; Luck et al. 1993; Luck and Ford 1998; Sutton et al. 1965; Treisman and Gelade 1980) for its relationship to active perception. Our hypotheses were that 1) EEG can be used to capture the cortical dynamics of walking in sensorimotor, anterior cingulate, and posterior parietal areas using independent component analysis and source localization, and 2) gait dynamics and the stress response would vary by environment and task. By using similar tasks indoors in a laboratory on a treadmill with virtual reality, and outdoors in an arboretum on natural terrain, this study provides new insights into the challenges faced conducting brain and body imaging studies in the real world.

Materials and Methods

Participants

This study consists of forty-nine healthy adults (20 males, 29 females) between the ages of 18-45 (average age 22.7). All participants were required to be free of any history of neurological or physical impairments and be in good enough shape that they could walk on a treadmill one hour while carrying a fifteen-pound load without issue. Both the University of Michigan Internal Review Board and the U.S. Army Institutional Review Board approved all study procedures and all subjects provided signed consent prior to participating in the study.

Testing Environments

Virtual reality environment

We designed a 3D animated environment (Figure 5-1A) using Google SketchUp to simulate a virtual park that was displayed as a video on a projector screen directly in front of the treadmill (Figure 5-1B) set at 0.7 m/s moving at the same pace as the video. Within the virtual landscape, there were a total of 50 animated target flags (bright green) and 150 animated non-target flags (dark green) split evenly between the *non-stress* and *stress* conditions (described below) (Figure 5-1A). All experiments started with a 20 minute baseline condition in which no flags were displayed. The placement of the target flag locations as well as their position relative to environmental objects were meant to simulate how flags were placed in the real world environment.

Real world environment

Subjects walked outdoors on a marked trail path (Figure 5-1B) at an arboretum (Nichols Arboretum, Ann Arbor, MI) while open to the public. The trail path was well marked and varied in terrain (e.g. gravel, wood chips, board walk, grass, mud, etc.) for approximately 2 miles (Figure 5-2). A total of 50 target flags (bright green) and 150 non-target flags (dark green) split evenly between the *non-stress* and *stress* conditions. The flags were 2" x 3" attached to a 15" pole (Figure 5-1A). During the first twenty minute baseline walking condition no flags were present. Subjects were instructed to walk straight along the path at a slow to moderate pace matching the indoor treadmill speed (0.7 ms/s) and were not allowed to stop walking at any time during the experiment. Auditory cues given by the experimenter were used to control the speed of the subject if necessary. Flags were placed within 10 feet off the marked path and not placed higher than 10 feet off the ground. All flags were visible from the trail as subjects were not allowed to deviate from the path.

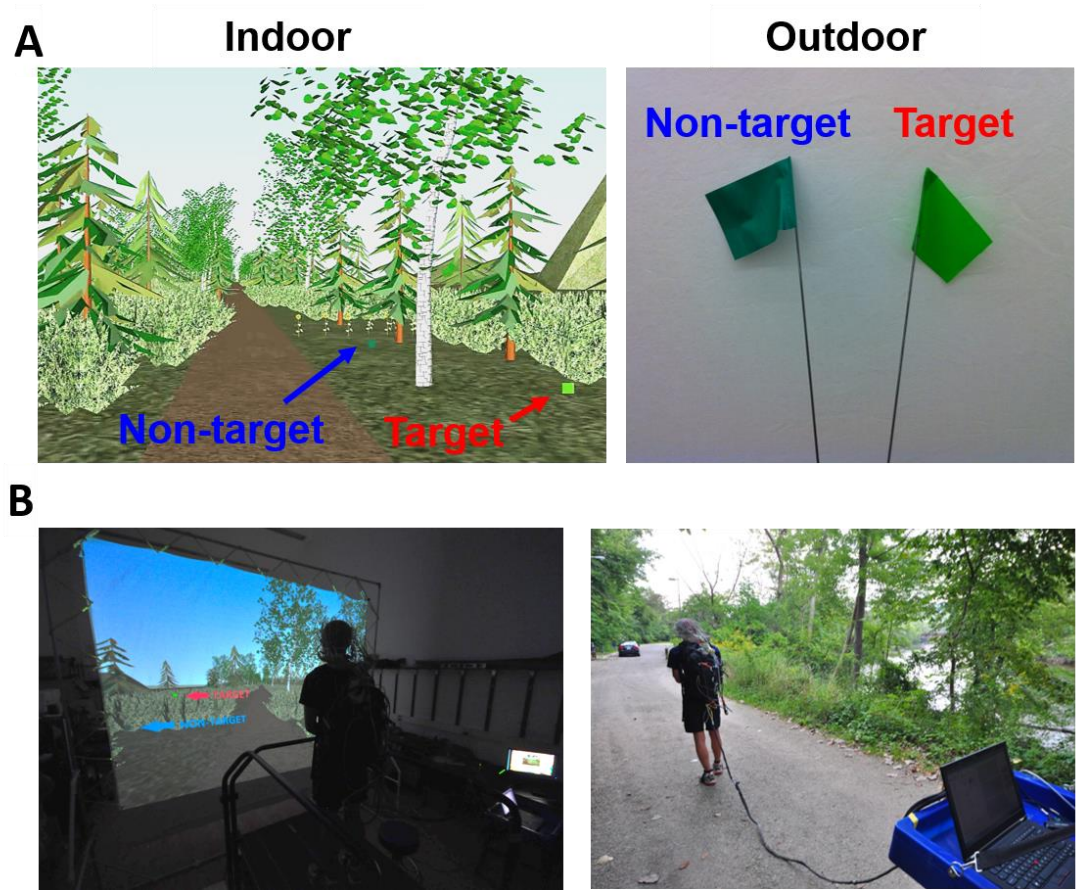

Figure 5-1. Indoor and outdoor environments with example flags. (A) Left panel shows a screenshot from the virtual environment video with a non-target (dark green) and target (bright green) flag placed to the right of the walking path indicated by arrows. Right panel shows a real non-target (dark green) and target (bright green) flag that were used for the outdoor environment. (B) Left panel shows an example subject standing on the treadmill in front of the projector screen. Right panel shows an example subject walking along the outdoor path with an experimenter carrying a laptop on a tray monitoring all measurement devices.

Protocol

Environment order was randomized across subjects and both consisted of the same walking and visual search conditions. First, subjects always started with a 20 minute baseline walking condition in which no flags were present in the environment. After baseline walking was complete the visual search task began immediately without interruption. The goal of the task was

to search for bright green flags (targets) within the environment and to ignore distractor dark green flags (non-targets). Subjects were instructed to press a button using a joystick when they saw a target bright green flag and to ignore (not press anything) when they saw a non-target dark green flag. We asked subjects to hold eye gaze fixation for at least one second on all flags when possible. The visual search task was split into 2 conditions, ~20 minutes each: 1) Normal (referred to as "*non-stress*") – subjects were told each correct flag identified would earn an extra $0.25 toward their compensation for the study completion and 2) Induced Stress (referred to as "*stress*") - in addition to earning $0.25 per correctly identified target flag subjects were also told they would be penalized $1.00 for every unidentified (missed) target flag and a loud siren was played by the experimenter immediately after the subject walked passed the unidentified target flag. To further induce stress, subjects were given random false negative siren noises indicating a missed target flag (approximately once every 2 minutes, 10 times total) regardless of task performance. Subjects were naïve to the random penalties during the task, but were debriefed after the completion of all experiments. The 20 minute baseline walking condition was always first, but the order of the 2 visual search conditions (*non-stress* and *stress*) was randomized.

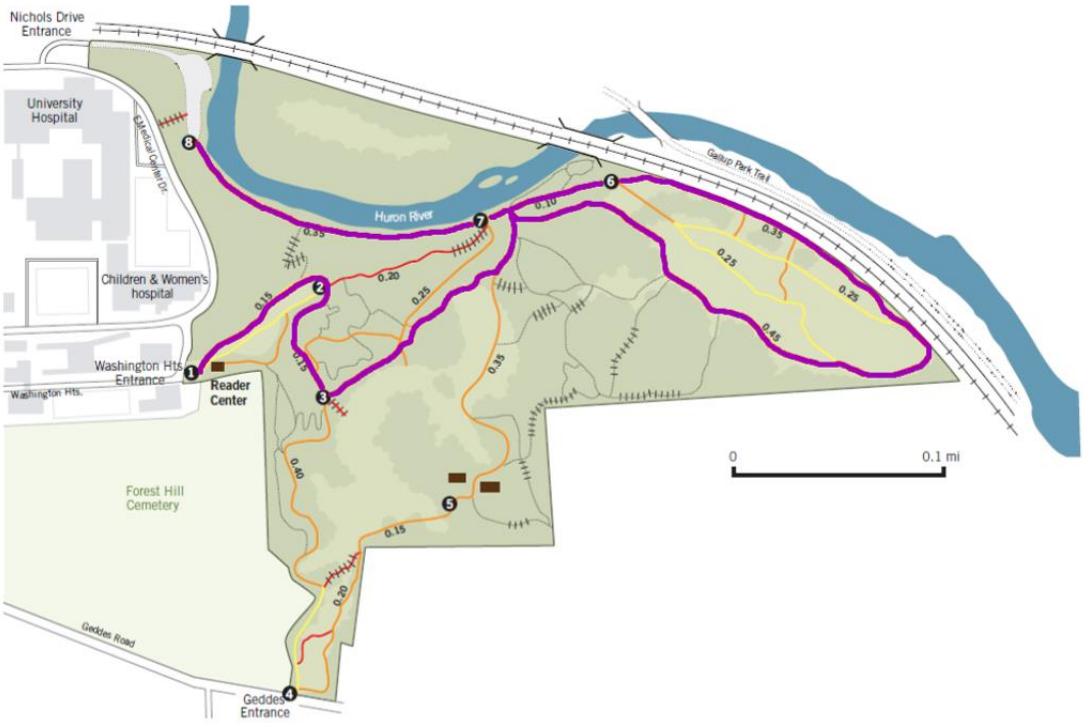

Figure 5-2. Trail map for Nichols Arboretum, Ann Arbor, MI. Thick purple line indicates walking path used for experiment. The trail started at point 1 and continued through points 2 and 3. Once subjects arrived near the river at point 7 they walked to the right toward point 6 and looped back around until continuing past point 7 until the end position at point 8. Total distance walked was approximately 2 miles.

Equipment and Data Processing

Instrumented treadmill

Subjects walked on an instrumented, split-belt treadmill (sampling rate: 1000 Hz; Bertec, Columbus, OH) consisting of two separate belts, each with its own motor, for the left and right side of the walking surface. Each belt contained separate force transducers which were used for the collection of 6 degrees of freedom ground reaction forces from the left and right foot separately. We used a threshold of 30 Newtons vertical ground reaction force to mark heel strikes and toe-offs for each foot.

Inertial measurement units

Subjects wore 6 inertial measurement units (sampling rate: 128 Hz; APDM Opal, Portland, OR) attached to both feet, both ankles, waist, and chest for both indoor and outdoor environments (Figure 3A). Each inertial measurement contained 3D accelerometers, gyroscopes, and magnetometers. We used the gait events determined from the instrumented treadmill ground reaction forces to align with the inertial measurement units. The inertial measurement units on the top of the toe box provided the most reliable data for matching gait events to the treadmill using peaks in anterior-posterior acceleration. The gait events from the inertial measurement units were recovered from the outdoor experiment and were synced to the EEG data (Figure 3B) and used in pre-processing for artifact detection removal. Stride duration was computed by taking the average stride time (right heel strike to right heel strike) across all gait cycles within each condition.

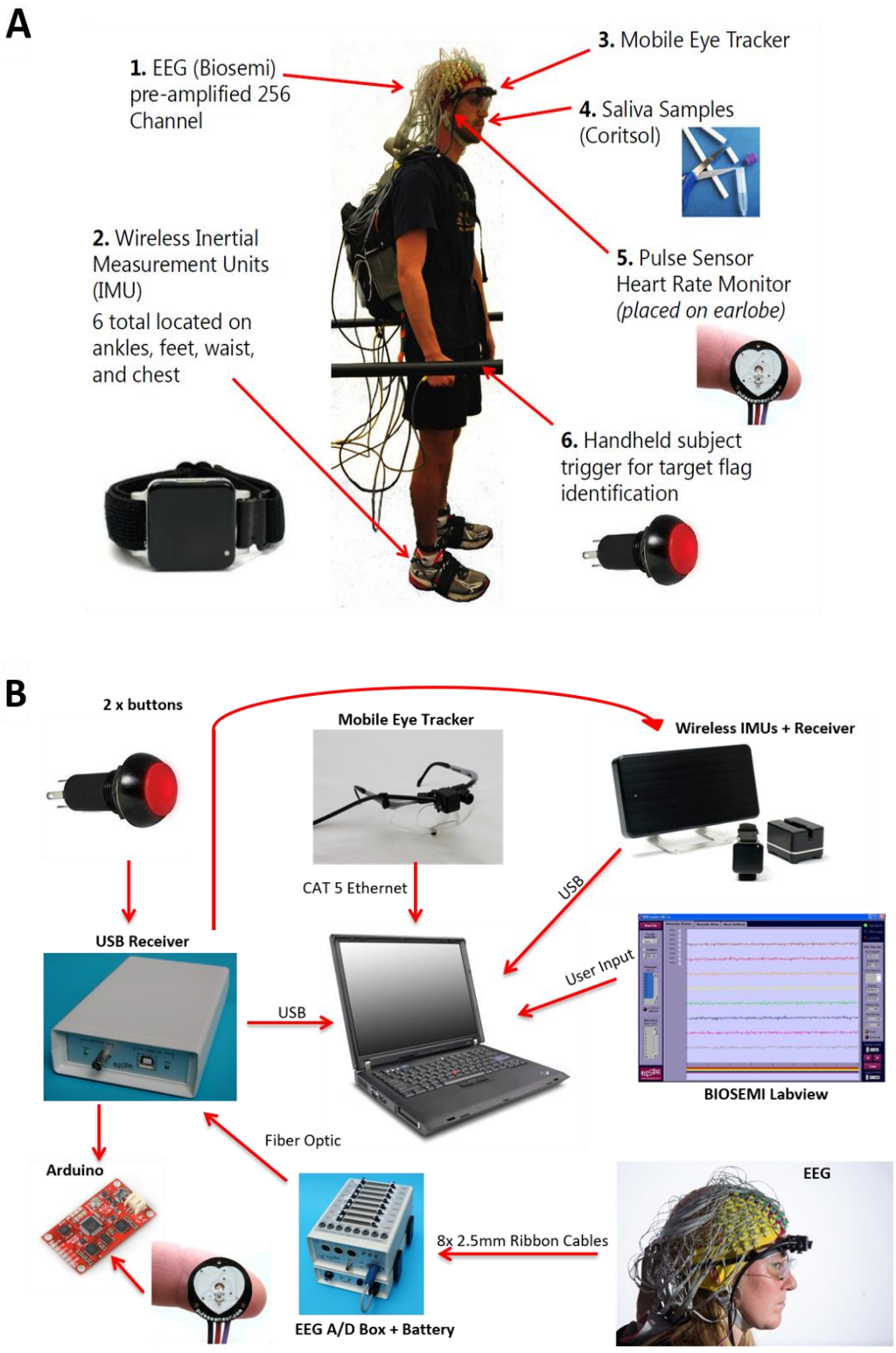

Figure 5-3. Layout of all recording devices shown on example subject. (A) All measurement devices and position of each placed on an example subject. (B) Layout of recording devices and how they were connected to each other for data collection. The EEG A/D box, battery, EEG

USB receiver, Arduino, and mobile eye tracker were all contained into backpack worn by subject. The laptop and wireless IMU receiver were carried externally by an experimenter following behind the subject.

Cortisol

The SalivaBio Oral Swab saliva collection method was used to obtain salivary cortisol samples (Salimetrics, Newmarket, UK) from all subjects (Figure 3A). Subjects were informed ahead of the experiments to not to consume any food or beverages (other than water) one hour prior to testing. Subjects were not allowed to eat during the duration of testing and only water was given during breaks. A total of 8 saliva samples (4 indoors, 4 outdoors) were collected during testing as follows: before the start of each experiment ("initial"), after the baseline walking condition ("baseline"), after the first visual search condition, and after the second visual search condition for both indoor and outdoor environments. Samples were taken approximately 20 minutes apart. Collections were obtained by placing an oral swab under the subject's tongue for two minutes. Swabs were then removed and placed in storage tubes that were then stored in an ice chest at below 4°C during testing. After testing samples were transferred to a freezer and kept below -20 °C until analysis. Saliva swabs were analyzed in a university lab using the Salimetrics Salivary Cortisol ELISA Kit (Salimetrics, Newmarket, UK) and cortisol concentrations (µg/dL) were obtained from each sample. In order to normalize results across subjects the initial sample taken before the start of the experiment for each respective environment served as a baseline. The concentration for each of the 3 samples within each environment were taken after the end of each testing condition were subtracted from the initial sample and the concentration differences were used for statistics.

Heart Rate

Heart rate was measured using the photoplethysmogram (PPG) signal and recorded from a Pulse Sensor heart rate monitor (sampling rate: 500 Hz; World Famous Electronics LLC, New York, NY) attached to each subject's right earlobe and logged through an external Arduino (Figure 3B).

Heart Rate Analysis

Each subject's raw heart beat data was manually screened and visible artifacts were corrected. Inter-beat intervals were then calculated using the distances between peaks of consecutive beats. Inter-beat interval outliers were then identified using common statistical thresholds (i.e. standard deviation, percent change/range) and corrected by linear interpolation. Heart rate variability analysis was processed using Kubios (Tarvainen et al. 2009). The software was used to determine the time domain measure mean inter-beat intervals (R-R interval) as well as frequency domain measures like standard deviation of normal-to-normal interval, relative low frequency (0.4-1.2 Hz) power, and relative high frequency (1.2- 4 Hz) power.

Eye Tracker

Each subject was fitted with Mobile Eye XG eye tracking glasses (sampling rate: 30 Hz; Applied Science Laboratory, Boston, MA) accurate within 0.5 to 1 degree (Figure 3A) and calibrated indoors to ensure proper alignment. The eye tracker produced scene videos with a visual crosshair marking the location of subject's eye gaze. All eye tracking videos were examined off-line by reviewers to mark notable events such as eye fixations to flags, faces, and animals. All timestamps were confirmed by at least two different reviewers for consistency.

Video

High definition video recordings of the all experiments were captured using a high definition camcorder (sampling rate: 30 Hz; Canon USA) handheld by an experimenter. Video recordings were synced to all measurement devices and reviewed to determine timestamps of relevant environmental variables like terrain changes, background talking, noises, bystanders, etc.

EEG

Subjects were fitted with a high density, pre-amplified 256-channel EEG cap (sampling rate: 512 Hz; Biosemi Activetwo, Amsterdam, Netherlands) (Figure 3B) along with 8 additional external sensors placed on the neck of the subject to record neck muscle electromyographic (EMG) activity. Electrodes positions were digitized and mapped with a 3D digitizer (Zebris, Germany) to make subject-specific head models. We used electrode gel placed underneath each sensor and kept all offsets below 20 mV as recommended by Biosemi for optimal data quality. If anytime during the experiments electrode offsets went above 20 mV, more electrode gel was applied until threshold was reached.

We performed All EEG analyses in MATLAB (The MathWorks, Natick, MA) using custom scripts based on EEGLAB (Delorme and Makeig 2004). EEG was downsampled to 256 Hz and high pass filtered at 1 Hz to remove drift. Common average reference was applied and the EEGLAB plug-in, Cleanline (https://www.nitrc.org/projects/cleanline/) was used to remove 60 Hz line noise. In order to reduce the effects of gait-related movement artifact from the EEG data, we first removed EEG channels that were found to be highly correlated to the gait cycle as described by Anderson and colleagues (Oliveira, Schlink, David Hairston, et al. 2017). Briefly,

individual EEG channel activations were smoothed with a 128 point moving average filter and then split into individual gait cycles from right heel strike to right heel strike. Each channel's mean amplitude for each time point across all gait cycles was used to create an average waveform template. Every individual gait cycle for each channel was cross-correlated against the average waveform. Individual channels which were highly correlated ($r > 0.4$) to the gait cycles for more than 75% of the total number of gait cycles were removed. Next we used standard cleaning methods (i.e., range, SD, kurtosis) to reject any further bad channels. All clean channels were re-referenced to common average. We then applied adaptive mixture independent component analysis (AMICA 15) (J. A. Palmer et al. 2008) using Principal Component Analysis to parse the data into 150 spatially fixed, maximally temporally independent component (IC) signals (Onton et al. 2006) per subject. We used the DIPFIT function in EEGLAB (Oostenveld and Oostendorp 2002) to model each independent component as an equivalent current dipole within a boundary element head model based on the Montreal Neurological Institute standard brain (Quebec). All sources indicative of eye blinks, eye movements, or muscle artifact (T.-P. Jung, Makeig, Westerfield, et al. 2000) were marked for removal. We removed the remaining independent components from further analysis if their best-fit equivalent current dipole accounted for less than 85% of the variance seen at the scalp (Gwin et al. 2011), or if their location was outside the boundary of the scalp.

Group analyses were limited to the number of subjects that included clean EEG signal for all conditions (*baseline* walking, *non-stress* visual search, *stress* visual search) within both environments (indoor, outdoor) and had gait event timings properly synchronized with EEG. Due to missing data cause by various device malfunction like syncing errors, gait detection errors,

etc. this limited our group to 29 of the 49 total subjects. All following EEG analyses were performed on this subset. To cluster the neural independent components obtained from independent component analyses, we used a k-means clustering algorithm across all subjects on vectors jointly grouped by similarities in dipole location, scalp topography, and frequency spectra (Gwin et al. 2010; T.-P. Jung, Makeig, Humphries, et al. 2000). We set the number of clusters to 13 to agree with previous studies from our lab (Bradford et al. 2016; Gwin et al. 2011; Sipp et al. 2013) and removed components to an outlier cluster if they were 3 standard deviations from the mean. Four of the 13 clusters (Figure 5-4) contained at least half of all subjects analyzed and were located in cortical areas that were most relevant for the locomotor task and were similar to those found in previous studies (Bradford et al. 2016; Gwin et al. 2011; Sipp et al. 2013): Left Sensorimotor (27 sources, 14 subjects), Right Sensorimotor (21 sources, 16 subjects), Anterior Cingulate (29 sources, 21 subjects), and Posterior Parietal (21 sources, 15 subjects). All further analyses were performed only on these four clusters. For spectral analysis, we computed log power spectra for each cluster for six conditions: (1) Indoor baseline walking, (2) Indoor non-stress visual search, (3) Indoor stress visual search, (4) Outdoor baseline walking, (5) Outdoor non-stress visual search, and (6) Outdoor stress visual search. A repeated measures ANOVA test was used to evaluate mean spectral frequency band power differences among conditions ($\alpha = 0.05$). Theta band was defined as 4-7 Hz, alpha band 8-12 Hz, beta band 13-30 Hz, and gamma band 31-50 Hz. To avoid substantial line noise present near 60 Hz, we limited gamma band to 50 Hz.

For time-frequency analyses, we examined the same six conditions. All conditions for each subject were epoched at each right heel strike (RHS) to produce discrete gait cycle trials across

the experiment and gait cycles with latencies outside of 3 standard deviations from the mean were removed. We computed a single trial time-frequency log spectrogram for each independent component source activity using three-cycle Morlet wavelets for every individual gait cycle. The spectrograms were time-locked to all subsequent gait events (i.e., left toe off, left heel strike, right toe off) and linearly time warped so each gait event occurred at the same latency in every trial (Gwin et al. 2011; Makeig 1993b). To visualize spectral changes within the gait cycle, we subtracted a baseline (calculated as the average log spectrum across all gait cycles within each condition) from the spectrum at each time point. The resulting plots show spectral change from baseline and are referred to as event-related spectral perturbations (ERSPs) (Gwin et al. 2011; Onton et al. 2006). We averaged the ERSP plots across each independent component in each cluster to make a grand average ERSP for each cluster across all conditions (Figure 10). We used a 200-iteration bootstrapping method to find statistical differences ($p < 0.05$) from baseline frequency power across the gait cycle for each condition and ERSP data were significance masked, such that all nonsignificant regions were set to zero (green).

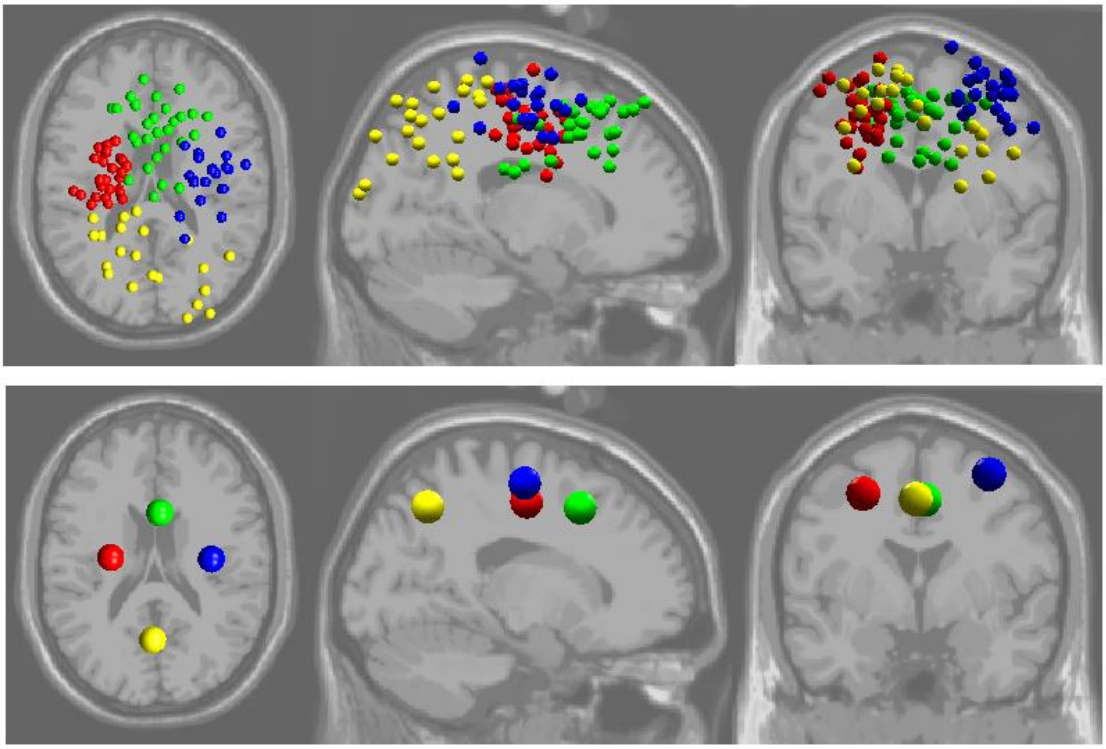

Figure 5-4. Clusters of independent component EEG sources plotted on the Montreal Neurological Institute brain. Left sensorimotor (red), right sensorimotor (blue), anterior cingulate (green), and posterior parietal (yellow). Top: small spheres indicate the equivalent current dipole locations of each clustered independent component source. Bottom: larger spheres show the locations of the cluster centroids.

EMG

To assess the potential of neck muscle electromyography (EMG) effects in EEG results, we used the 8 external EMG channels placed as bipolar pairs on two left and two right neck muscles (Levator Scapulae and Splenius Capitis) to examine neck muscle activity across the gait cycle. For each of the four muscles, we subtracted the difference in EEG signal between each bipolar pair, detrended the signal, applied a 20 Hz high-pass filter and rectified the amplitude. We used a Butterworth low pass filter at 6 Hz to obtain the linear envelope of the EMG signal. Each of the four EMG signals were epoched into individual gait cycles separated by indoor and outdoor environment and then averaged across all gait cycles for a grand average. The grand average gait

cycle EMG signal for each environment was divided by the maximum peak amplitude found across all conditions in order to normalize EMG power for individual subjects. Finally, the average of all subjects for each environment was obtained for a grand average, normalized EMG gait cycle linear envelope.

Statistical Analysis

All statistical analyses except event-related spectral perturbations (ERPs) were carried out using SPSS Statistics 19 (IBM SPSS Statistics 19.0, Armonk, NY). For all variables of interest we used a two-way repeated measures ANOVA with factors of environment (indoor vs outdoor) and condition (*baseline* walking, *non-stress* visual search, *stress* visual search) using the order of environment and order of stress condition as covariates with alpha = 0.05.

Results

Gait

Stride duration (Figure 5-5) was significant for both environment ($F = 28.64$, $p < 0.001$) and conditions ($F = 13.47$, $p < 0.001$). Pairwise comparisons showed indoor treadmill walking used a longer stride duration (mean = 1425.76 ms, std. error = 39.04 ms) compared to outdoors (mean = 1210.95 ms, std. error = 15.41 ms). *Baseline* walking in both environments was significantly slower ($p < 0.001$) than both *non-stress* (mean difference = -75.44 ms, std. error = 15.97 ms) and *stress* (mean = -76.94 ms, std. error = 14.55 ms) visual search conditions. However, *non-stress* and *stress* visual search conditions were not significantly different in either environment.

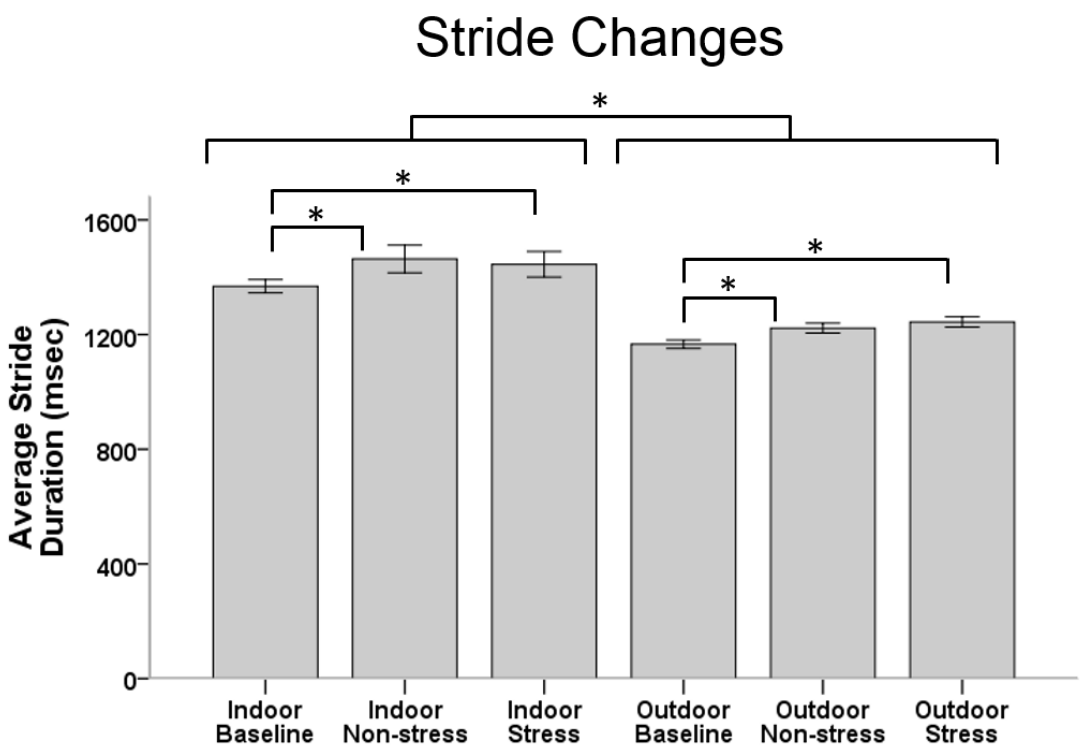

Figure 5-5. Group average stride duration changes across environments and conditions. Stride duration was measured as mean right heel strike to right heel strike gait cycles time (in milliseconds) for each subject. * $p < 0.05$

Cortisol

Cortisol concentrations (differences from initial samples) (Figure 5-6) were only significant for conditions ($F = 3.27$, $p = 0.049$) but not for environment. Pairwise comparisons showed cortisol concentration for outdoor *baseline* walking was significantly greater compared to both *non-stress* (mean = 0.014 µg/dL, std. error = 0.006 µg/dL) and *stress* (mean = 0.016 µg/dL, std. error = 0.006 µg/dL) visual search conditions. However, *non-stress* and *stress* visual search conditions were not significantly different in either environment.

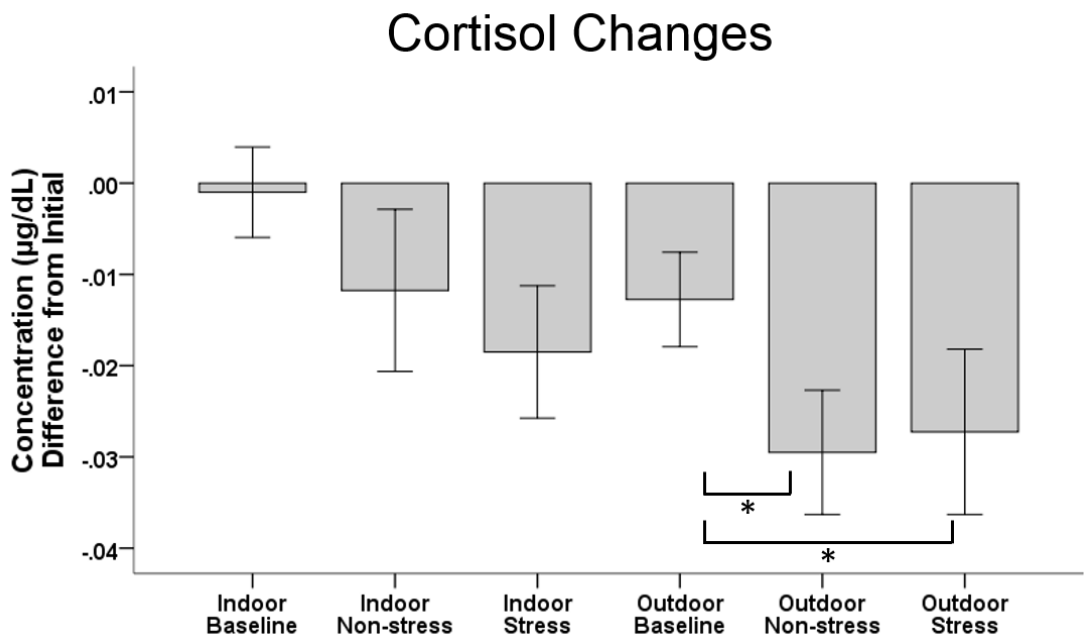

Figure 5-6. Group average salivary cortisol changes across environments and conditions. Concentration (µg/dL) was measured as a difference from initial sample within each environment. * $p < 0.05$

Heart Rate and Heart Rate Variability (HRV)

The mean R-R inter-beat intervals (IBI) were significant for condition ($F = 7.37$, $p = 0.02$) but not for environment (Figure 5-7). Pairwise comparisons showed mean IBI was greater for outdoor *baseline* walking compared to *non-stress* (mean difference = 0.043 sec, std. error = 0.005 sec, $p < 0.001$) and *stress* (mean difference = 0.047 sec, std. error = 0.007 sec, $p < 0.001$) visual search conditions. However, *non-stress* and *stress* visual search conditions were not significantly different in either environment.

The standard deviation of the normal-to-normal RR interval (SD of NN) was significant for condition ($F = 3.67$, $p = 0.03$) but not for environment. Pairwise comparisons showed mean SD of NN was significantly greater for outdoor *baseline* walking compared to *non-stress* (mean difference = 0.007 sec, std. error = 0.002 sec, $p = 0.005$) and *stress* (mean difference = 0.008 sec,

std. error = 0.002 sec, $p < 0.001$) visual search conditions. However, *non-stress* and *stress* visual search conditions were not significantly different in either environment.

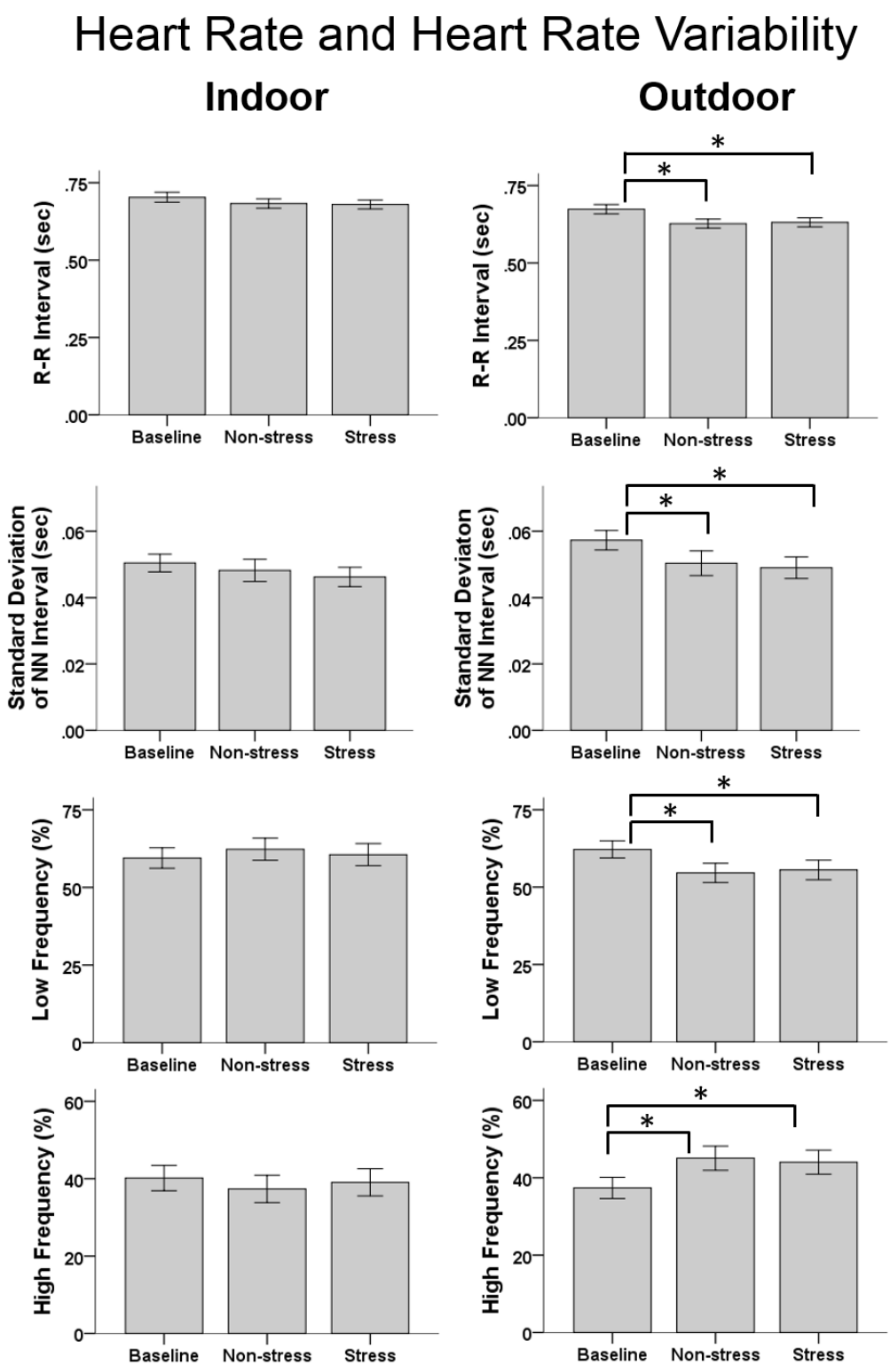

Figure 5-7. Group average heart rate and heart rate variability changes across environments and conditions. R-R interval is the time between successive peaks in the QRS complex. Standard deviation of the normal to normal RR interval represents the variability in

heart rate. Low frequency power represents 0.4-1.2 Hz and high frequency power is 1.2 to 4 Hz. * $p < 0.05$

EMG

The average gait cycle EMG linear envelops (Figure 5-8) for both left and right neck muscles (Levator Scapulae and Splenius Capitis) show that outdoor walking produced great amplitudes and more fluctuations of EMG activity compared to indoor walking. Both left and right neck muscles showed similar spikes of EMG activity at the end of toe off before heel strike.

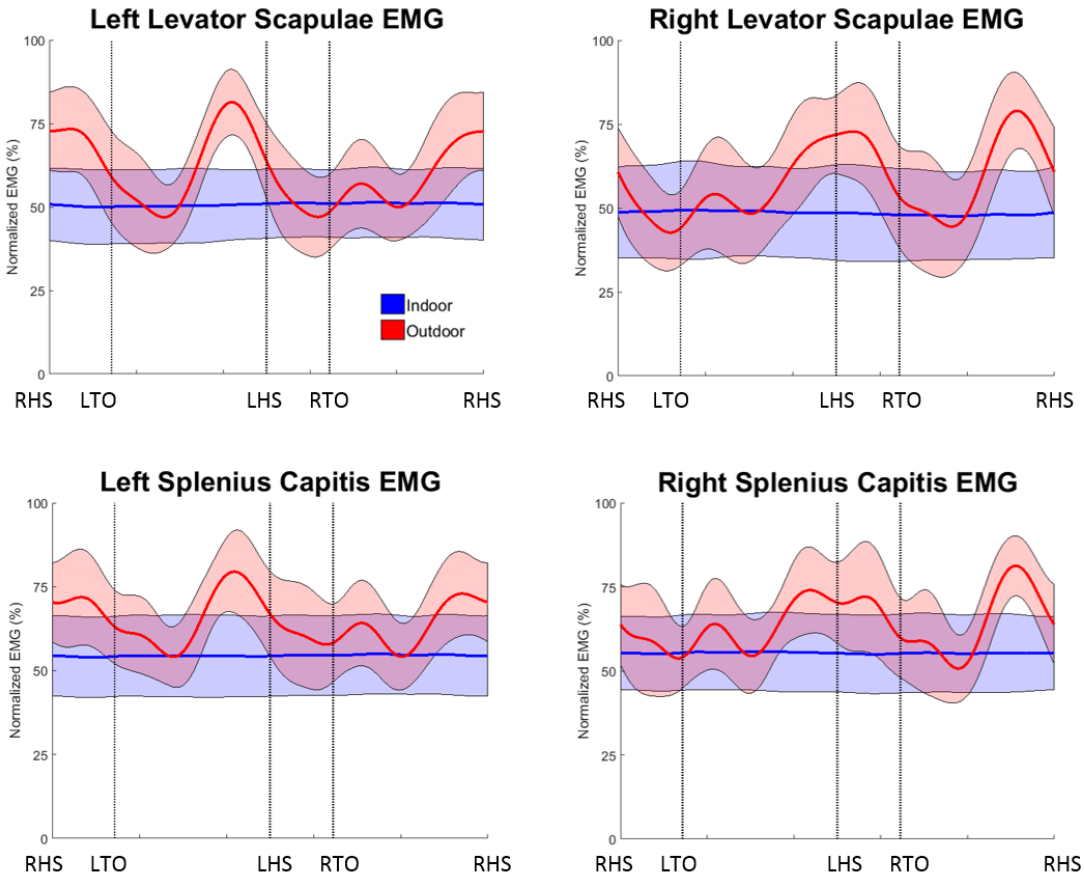

Figure 5-8. Grand average EMG envelopes. Plots shown for two left neck muscles (Levator Scapulae and Splenius Capitis) and same two right neck muscles across the average of all gait cycles normalized by subject. Red line represents indoor walking on a treadmill and blue line represents outdoor walking overground in arboretum. Shaded areas around lines represent +/-1

standard deviation from mean. RHS = right heel strike, LTO = left toe off, LHS = left heel strike, RTO = right toe off.

EEG Spectral Analysis

Table 5-1 presents all significant pairwise comparisons for each cortical cluster by frequency band. Left sensorimotor and right sensorimotor clusters showed very similar patterns (Figure 5-9). For both clusters, *outdoor non-stress* visual search and *outdoor stress* visual search conditions were significantly greater in theta power compared to *baseline* walking. Left sensorimotor also showed significantly greater theta (4-7 Hz) power in the *indoor stress* visual search condition compared to *baseline* walking. Alpha power in left sensorimotor was significantly greater for *indoor non-stress* visual search compared to *stress* visual search condition, while right sensorimotor showed significantly greater alpha (8-12 Hz) power in *outdoor non-stress* vs *stress* visual search. Left sensorimotor showed significant beta (13-30 Hz) power increase for *indoor non-stress* visual search compared to *stress* visual search. Anterior cingulate showed significant increases in theta power for *indoor* and *outdoor stress* visual search conditions compared to *baseline* walking within each environment. Gamma (31-50 Hz) power was also significantly increased for *indoor stress* visual search compared to *indoor non-stress* visual search. *Outdoor stress* visual search has greater gamma power than both *non-stress* visual search and *baseline* walking. Posterior parietal area showed greater theta power for all visual search conditions compared to *baseline* walking within each environment. Both alpha and beta power was significantly higher for *indoor baseline* walking compared to both *indoor non-stress* and *stress* visual search conditions. Gamma power was greater for *indoor stress* visual search compared to *indoor non-stress* visual search.

Table 5-1. Significant spectral differences between pairs of conditions.

	Theta (4-7 Hz)	Alpha (8-12 Hz)	Beta (13-30 Hz)	Gamma (31-50 Hz)
Left Sensorimotor Cortex	In S > In B (p=0.002) Out N > Out B (p=0.009) Out S > Out B (p=0.001)	In N > In S (p=0.031)	In N > In S (p=0.038)	
Right Sensorimotor Cortex	Out N > Out B (p=0.011) Out S > Out B (p=0.020)	Out N > Out S (p=0.017)		
Anterior Cingulate	In S > In B (p=0.021) Out S > Out B (p=0.018)			In S > In N (p=0.028) Out S > Out B (p=0.023) Out S > Out N (p=0.007)
Posterior Parietal	In N > In B (p=0.009) In S > In B (p=0.014) Out N > Out B (p=0.006) Out S > Out B (p<0.001)	In B > In N (p=0.039) In B > In S (p=0.030)	In B > In N (p=0.017) In B > In S (p=0.021)	In S > In N (p=0.002)

In B = Indoor baseline walking, In N = Indoor non-stress visual search, In S = Indoor stress visual search, Out B = Outdoor baseline walking, Out N = Outdoor non-stress visual search, Out S = Outdoor stress visual search.

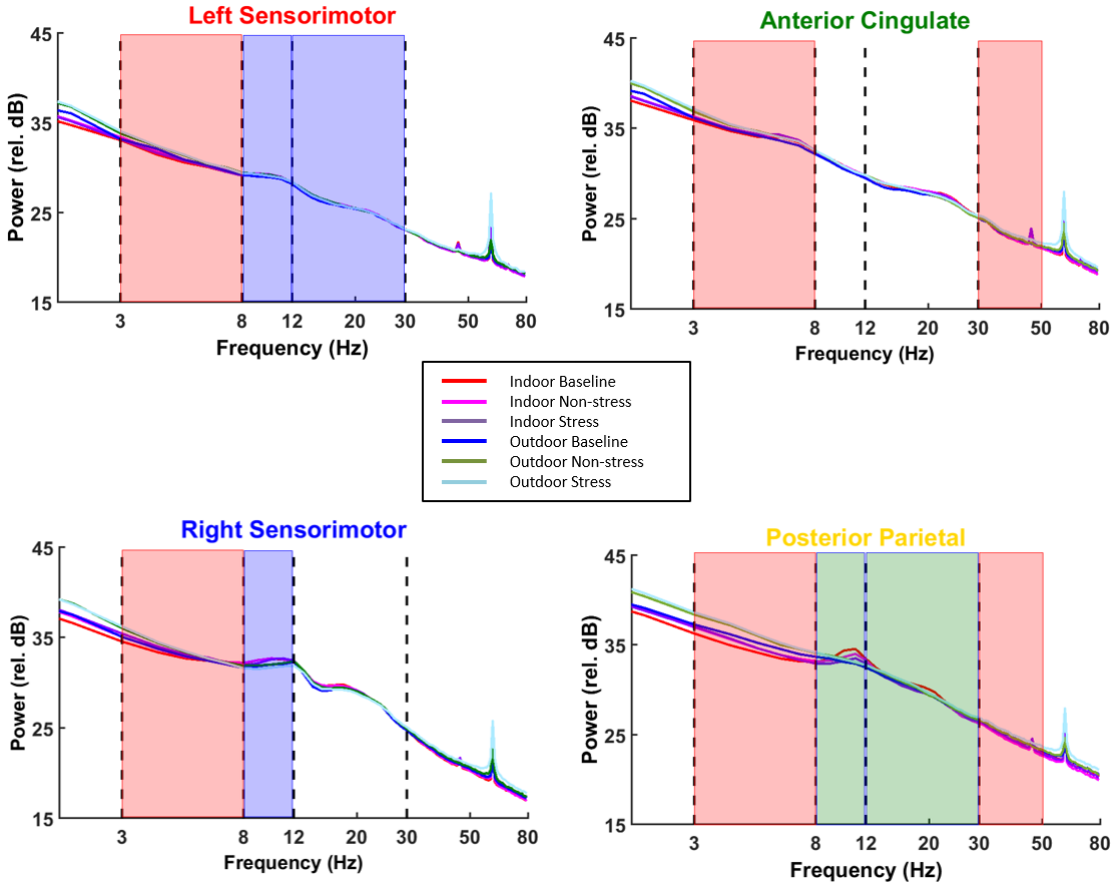

Figure 5-9. Grand average spectral power for each electrocortical cluster. Conditions are indoor *baseline* walking (red), indoor *non-stress* visual search (magenta), indoor *stress* visual search (purple), outdoor *baseline* walking (blue), outdoor *non-stress* visual search (green), outdoor *stress* visual search (light blue). The dashed lines mark boundaries of frequency bands—theta (3-7 Hz), alpha (8-12 Hz), beta (13-30.Hz), and gamma (31-80 Hz). Red shaded regions indicate at least one or both visual search conditions are significantly greater than *baseline* walking conditions. Green shaded region indicates at both visual search conditions are significantly less than *baseline* walking conditions during indoors. Blue shaded regions indicate *non-stress* visual search is significantly greater than *stress* visual search. For specific pairwise statistics see Table 5-1.

ERSP fluctuations across the gait cycle

All four brain areas showed significant spectral power fluctuations in theta, alpha, beta, and gamma bands across the gait cycle during *indoor baseline* walking, *indoor non-stress* visual search,, *indoor stress* visual search, *outdoor baseline* walking, *outdoor non-stress* visual search, *and outdoor stress* visual search (Figure 5-10). Left sensorimotor *indoor baseline* walking showed significant theta power desynchronizations during left swing phase and synchronizations during right foot swing phase. There was also a significant beta and gamma power synchronization at the end of left foot swing phase going into double support. During *indoor non-stress* visual search only a theta synchronization around left foot sing phase and desynchronization around right foot swing phase was significant. And during *indoor stress* visual search there was significant beta and gamma synchronizations at the beginning of left foot swing phase as well as theta, and beta desynchronizations during right foot swing phase. All outdoor conditions showed a similar pattern of alternating theta, alpha and beta synchronizations around both double support phases with theta, alpha, and beta desynchronizations around both swing phases.

Right sensorimotor area *indoor baseline* walking showed significant alpha and beta synchronizations during end of left foot swing and beginning of double support and alpha desynchronization during the opposite double support phase. This same pattern happened for *indoor non-stress* visual search as well. There were no significant fluctuations during *indoor stress* visual search. All outdoor conditions showed a similar pattern of alternating theta, alpha, beta, and gamma synchronizations during first double support phase with right foot forward and only theta synchronization during double support with left foot forward. There were significant theta, alpha, beta, and gamma desynchronizations during both swing phases.

Anterior cingulate area *indoor baseline* walking showed only alpha synchronization at left foot forward double support phase. *Indoor non-stress* visual search showed a small fluctuation of alpha desynchronization during right foot forward double support phase followed by alpha synchronization during left foot swing phase. *Indoor stress* visual search showed theta desynchronization during right foot forward double support phase and alpha synchronization during right foot swing phase. All outdoor conditions showed a similar pattern of alternating theta, alpha and beta synchronizations around both double support phases with theta, alpha, and beta desynchronizations around both swing phases.

Posterior parietal cortex *indoor baseline* walking showed only a small alpha desynchronization during left foot swing phase and alpha synchronization during right foot swing phase. *Indoor non-stress* visual search showed theta synchronization during right foot forward double support phase and theta desynchronization during end of left foot swing phase. *Indoor stress* visual search showed theta and alpha synchronizations during right foot forward double support

followed by alpha and beta desynchronizations during left foot swing phase. *Outdoor baseline* walking showed alpha synchronization during left foot forward double support phase followed by theta and alpha desynchronization during right foot swing phase. *Outdoor non-stress* visual search showed theta, alpha, and beta desynchronizations during left foot swing phase followed by theta and alpha synchronizations during double support. There was a significant alpha, beta, and gamma power synchronization at the end of right foot swing phase. And *outdoor stress* visual search showed a theta and alpha synchronization during right foot forward double support followed by theta and alpha desynchronizations during left foot swing phase. There was also alpha and beta desynchronizations during right foot swing phase as well as gamma synchronization during right foot swing phase.

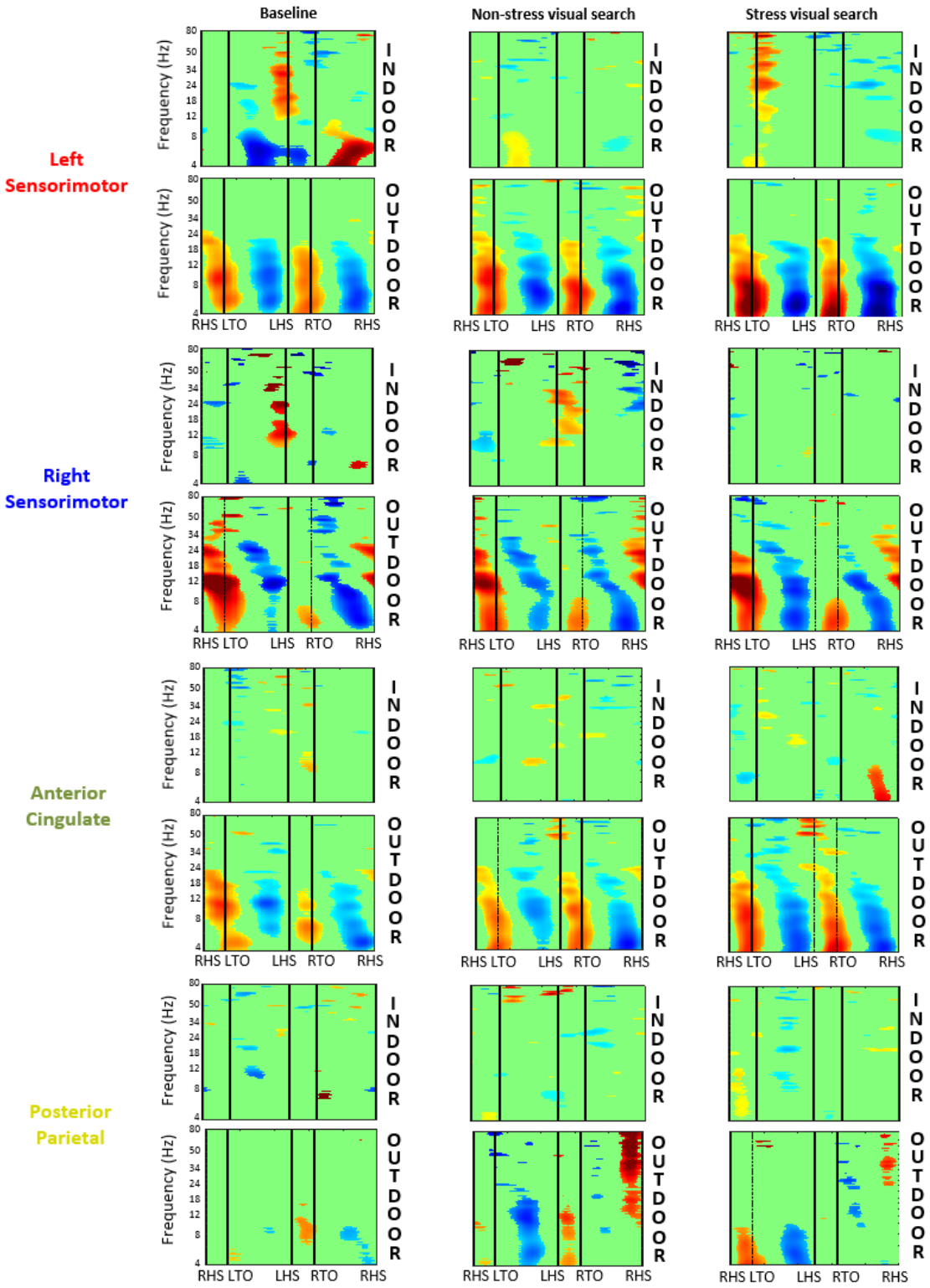

Figure 5-10. Grand average normalized spectrograms. Plots are significance masked (p = 0.05) for left sensorimotor, right sensorimotor, anterior cingulate, and posterior parietal clusters for all conditions in each environment. Left column indicates baseline walking, middle column indicates non-stress visual search, and right column indicates stress visual search. Environment is

indicated by vertical titles to the right of plots. All plots represent one gait cycle from right heel strike (RHS) to RHS, with left toe off (LTO), left heel strike (LHS), and right toe off (RTO) designated by dashed vertical lines. Nonsignificant values were set to zero (green).

Discussion

The results presented confirm that we were able to localize cortical EEG activity in left sensorimotor, right sensorimotor, anterior cingulate, and posterior parietal clusters for both indoor and outdoor walking. We were also able to combine EEG with other multi-modal imaging devices including heart rate, eye tracking, inertial measurement units, and salivary cortisol to find behavior differences between normal walking and walking during visual search for both indoor and outdoor environments. However, the behavioral and neural results show mixed patterns that aren't entirely clear.

Behavioral Differences

We found that gait stride duration significantly increased during both *non-stress* and *stress* visual search tasks compared to *baseline* walking for both indoor and outdoor environments. Stride duration was also significantly longer indoors than it was outdoors. While we can't say for certain whether or not walking speed decreased, longer stride durations suggest that subjects took longer steps when dual-tasking during visual search compared to normal walking. Past studies have similarly found that adding cognitive tasks while walking slows down walking speeds (Beauchet et al. 2005; Patel, Lamar, and Bhatt 2014). This isn't surprising outdoors when subjects walked self-paced as they were not allowed to stop at any time during the visual search task. However, the same increase in stride duration during indoors while on a set treadmill speed (0.7 m/s) does indicate that subjects adjusted their overall walking pattern during visual search. Stride duration was also the only measure to show a significant difference from indoor to

outdoor with subjects walking with a shorter stride duration outside. This also seems reasonable as preferred walking speed is in the range of 1.3 m/s for healthy adults (Bastien et al. n.d.), but here we chose to keep the treadmill at slower speeds to minimize motion related artifact in EEG (Kline et al. 2015).

Cortisol results only showed significant differences between outdoor *baseline* walking and both visual search conditions. There were no significant differences between *non-stress* and *stress* visual search nor any differences for any of the conditions indoors. The decrease in cortisol concentration seems contradictory given that previous studies have shown that cortisol concentration increases with mental stress (Tsigos and Chrousos 2002). However, one potential reason for this pattern might be caused by the nature of the latency response in salivary cortisol. It has been shown that measuring cortisol 21-40 minutes after the stressor elicits the peak cortisol response (Dickerson and Kemeny 2004). In this study we took our cortisol measurements immediately following each condition. Since each condition lasted for approximately 20 minutes, our cortisol measurements might be reflecting the stress levels from the beginning of each condition rather than the end. Another possibility is that our experimental design was not using a strong enough stressor in our *stress* visual search condition. We tried to induce stress using negative feedback penalties for missing target flags along with uncontrollability in when subjects would be penalized. While previous studies have shown that motivated performance with uncontrollability show a significant effect size in cortisol increase (Dickerson and Kemeny 2004), that effect size tends to be much smaller compared to other stressors like social-evaluative threat. It could be that our outdoor task was confounded with social-evaluative threat by the

nature of being outside in a heavily trafficked public space wearing unusual equipment like an EEG cap and mobile eye tracker.

Surprisingly, heart rate and heart rate variability showed no significant differences across any conditions for the indoor environment. However, in the outdoor environment inter-beat interval decreased for both visual search conditions compared to baseline walking indicating an elevated heart rate. Heart rate variability results showed that standard deviation of the normal-to-normal RR peak decreased, low frequency (0.4-1.2 Hz) power decreased, and high frequency (1.2 to 4 Hz) power increased for both visual search conditions compared to *baseline* walking. Heart rate variability decreases have been shown to indicate acute mental stress (Steptoe et al. 2002) and our results suggest that the outdoor visual search task was more stressful than normal *baseline* walking. The frequency domain results of heart rate variability showed a significant decrease in low frequency along with significant high frequency power during both visual search conditions. These results conflict with previous studies that have shown the opposite pattern of low frequency power increases and high frequency power decreases related to physiological stress (Delaney and Brodie 2000). However, the frequency domain measurements of heart rate variability and their relationship to stress are unclear in previous studies. One study conducted a review of across stress literature citing low frequency power results and found that many showed no relationship of low frequency power and laboratory physiological challenges (Goldstein et al. 2011). From both cortisol and heart rate results it is clear that baseline walking and walking during visual search elicited different behavioral patterns outdoors, but we can't say for sure if these differences are directly related to our induced stress procedures or if the involvement of

physical exercise also played a role. However, the lack of significant difference in the indoor condition may indicate that the outdoor differences are not entirely due to the effects of exercise.

Theta band differences between conditions

Our EEG spectral results showed significant decreases in theta (4-7 Hz) power across all clusters during baseline walking compared to one or both visual search conditions. This was consistent for both indoor and outdoor environments with the exception of right sensorimotor only showing both visual search conditions having greater theta frequency power compared to *baseline* walking in outdoors. The ERSP results similarly show that theta power tends to increase in synchronizations around one or both double support phases of the gait cycle, near heel strikes and toe-offs, going from *baseline* to visual search. The ERSP patterns also show more theta synchronizations during double support and desynchronizations during swing phase in all the outdoor conditions compared to their analogues in the indoor environment. This increase in theta power particularly around double support phase going from normal *baseline* walking to a more complex motor task has been shown in previous studies. One study showed this same pattern of theta band increases in the same cortical regions with a similar increase in synchronizations around double support phase when subjects walked on an incline treadmill compared to level walking (Bradford et al. 2016). Another study showed significant theta synchronizations around double support phase in anterior cingulate, left premotor, right motor, and prefrontal parietal clusters when walking on an active treadmill compared to passive walking. They also showed that same pattern of theta synchronizations during both active and passive treadmill walking relative to standing (Bulea et al. 2015). Balance beam walking similarly showed increase theta power compared to normal walking in anterior cingulate, anterior parietal, right sensorimotor,

medial sensorimotor, and dorsolateral prefrontal cortex (Sipp et al. 2013). Theta power was also shown to increase during postural stance in the transition-to-stability stage and then decrease during falls (Slobounov et al. 2009). Together, these past findings along with the results from this current study support that theta power increases with more challenging motor demands and might be particularly critical in the transitional stability stages of gait.

Alpha and Beta synchronizations and desynchronizations

Our ERSP results revealed a common pattern across all the clusters showing significant alpha (8-12 Hz) and beta (13-30 Hz) power alternations of synchronizations around double support and desynchronizations around swing phase for all conditions outdoors that was not present in the indoor conditions. Previous studies have also shown similar patterns in alpha and beta power fluctuations during treadmill walking (Bradford et al. 2016; Bruijn et al. 2015; Bulea et al. 2015; Gwin et al. 2011; Oliveira, Schlink, Hairston, et al. 2017; Sipp et al. 2013). Beta desynchronizations have been shown to represent an "active state" used by the brain for the promotion of sensorimotor integration of ongoing voluntary movement (Buneo and Andersen 2006; Engel and Fries 2010). Similarly, one study doing dual-task walking using EEG outdoors showed increase beta desynchronizations across sensorimotor, prefrontal, frontal, and parietal cortices when walking while texting compared to walking and talking (Pizzamiglio et al. 2017). They concluded that beta desynchronizations promote stronger sensorimotor integration and is needed for maintaining gait stability and spatial navigations while performing a secondary cognitive task. These previous findings along with our currents results showing increased beta desynchronizations across all cluster in outdoor walking compared to indoor walking might

suggest that outdoor walking utilizes more sensory integration in outdoor overground walking compared to the steady walking indoors on a treadmill.

Limitations

One concern when doing mobile EEG is that spectral fluctuations could be influenced by non-neural artifact. Accelerometers on the head have been used to show that frequencies up to 15 Hz in EEG can be affected by head motion (Castermans et al. 2014). However, another study used a wig placed over a non-conductive swim cap to record EEG signals not related to neural activity in order to determine the extent to which motion related artifact might contaminate EEG results and they found that accelerometers on the head were not a good predictor of EEG artifact (Kline et al. 2015). They also noted that slower walking speeds dramatically reduced the effect of alpha and beta fluctuations related to movement artifact. In this study we chose to use 0.7 m/s as the walking speed for the treadmill and restricted subjects to a similar slow walking pace outdoors in the arboretum.

Another possibility for the spectral fluctuation patterns differing so much between the indoor and outdoor environment is that we concatenated all EEG sessions together before pre-processing and using independent component analysis with source localization. This method was chosen in order to obtain the same neural components within each subject so that clusters could be compared across all conditions and both environments. We also presented the neck muscle EMG activity (Figure 5-8) for both indoor and outdoor walking with outdoor walking showing higher amplitudes for all muscles. Those results suggest that EEG indoors has less head movement and neck activation compared to outdoors, which might be caused by a larger range of head motion

during visual search in the real world. So even though both the indoor and outdoor walking tasks should be similar in representing locomotion, it could be that the differences in neural and muscle activity in each environment are large enough such that our single model used for independent component analysis was not well fit to both environments. One study has shown that using a multiple model approach to independent component analysis of EEG data from concatenated walking and sitting conditions produced competing models in which no single model showed high probability of likelihood for both walking and sitting data (Artoni et al. 2017). They showed that multiple models were needed in order to best parse the walking and sitting EEG data separately. However, that same study used a rigorous cleaning methodology to analyze EEG spectral power across the gait cycle of normal treadmill walking in order to best reduce noise and motion related artifact, but they found very similar patterns of increased alpha and beta power synchronizations during double support and desynchronizations during swing phase in both motor and non-motor sources. While we acknowledge the limitations in our ability to ensure our EEG data was not partially contaminated by non-neural sources like noise, muscle, and motion related artifact, the pattern of spectral results we show draw similar conclusions from other mobile EEG studies.

Conclusions

Using mobile brain and body imaging is becoming a popular approach to conducting studies in the real world. However, there are still significant challenges to recording and interpreting data from behavioral and neural modalities. Our results demonstrate the feasibility of using mobile brain and body imaging both indoors with virtual reality and outdoors in a real world environment to understand the behavioral and neural dynamics related to locomotion and stress

during a visual search task. Future studies should continue to expand on these methods and find new ways of uncovering how the brain and body interact outside of traditional laboratory settings.

Chapter 6 Discussion and Conclusions

The goal of this dissertation was to push the design and applications forward for mobile brain and body imaging (MoBI) using high density electroencephalography (EEG) to study complex motor tasks in more natural environments. In this dissertation I completed two main projects meant to 1) explore new methods for using mobile EEG in a split-belt motor adaptation walking task to better understand gait dynamics with perturbations, 2) advance the field of MoBI research by testing the feasibility of using a portable system in virtual reality and the real world, 3) determine if the P300 (positive peak amplitude around 250-400ms after stimulus onset) evoked potential present in previous EEG studies could be seen in both environments while walking and performing a visual search task, and 4) quantify the behavioral and electrocortical activity patterns related to locomotion and gait dynamics using the MoBI setup in indoor treadmill walking and outdoor overground walking.

One of the main findings of study 1 were that left and right sensorimotor areas, anterior cingulate, and posterior parietal cortex all showed similar increases in theta (4-7 Hz) frequency fluctuations during motor adaptation compared to normal walking. This was particularly present around double support, when both feet were on the ground and stabilized for balance, which supports previous research that has shown theta power might play an important role in coordination and balance during more demanding motor tasks compared to normal walking. One previous study (Bradford et al. 2016) also showed increase theta band power when subjects

walked on an incline treadmill compared to level walking. Another study (Sipp et al. 2013) showed subjects walking on a balance beam had sustained theta power increases across the same neural sources compared to normal walking.

We also saw similar increases in alpha (8-12 Hz) fluctuations as well in all clusters. These fluctuations showed up as desynchronizations during swing phase and synchronizations during double support. They were most present during asymmetric walking compared to normal walking and may suggest alpha power also plays a key role in complex movements that happen during the transition phases of swing to stance. Alpha power seems to show interesting dynamics in many complex walking studies (Bulea et al. 2015; Oliveira, Arguissain, and Andersen 2018; Wagner et al. 2012), but its exact function in motor areas are still unknown.

Interestingly, another finding from study 1 was that left sensorimotor and right sensorimotor showed a lateralized difference in beta (13-30 Hz) power with left sensorimotor showing a decrease in beta power during swing phase from pre to post adaptation as well as increased beta synchronizations during double support. These beta power modulations in left sensorimotor areas might suggest that the left sensorimotor area plays a larger role in sensing loss of balance during walking compared to right sensorimotor area. Many other studies have noted similar lateralized differences (Bradford et al. 2016; Bruijn et al. 2015; Serrien et al. 2006; Sipp et al. 2013) and have theorized why these motor areas would control different functions, but there is no consensus yet.

And the last finding from this study was that posterior parietal cortex showed very different fluctuation patterns during split-belt walking compared to normal walking particularly in higher frequencies like beta and gamma (31-80 Hz) power. Previous research in cats (Beloozerova and Sirota 1993; Drew et al. 2008, 2004; Lajoie et al. 2010; Widajewicz et al. 1994) have noted the parietal areas involvement in interlimb coordination during locomotion. Our findings support previous research that has also concluded that parietal area is important in motor planning and error correction during challenging walking conditions.

One of the main limitations for this study was that it was difficult to determine if mechanical or movement related artifacts were still present in the EEG data after cleaning. Over the course of many years I tried numerous cleaning and processing methods to look at the data in different ways. By analyzing muscle EMG activity from the neck electrodes I noticed some overlap in the EEG spectral fluctuations and wanted to find better ways to incorporate that activity back into the data processing steps to try and cancel it out. By including the neck electrode activity and using Ensemble Empirical Mode Decomposition (EEMD) before running independent component analysis (ICA) I was able to specifically target and parse out the highest frequency noise contributors to the data and remove those sources from the channels. Then I found that applying Canonical Correlation Analysis (CCA) to the cleaned channels I could localize components that were cyclical in nature and at low frequencies that aligned with the stepping frequencies. That helped to remove potential sources of movement related artifact. From there I could use adaptive mixture ICA (AMICA) to best separate the clean channel data into the most independent neural sources possible (Delorme et al. 2012). While I can't be certain that I was able to successfully separate out all mechanical and motion artifact from the EEG data, I am

satisfied with the end result and feel that the overall pattern of results I found look similar to and not significantly more noisy than other studies using complex walking tasks and similar methodologies.

The second project comprised of a large scale experiment that had multiple components. While this project was one experiment, there were many findings and challenges that could be split into multiple studies. The first study from this project was purely methods based. To the best of our knowledge nobody has tried to record high density EEG data outdoors in the real world while also using an indoor virtual reality component for comparison. This involved creating a custom system of both hardware and software devices to accomplish. One of the main challenges from this endeavor was that all the data streams from the MoBI device would need to be synced and monitored carefully such that experimental events could be labeled and coded into the data set for future public use. Designing the setup took careful planning and required building custom software to coordinate all devices together. This system was setup with EEG as the primary recording device and all other measuring equipment would be time locked to the EEG data. This allowed for adding unique and interesting tags that could be encoded into the data set in ways that have never been done before. Other team members and myself were able to use video data from the subject eye tracker as well as videos recorded externally from a high definition camcorder to post-hoc mark any timestamps in the data that could be of interest for other researchers unrelated to our field of study. The final data set includes tens of thousands of event labels pre-coded into the EEG data sets with a structured labeling system and key. The first study was a documentation of the data descriptions and methodology we used to complete this task and includes the full data set that has been made available to the public.

For the second study of this project, our main finding was that we could use the EEG data in coordination with the mobile eye tracker to detect a significant positive amplitude waveform around 300 ms to detect target vs distractor flags in both the indoor virtual visual search task as well as the analogous outdoor real world task. This is significant because previous ERP studies using visual search have focused on using computer screens with subjects forced to look straight ahead. Our study instead used a free viewing visual search task in which the subjects were allowed to freely gaze the entire environment. While more recent ERP studies have explored and compared this type of free viewing visual search to traditional oddball paradigms (Kamienkowski et al. 2012; Kaunitz et al. 2014) those were still using pictures of natural scenes rather than using real environments. There have also been previous work that has shown the P300 response is detectable while in mobile walking situations (Debener et al. 2012; Gramann, Gwin, et al. 2010). The findings from this study now confirm that using a free viewing visual search task in the real world can also elicit a similar positive amplitude increase around 300 ms which can be captured by EEG and mobile eye tracking. The limitations from our results were that we were not able to find earlier ERP components like P1 (positive peak at 100 ms), N1 (negative peak at 150 ms), and P2 (positive peak at 200 ms). This is most likely caused by the different method we used in time locking stimulus onset to eye gaze fixation on a target or distractor flag rather than traditional onset based on the moment when a stimulus is presented on a screen. Because of the nature of using a free viewing task in which stimuli were always present in the environment, we had to rely on fixation-event related potentials (fERPs). This method also produces more variability in determining the fixation onset as we relied on eye tracking videos recorded at 30 frames/sec, which limits the consistency of precise timestamps. Another challenge

was that the effect of attention and engagement outdoors compared to indoors might be different. There has been previous work noting that attentional engagement might modulate the temporal effects during free viewing (Corbetta et al. 1998; Melcher and Colby 2008). Since we were outdoors in a public space we had no method of control for subject attention. However, by showing we were able to still capture the positive amplitude waveform around 300ms in these environments under such uncontrollable conditions suggests that this evoked response is quite robust and could be used as a potential biomarker for other applications to take advantage of like brain-computer interface (BCI) devices.

And finally, the last study from this project showed that there were many significant behavioral and neural differences between normal walking and visual search walking during non-stress and stress induced conditions, as well as between the indoor and outdoor environments. We found that gait kinematics, salivary cortisol, heart rate, and heart rate variability consistently showed that walking normally outdoors during the baseline condition was significantly different than during both of the visual search conditions. However, the pattern of results were mixed and the conclusions are unclear. Stride duration was significantly longer in baseline walking compared to both visual search conditions in each environment and that stride was significantly shorter in outdoors compared to indoors. This seems reasonable as the visual search task is more challenging and previous studies have shown that cognitive tasks while walking modulates gait patterns (Kline, Poggensee, and Ferris 2014b). Salivary cortisol concentrations decreased during the visual search conditions while outdoors, which was unexpected, but other studies have also showed that cortisol is sensitive to both the timing of the samples and the types of paradigms being used (Dickerson and Kemeny 2004). It is possible that outside variables like social-

evaluative threat have affected our cortisol results as the act of doing this experiment outdoors in public might have played a larger role than the stress induced by the actual visual search task. This might also be a factor in why we were not able to see significant differences between the non-stress and induced stress conditions outdoors. Heart rate and hear rate variability consistently showed that baseline walking was significantly different than both visual search conditions but only outdoors. The inter-beat interval was reduced (faster heat rate) when subjects were performing the visual search tasks compared to baseline walking. And heart rate variability showed that the standard deviation of normal-to-normal R intervals (SD of NN) decreased when subjects performed the visual search tasks compared to baseline walking. These patterns are in line with previous research (Delaney and Brodie 2000; Steptoe et al. 2002) showing the same changes during more difficult and stressful tasks, but the frequency domain results showed the opposite effect as previous research in that low frequency (0.4-1.2 Hz) power decreased and high frequency (1.2-4 Hz) power increased during the visual search tasks compared to baseline walking. However, there are also conflicting reports about the role of low and high frequency components in heart rate variability (Goldstein et al. 2011). There were also no significant changes indoors for any condition.

The main findings from EEG results were that theta power fluctuations around double support increased across all the outdoor walking conditions compared to indoors. This is in line with the findings from my first study showing theta power fluctuation increases during split-belt walking compared to normal walking. Similarly, the previously mentioned literature from my first study supports that theta power plays an important role in gait dynamics for more challenging motor task compared to normal walking on a treadmill. Another finding was that alpha and beta power

fluctuations showed significant increases in synchronizations and desynchronizations around both double support and swing phases, respectively, for all outdoor conditions compared to indoors. Again, this is similar to the previous findings I saw in the split-belt study with both alpha and beta power being more active in asymmetric walking and suggesting those frequencies play a role in coordination and motor planning. There were similar concerns with this EEG data regarding noise and movement related artifact. We chose to use a very slow walking speed of 0.7 m/s since previous work (Kline et al. 2015) has shown that lower walking speeds are less likely to be affected by motion artifacts. Another major concern was that we chose to analyze the EEG data from both indoor and outdoor sessions concatenated together so that we could separate the same neural sources in each environment and compare them directly. A potential issue with this is that the ICA models assumes the sources are stationary and this might not be the case in both indoor and outdoor environments. While the walking tasks were meant to mirror each other in each environment, we can't be sure if the same neural sources are active in each. This could lead to models with poor fit. However, other studies (Artoni et al. 2017) that have explored this exact issues using similar methods and took great care in avoiding this issue by doing rigorous cleaning steps and using multiple models, but their EEG walking results showed similar patterns of synchronization and desynchronizations in the same neural sources that I found in this study.

Despite all the drawbacks and challenges I faced in each of my studies, I feel the work I presented shows results in line with previous research and that I was successful in advancing the ways in which brain and body imaging can be used in non-traditional environments. To the best of my knowledge, this MoBI study was the first to use high density EEG outdoors with as many multi-modal sensors and as many subjects. Completing the same task simulated indoors on a

treadmill with virtual reality was also novel and important in showing how these types of simulated environments relate to the real world. As more research is pushing towards using virtual reality and also exploring natural settings outside of traditional laboratories, this work was important for taking those first steps.

Bibliography

Admon, Roee et al. 2017. “Distinct Trajectories of Cortisol Response to Prolonged Acute Stress Are Linked to Affective Responses and Hippocampal Gray Matter Volume in Healthy Females.”

Al-Subari, K. et al. 2015. “EMDLAB: A Toolbox for Analysis of Single-Trial EEG Dynamics Using Empirical Mode Decomposition.” *Journal of Neuroscience Methods* 253:193–205.

Alonso-Prieto, E., M. A. Alvarez-González, O. Fernández-Concepción, A. Jiménez-Conde, and C. Machado. 2002. “[Usefulness of P300 as a Tool for Diagnosing Alterations in Sustained Attention in Ischemic Cerebrovascular Disease].” *Revista de Neurologia* 34(12):1105–9.

Artoni, Fiorenzo et al. 2017. “Unidirectional Brain to Muscle Connectivity Reveals Motor Cortex Control of Leg Muscles during Stereotyped Walking.” *NeuroImage* 159:403–16.

Aziz-Zadeh, Lisa, Sook-Lei Liew, and Francesco Dandekar. 2013. “Exploring the Neural Correlates of Visual Creativity.” *Social Cognitive and Affective Neuroscience* 8(4):475–80.

Bastien, G. J., Ae P. A. Willems, Ae B. Schepens, and N. C. Heglund. n.d. “Effect of Load and Speed on the Energetic Cost of Human Walking.”

Beauchet, Olivier, Véronique Dubost, François R. Herrmann, and Reto W. Kressig. 2005. “Stride-to-Stride Variability While Backward Counting among Healthy Young Adults.” *Journal of NeuroEngineering and Rehabilitation* 2(1):26.

Beloozerova, I. N. and M. G. Sirota. 1993. “The Role of the Motor Cortex in the Control of Accuracy of Locomotor Movements in the Cat.” *The Journal of Physiology* 461(1):1–25.

Benjamini, Yoav and Daniel Yekutieli. 2001. *THE CONTROL OF THE FALSE DISCOVERY RATE IN MULTIPLE TESTING UNDER DEPENDENCY*. Vol. 29.

Bischof, Walter F. and Pierre Boulanger. 2003. *Spatial Navigation in Virtual Reality Environments: An EEG Analysis*. Vol. 6.

Bradford, J. Cortney, Jamie R. Lukos, and Daniel P. Ferris. 2016. “Electrocortical Activity Distinguishes between Uphill and Level Walking in Humans.” *Journal of Neurophysiology* 115(2):958–66.

Braun, Jochen and Bela Julesz. 1998. “Withdrawing Attention at Little or No Cost: Detection and Discrimination Tasks.” *Perception & Psychophysics* 60(1):1–23.

Brouwer, A. M., B. Reuderink, J. Vincent, M. A. J. van Gerven, and J. B. F. van Erp. 2013. “Distinguishing between Target and Nontarget Fixations in a Visual Search Task Using Fixation-Related Potentials.” *Journal of Vision* 13(3):17–17.

Bruijn, Sjoerd M., Jaap H. Van Dieën, and Andreas Daffertshofer. 2015. “Beta Activity in the Premotor Cortex Is Increased during Stabilized as Compared to Normal Walking.” *Frontiers in Human Neuroscience* 9(October):1–13.

Brunner, Clemens, Martin Billinger, Martin Seeber, Timothy R. Mullen, and Scott Makeig. 2016. “Volume Conduction Influences Scalp-Based Connectivity Estimates.” *Frontiers in Computational Neuroscience* 10(November):1–4.

Brütsch, Karin et al. 2010. “Influence of Virtual Reality Soccer Game on Walking Performance

in Robotic Assisted Gait Training for Children." *Journal of NeuroEngineering and Rehabilitation* 7(1):15.
Bulea, Thomas C., Jonghyun Kim, Diane L. Damiano, Christopher J. Stanley, and Hyung-Soon Park. 2015. "Prefrontal, Posterior Parietal and Sensorimotor Network Activity Underlying Speed Control during Walking." *Frontiers in Human Neuroscience* 9(May).
Buneo, Christopher A. and Richard A. Andersen. 2006. "The Posterior Parietal Cortex: Sensorimotor Interface for the Planning and Online Control of Visually Guided Movements." *Neuropsychologia* 44(13):2594–2606.
Castermans, Thierry, Matthieu Duvinage, Guy Cheron, and Thierry Dutoit. 2014. "About the Cortical Origin of the Low-Delta and High-Gamma Rhythms Observed in EEG Signals during Treadmill Walking." *Neuroscience Letters* 561:166–70.
Castermans, Thierry, Matthieu Duvinage, Guy Cheron, and Thierry Dutoit. 2012. "EEG AND HUMAN LOCOMOTION Descending Commands and Sensory Feedback Should Be Disentangled From Artifacts Thanks to New Experimental Protocols Position Paper." *Proceedings of the International Conference on Bio-Inspired Systems and Signal Processing* 309–14.
Chin-Teng Lin et al. 2007. "EEG-Based Assessment of Driver Cognitive Responses in a Dynamic Virtual-Reality Driving Environment." *IEEE Transactions on Biomedical Engineering* 54(7):1349–52.
Christensen, Lars O. D., Jacob Buus Andersen, Thomas Sinkjaer, and Jens Nielsen. 2001. "Transcranial Magnetic Stimulation and Stretch Reflexes in the Tibialis Anterior Muscle during Human Walking." *The Journal of Physiology* 531(2):545–57.
Clays, Els et al. 2011. "The Perception of Work Stressors Is Related to Reduced Parasympathetic Activity." *International Archives of Occupational and Environmental Health* 84(2):185–91.
Corbetta, Maurizio et al. 1998. "A Common Network of Functional Areas for Attention and Eye Movements." *Neuron* 21(4):761–73.
Correa, Ángel, Juan Lupiáñez, Eduardo Madrid, and Pío Tudela. 2006. "Temporal Attention Enhances Early Visual Processing: A Review and New Evidence from Event-Related Potentials." *Brain Research* 1076(1):116–28.
Cruz-Neira, Carolina, Daniel J. Sandin, Thomas A. DeFanti, Robert V. Kenyon, and John C. Hart. 1992. "The CAVE: Audio Visual Experience Automatic Virtual Environment." *Communications of the ACM* 35(6):64–72.
Debener, Stefan, Falk Minow, Reiner Emkes, Katharina Gandras, and Maarten de Vos. 2012. "How about Taking a Low-Cost, Small, and Wireless EEG for a Walk?" *Psychophysiology* 49(11):1617–21.
Delaney, J. P. and D. A. Brodie. 2000. "Effects of Short-Term Psychological Stress on the Time and Frequency Domains of Heart-Rate Variability." *Perceptual and Motor Skills* 91(2):515–24.
Delorme, Arnaud and Scott Makeig. 2004. "EEGLAB: An Open Source Toolbox for Analysis of Single-Trial EEG Dynamics Including Independent Component Analysis." *Journal of Neuroscience Methods* 134(1):9–21.
Delorme, Arnaud, Jason Palmer, Julie Onton, Robert Oostenveld, and Scott Makeig. 2012. "Independent EEG Sources Are Dipolar." *PLoS ONE* 7(2).
Dickerson, Sally S. and Margaret E. Kemeny. 2004. "Acute Stressors and Cortisol Responses: A Theoretical Integration and Synthesis of Laboratory Research." *Psychological Bulletin* 130(3):355–91.

Diemer, Julia, Georg W. Alpers, Henrik M. Peperkorn, Youssef Shiban, and Andreas MÃ¼hlberger. 2015. “The Impact of Perception and Presence on Emotional Reactions: A Review of Research in Virtual Reality.” *Frontiers in Psychology* 6:26.

Dobkin, Bruce H., Ann Firestine, Michele West, Kaveh Saremi, and Roger Woods. 2004. “Ankle Dorsiflexion as an FMRI Paradigm to Assay Motor Control for Walking during Rehabilitation.” *NeuroImage* 23(1):370–81.

Drew, Trevor, John Kalaska, and Nedialko Krouchev. 2008. “Muscle Synergies during Locomotion in the Cat: A Model for Motor Cortex Control.” *The Journal of Physiology* 586(5):1239–45.

Drew, Trevor, Stephen Prentice, and Bénédicte Schepens. 2004. “Cortical and Brainstem Control of Locomotion.” *Progress in Brain Research* 143:251–61.

Eckstein, M. P. 2011. “Visual Search: A Retrospective.” *Journal of Vision* 11(5):14–14.

Engel, Andreas K. and Pascal Fries. 2010. “Beta-Band Oscillations—signalling the Status Quo?” *Current Opinion in Neurobiology* 20(2):156–65.

Farwell, L. A. and E. Donchin. 1988. “Talking off the Top of Your Head: Toward a Mental Prosthesis Utilizing Event-Related Brain Potentials.” *Electroencephalography and Clinical Neurophysiology* 70(6):510–23.

Friman, Ola, Magnus Borga, Peter Lundberg, and Hans Knutsson. 2004. “Detection and Detrending in FMRI Data Analysis.” *NeuroImage* 22(2):645–55.

Goldstein, David S., Oladi Bentho, Mee Yeong Park, and Yehonatan Sharabi. 2011. “Low-Frequency Power of Heart Rate Variability Is Not a Measure of Cardiac Sympathetic Tone but May Be a Measure of Modulation of Cardiac Autonomic Outflows by Baroreflexes.” *Experimental Physiology* 96(12):1255–61.

Gramann, Klaus et al. 2011. “Cognition in Action: Imaging Brain/Body Dynamics in Mobile Humans.” *Reviews in the Neurosciences* 22(6):593–608.

Gramann, Klaus, Julie Onton, et al. 2010. “Human Brain Dynamics Accompanying Use of Egocentric and Allocentric Reference Frames during Navigation.” *Journal of Cognitive Neuroscience* 22(12):2836–49.

Gramann, Klaus, Daniel P. Ferris, Joseph Gwin, and Scott Makeig. 2014. “Imaging Natural Cognition in Action.” *International Journal of Psychophysiology* 91(1):22–29.

Gramann, Klaus, Joseph T. Gwin, Nima Bigdely-Shamlo, Daniel P. Ferris, and Scott Makeig. 2010. “Visual Evoked Responses During Standing and Walking.” *Frontiers in Human Neuroscience* 4(October):1–12.

Graupner, Sven-Thomas, Boris M. Velichkovsky, Sebastian Pannasch, and Johannes Marx. 2007. “Surprise, Surprise: Two Distinct Components in the Visually Evoked Distractor Effect.” *Psychophysiology* 44(2):251–61.

Groppe, David M., Thomas P. Urbach, and Marta Kutas. 2011. “Mass Univariate Analysis of Event-Related Brain Potentials/Fields I: A Critical Tutorial Review.” *Psychophysiology* 48(12):1711–25.

Gwin, J. T., K. Gramann, S. Makeig, and D. P. Ferris. 2010. “Removal of Movement Artifact From High-Density EEG Recorded During Walking and Running.” *Journal of Neurophysiology* 103(6):3526–34.

Gwin, Joseph T., Klaus Gramann, Scott Makeig, and Daniel P. Ferris. 2011. “Electrocortical Activity Is Coupled to Gait Cycle Phase during Treadmill Walking.” *NeuroImage* 54(2):1289–96.

Haefeli, Jenny, Stefanie Vögeli, Jan Michel, and Volker Dietz. 2011. “Preparation and

Performance of Obstacle Steps: Interaction between Brain and Spinal Neuronal Activity." *European Journal of Neuroscience* 33(2):338–48.
Hellhammer, Dirk H., Stefan Wüst, and Brigitte M. Kudielka. 2009. "Salivary Cortisol as a Biomarker in Stress Research." *Psychoneuroendocrinology* 34(2):163–71.
Heuninckx, Sofie, Nicole Wenderoth, Filiep Debaere, Ronald Peeters, and Stephan P. Swinnen. 2005. "Behavioral/Systems/Cognitive Neural Basis of Aging: The Penetration of Cognition into Action Control."
Hill, E. E. et al. 2008. "Exercise and Circulating Cortisol Levels: The Intensity Threshold Effect." *Journal of Endocrinological Investigation* 31(7):587–91.
Hillyard, S. A., R. F. Hink, V. L. Schwent, and T. W. Picton. 1973. "Electrical Signs of Selective Attention in the Human Brain." *Science (New York, N.Y.)* 182(4108):177–80.
Holden, Maureen K. 2005. "Virtual Environments for Motor Rehabilitation: Review." *CyberPsychology & Behavior* 8(3):187–211.
Hopf, J. M. et al. 2000. "Neural Sources of Focused Attention in Visual Search." *Cerebral Cortex* 10(12):1233–41.
Hotelling, Harold. 1936. "Relations Between Two Sets of Variates." *Biometrika* 28(3/4):321.
Hülsdünker, T., A. Mierau, C. Neeb, H. Kleinöder, and H. K. Strüder. 2015. "Cortical Processes Associated with Continuous Balance Control as Revealed by EEG Spectral Power." *Neuroscience Letters* 592:1–5.
Hutzler, Florian et al. 2007. "Welcome to the Real World: Validating Fixation-Related Brain Potentials for Ecologically Valid Settings." *Brain Research* 1172(1):124–29.
Jagla, Fedor and Igor Riecansky. 2007. *Saccadic Eye Movement Related Potentials Slovak Adaptation of the Schizotypal Personality Questionnaire View Project Polyphenols and Higher Brain Functions View Project*.
Jung, Tzyy-Ping, Scott Makeig, Marissa Westerfield, et al. 2000. "Removal of Eye Activity Artifacts from Visual Event-Related Potentials in Normal and Clinical Subjects." *Clinical Neurophysiology* 111(10):1745–58.
Jung, Tzyy-Ping, Scott Makeig, Colin Humphries, et al. 2000. "Removing Electroencephalographic Artifacts by Blind Source Separation." *Psychophysiology* 37(2):163–78.
Jung, Tzyy Ping et al. 2001. "Analysis and Visualization of Single-Trial Event-Related Potentials." *Human Brain Mapping* 14(3):166–85.
Jung, Tzyy Ping et al. 2000. "Removal of Eye Activity Artifacts from Visual Event-Related Potentials in Normal and Clinical Subjects." *Clinical Neurophysiology* 111(10):1745–58.
Kamienkowski, J. E., M. J. Ison, R. Q. Quiroga, and M. Sigman. 2012. "Fixation-Related Potentials in Visual Search: A Combined EEG and Eye Tracking Study." *Journal of Vision* 12(7):4–4.
Katayama, Jun'ichi, Yo Miyata, and Akihiro Yagi. 1987. "Sentence Verification and Event-Related Brain Potentials." *Biological Psychology* 25(2):173–85.
Kaunitz, Lisandro N. et al. 2014. "Looking for a Face in the Crowd: Fixation-Related Potentials in an Eye-Movement Visual Search Task." *NeuroImage* 89:297–305.
Kazai, Koji and Akihiro Yagi. 1999. "Integrated Effect of Stimulation at Fixation Points on EFRP (Eye-Fixation Related Brain Potentials)." *International Journal of Psychophysiology* 32(3):193–203.
Kersting, Uwe G. 2011. "Regulation of Impact Forces during Treadmill Running." *Footwear Science* 3(1):59–68.

Kline, Julia E., Helen J. Huang, Kristine L. Snyder, and Daniel P. Ferris. 2015. “Isolating Gait-Related Movement Artifacts in Electroencephalography during Human Walking.” *Journal of Neural Engineering* 12(4):46022.
Kline, Julia E., Katherine Poggensee, and Daniel P. Ferris. 2014a. “Your Brain on Speed: Cognitive Performance of a Spatial Working Memory Task Is Not Affected by Walking Speed.” *Frontiers in Human Neuroscience* 8(May):1–16.
Kline, Julia E., Katherine Poggensee, and Daniel P. Ferris. 2014b. “Your Brain on Speed: Cognitive Performance of a Spatial Working Memory Task Is Not Affected by Walking Speed.” *Frontiers in Human Neuroscience* 8:288.
Kranczioch, Cornelia, Stefan Debener, and Andreas K. Engel. 2003. “Event-Related Potential Correlates of the Attentional Blink Phenomenon.” *Cognitive Brain Research* 17(1):177–87.
Kranczioch, Cornelia, Catharina Zich, Irina Schierholz, and Annette Sterr. 2014. “Mobile EEG and Its Potential to Promote the Theory and Application of Imagery-Based Motor Rehabilitation.” *International Journal of Psychophysiology* 91(1):10–15.
Krusienski, Dean J. et al. 2006. “A Comparison of Classification Techniques for the P300 Speller.” *Journal of Neural Engineering* 3(4):299–305.
de Lafuente, Victor. 2013. “Conversion of Sensory Signals into Perceptual Decisions.” *Progress in Neurobiology* 103:41–75.
Lagopoulos, J. et al. 1998. “Dysfunctions of Automatic (P300a) and Controlled (P300b) Processing in Parkinson’s Disease.” *Neurological Research* 20(1):5–10.
Lajoie, Kim, Jacques-Étienne Andujar, Keir Pearson, and Trevor Drew. 2010. “Neurons in Area 5 of the Posterior Parietal Cortex in the Cat Contribute to Interlimb Coordination During Visually Guided Locomotion: A Role in Working Memory.” *Journal of Neurophysiology* 103(4):2234–54.
Lau, Troy M., Joseph T. Gwin, and Daniel P. Ferris. 2012. “How Many Electrodes Are Really Needed for EEG-Based Mobile Brain Imaging?” *Journal of Behavioral and Brain Science* 02(03):387–93.
Lau, Troy M., Joseph T. Gwin, and Daniel P. Ferris. 2014. “Walking Reduces Sensorimotor Network Connectivity Compared to Standing.” *Journal of NeuroEngineering and Rehabilitation* 11(1):1–10.
Liv Hansen, Naja and Jens Bo Nielsen. 2004. “The Effect of Transcranial Magnetic Stimulation and Peripheral Nerve Stimulation on Corticomuscular Coherence in Humans.” *The Journal of Physiology* 561(1):295–306.
Livingston, M. A., Zhuming Ai, J. E. Swan, and H. S. Smallman. 2009. “Indoor vs. Outdoor Depth Perception for Mobile Augmented Reality.” Pp. 55–62 in *2009 IEEE Virtual Reality Conference*. IEEE.
Luck, S. J. and M. A. Ford. 1998. “On the Role of Selective Attention in Visual Perception.” *Proceedings of the National Academy of Sciences of the United States of America* 95(3):825–30.
Luck, Steven J. (Steven John). 2005. *An Introduction to the Event-Related Potential Technique*. MIT Press.
Luck, Steven J., Silu Fan, and Steven A. Hillyard. 1993. “Attention-Related Modulation of Sensory-Evoked Brain Activity in a Visual Search Task.” *Journal of Cognitive Neuroscience* 5(2):188–95.
Luft, Andreas R. et al. 2002. “Comparing Brain Activation Associated with Isolated Upper and Lower Limb Movement across Corresponding Joints.” *Human Brain Mapping* 17(2):131–

40.
Mager, Ralph, Alex H. Bullinger, Andreas Roessler, Franz Mueller-Sphan, and Robert Stoermer. 2000. “Monitoring Brain Activity During Use of Stereoscopic Virtual Environments.” *CyberPsychology & Behavior* 3(3):407–13.
Makeig, Scott. 1993a. “Auditory Event-Related Dynamics of the EEG Spectrum and Effects of Exposure to Tones.” *Electroencephalography and Clinical Neurophysiology* 86(4):283–93.
Makeig, Scott. 1993b. “Auditory Event-Related Dynamics of the EEG Spectrum and Effects of Exposure to Tones.” *Electroencephalography and Clinical Neurophysiology* 86(4):283–93.
Makeig, Scott, Stefan Debener, Julie Onton, and Arnaud Delorme. 2004. “Mining Event-Related Brain Dynamics.” *Trends in Cognitive Sciences* 8(5):204–10.
Makeig, Scott, Klaus Gramann, Tzyy-Ping Jung, Terrence J. Sejnowski, and Howard Poizner. 2009. “Linking Brain, Mind and Behavior.” *International Journal of Psychophysiology* 73(2):95–100.
Makeig, Scott, Anthony J. Bell., Tzyy-Ping Jung, and Terrence J. Sejnowski. 1996. “Independent Component Analysis of Electroencephalographic Data.” *Advances in Neural Information Processing Systems* 8:145–51.
Malcolm, Brenda R., John J. Foxe, John S. Butler, and Pierfilippo De Sanctis. 2015. “The Aging Brain Shows Less Flexible Reallocation of Cognitive Resources during Dual-Task Walking: A Mobile Brain/Body Imaging (MoBI) Study.” *NeuroImage* 117:230–42.
Martinez-Conde, Susana, Jorge Otero-Millan, and Stephen L. Macknik. 2013. “The Impact of Microsaccades on Vision: Towards a Unified Theory of Saccadic Function.” *Nature Reviews Neuroscience* 14(2):83–96.
McCall, Cade and Jim Blascovich. 2009. “How, When, and Why to Use Digital Experimental Virtual Environments to Study Social Behavior.” *Social and Personality Psychology Compass* 3(5):744–58.
Melcher, David and Carol L. Colby. 2008. “Trans-Saccadic Perception.” *Trends in Cognitive Sciences* 12(12):466–73.
Meyerding, Stephan G. H. and Antje Risius. 2018. “Reading Minds: Mobile Functional near-Infrared Spectroscopy as a New Neuroimaging Method for Economic and Marketing Research—A Feasibility Study.” *Journal of Neuroscience, Psychology, and Economics*.
Mine, Mark R., Frederick P. Brooks, and Carlo H. Sequin. 1997. “Moving Objects in Space.” Pp. 19–26 in *Proceedings of the 24th annual conference on Computer graphics and interactive techniques - SIGGRAPH ’97*. New York, New York, USA: ACM Press.
Minguillon, Jesus, M. Angel Lopez-Gordo, and Francisco Pelayo. 2017. “Trends in EEG-BCI for Daily-Life: Requirements for Artifact Removal.” *Biomedical Signal Processing and Control* 31:407–18.
Miniussi, C., E. L. Wilding, J. T. Coull, and A. C. Nobre. 1999. “Orienting Attention in Time.” *Brain* 122(8):1507–18.
Mirelman, A. et al. 2011. “Virtual Reality for Gait Training: Can It Induce Motor Learning to Enhance Complex Walking and Reduce Fall Risk in Patients With Parkinson’s Disease?” *The Journals of Gerontology Series A: Biological Sciences and Medical Sciences* 66A(2):234–40.
Miyai, Ichiro et al. 2001. “Cortical Mapping of Gait in Humans: A Near-Infrared Spectroscopic Topography Study.” *NeuroImage* 14(5):1186–92.
Morton, S. M. 2006. “Cerebellar Contributions to Locomotor Adaptations during Splitbelt Treadmill Walking.” *Journal of Neuroscience* 26(36):9107–16.

Mullen, Tim et al. 2013. “Real-Time Modeling and 3D Visualization of Source Dynamics and Connectivity Using Wearable EEG.” Pp. 2184–87 in *2013 35th Annual International Conference of the IEEE Engineering in Medicine and Biology Society (EMBC)*. IEEE.

Münte, Thomas F., Mike Matzke, and Sönke Johannes. 1997. “Brain Activity Associated with Syntactic Incongruencies in Words and Pseudo-Words.” *Journal of Cognitive Neuroscience* 9(3):318–29.

Ojeda, Alejandro, Nima Bigdely-Shamlo, and Scott Makeig. 2014. “MoBILAB: An Open Source Toolbox for Analysis and Visualization of Mobile Brain/Body Imaging Data.” *Frontiers in Human Neuroscience* 8:121.

Oliveira, Anderson S., Bryan R. Schlink, W. David Hairston, Peter König, and Daniel P. Ferris. 2017. “A Channel Rejection Method for Attenuating Motion-Related Artifacts in EEG Recordings during Walking.” *Frontiers in Neuroscience* 11(APR):1–17.

Oliveira, Anderson S., Bryan R. Schlink, W. David Hairston, Peter König, and Daniel P. Ferris. 2017. “Restricted Vision Increases Sensorimotor Cortex Involvement in Human Walking.” *Journal of Neurophysiology* 118(4):1943–51.

Oliveira, Anderson Souza, Federico Gabriel Arguissain, and Ole Kæseler Andersen. 2018. “Cognitive Processing for Step Precision Increases Beta and Gamma Band Modulation During Overground Walking.” *Brain Topography* 0(0):1–11.

Onton, Julie and Scott Makeig. 2006. “Information-Based Modeling of Event-Related Brain Dynamics.” *Progress in Brain Research* 159:99–120.

Onton, Julie, Marissa Westerfield, Jeanne Townsend, and Scott Makeig. 2006. “Imaging Human EEG Dynamics Using Independent Component Analysis.” *Neuroscience and Biobehavioral Reviews* 30(6):808–22.

Oostenveld, Robert and Thom F. Oostendorp. 2002. “Validating the Boundary Element Method for Forward and Inverse EEG Computations in the Presence of a Hole in the Skull.” *Human Brain Mapping* 17(3):179–92.

Ossandon, J. P., A. V. Helo, R. Montefusco-Siegmund, and P. E. Maldonado. 2010. “Superposition Model Predicts EEG Occipital Activity during Free Viewing of Natural Scenes.” *Journal of Neuroscience* 30(13):4787–95.

Palmer, J. A., S. Makeig, K. Kreutz-Delgado, and B. D. Rao. 2008. “Newton Method For the ICA Micture Model.” *Proceedings of the 33rd IEEE International Conference on Acoustics and Signal Processing* 1805–8.

Palmer, J. A., S. Makeig, K. Kreutz-Delgado, and B. D. Rao. 2008. “Newton Method for the ICA Mixture Model.” Pp. 1805–8 in *2008 IEEE International Conference on Acoustics, Speech and Signal Processing*. IEEE.

Palmer, Jason A., Kenneth Kreutz-Delgado, and Scott Makeig. 2006. “Super-Gaussian Mixture Source Model for ICA.” *Lecture Notes in Computer Science (Including Subseries Lecture Notes in Artificial Intelligence and Lecture Notes in Bioinformatics)* 3889 LNCS:854–61.

Patel, P., M. Lamar, and T. Bhatt. 2014. “Effect of Type of Cognitive Task and Walking Speed on Cognitive-Motor Interference during Dual-Task Walking.” *Neuroscience* 260:140–48.

Patel, Salil H. and Pierre N. Azzam. 2005. “Characterization of N200 and P300: Selected Studies of the Event-Related Potential.” *International Journal of Medical Sciences* 2(4):147–54.

Petersen, T. H., M. Willerslev-Olsen, B. A. Conway, and J. B. Nielsen. 2012. “The Motor Cortex Drives the Muscles during Walking in Human Subjects.” *Journal of Physiology* 590(10):2443–52.

Peterson, S. M., E. Furuichi, and D. P. Ferris. 2018. “Effects of Virtual Reality High Heights

Exposure during Beam-Walking on Physiological Stress and Cognitive Loading." *PLoS ONE* 13(7):1–17.
Pizzamiglio, Sara, Usman Naeem, Hassan Abdalla, and Duncan L. Turner. 2017. "Neural Correlates of Single- and Dual-Task Walking in the Real World." *Frontiers in Human Neuroscience* 11(September):1–12.
Polich, J. and A. Kok. 1995. "Cognitive and Biological Determinants of P300: An Integrative Review." *Biological Psychology* 41(2):103–46.
Polich, John. 1987. "Comparison of P300 from a Passive Tone Sequence Paradigm and an Active Discrimination Task." *Psychophysiology* 24(1):41–46.
Presacco, A., R. Goodman, L. Forrester, and J. L. Contreras-Vidal. 2011. "Neural Decoding of Treadmill Walking from Noninvasive Electroencephalographic Signals." *Journal of Neurophysiology* 106(4):1875–87.
Pugnetti, Luigi, Michael Meehan, and Laura Mendozzi. 2001. "Psychophysiological Correlates of Virtual Reality: A Review." *Presence: Teleoperators and Virtual Environments* 10(4):384–400.
Raethjen, Jan et al. 2008. "Cortical Representation of Rhythmic Foot Movements." *Brain Research* 1236:79–84.
Rämä, Pia and Thierry Baccino. 2010. "Eye Fixation-Related Potentials (EFRPs) during Object Identification." *Visual Neuroscience* 27(5–6):187–92.
Ravden, D. and J. Polich. 1999. "On P300 Measurement Stability: Habituation, Intra-Trial Block Variation, and Ultradian Rhythms." *Biological Psychology* 51(1):59–76.
Reisman, D. S. 2005. "Interlimb Coordination During Locomotion: What Can Be Adapted and Stored?" *Journal of Neurophysiology* 94(4):2403–15.
Reisman, Darcy S., Heather McLean, and Amy J. Bastian. 2010. "Split-Belt Treadmill Training Poststroke: A Case Study." *Journal of Neurologic Physical Therapy* 34(4):202–7.
Reisman, Darcy S., Robert Wityk, Kenneth Silver, and Amy J. Bastian. 2007. "Locomotor Adaptation on a Split-Belt Treadmill Can Improve Walking Symmetry Post-Stroke." *Brain* 130(7):1861–72.
Roe, Jenny J., Peter A. Aspinall, Panagiotis Mavros, and Richard Coyne. 2013. "Engaging the Brain: The Impact of Natural versus Urban Scenes Using Novel EEG Methods in an Experimental Setting." *Environmental Sciences* 1(2):93–104.
Roemmich, Ryan T., Andrew W. Long, and Amy J. Bastian. 2016. "Seeing the Errors You Feel Enhances Locomotor Performance but Not Learning." *Current Biology* 26(20):2707–16.
Safieddine, Doha et al. 2012. "Removal of Muscle Artifact from EEG Data: Comparison between Stochastic (ICA and CCA) and Deterministic (EMD and Wavelet-Based) Approaches." *Eurasip Journal on Advances in Signal Processing* 2012(1):1–15.
Sahyoun, C., A. Floyer-Lea, H. Johansen-Berg, and P. M. Matthews. 2004. "Towards an Understanding of Gait Control: Brain Activation during the Anticipation, Preparation and Execution of Foot Movements." *NeuroImage* 21(2):568–75.
De Sanctis, Pierfilippo, John S. Butler, Brenda R. Malcolm, and John J. Foxe. 2014. "Recalibration of Inhibitory Control Systems during Walking-Related Dual-Task Interference: A Mobile Brain-Body Imaging (MOBI) Study." *NeuroImage* 94:55–64.
Sandstrom, Noah J., Jordy Kaufman, and Scott A. Huettel. 1998. "Males and Females Use Different Distal Cues in a Virtual Environment Navigation Task." *Cognitive Brain Research* 6(4):351–60.
Scanlon, Joanna E. M., Kimberley A. Townsend, Danielle L. Cormier, Jonathan W. P. Kuziek,

and Kyle E. Mathewson. 2017. “Taking off the Training Wheels: Measuring Auditory P3 during Outdoor Cycling Using an Active Wet EEG System.” *Brain Research*.
Schlink, Bryan R. et al. 2017. “Independent Component Analysis and Source Localization on Mobile EEG Data Can Identify Increased Levels of Acute Stress.” *Frontiers in Human Neuroscience* 11:310.
Seeber, Martin, Reinhold Scherer, Johanna Wagner, Teodoro Solis-Escalante, and Gernot R. Müller-Putz. 2015. “High and Low Gamma EEG Oscillations in Central Sensorimotor Areas Are Conversely Modulated during the Human Gait Cycle.” *NeuroImage* 112:318–26.
Serrien, Deborah J., Richard B. Ivry, and Stephan P. Swinnen. 2006. “Dynamics of Hemispheric Specialization and Integration in the Context of Motor Control.” *Nature Reviews Neuroscience* 7(2):160–67.
Severens, M., B. Nienhuis, P. Desain, and J. Duysens. 2012. “Feasibility of Measuring Event Related Desynchronization with Electroencephalography during Walking.” *Proceedings of the Annual International Conference of the IEEE Engineering in Medicine and Biology Society, EMBS* 8:2764–67.
Sinclair, Jonathan, Sarah J. Hobbs, Laurence Protheroe, Christopher J. Edmundson, and Andrew Greenhalgh. 2013. “Determination of Gait Events Using an Externally Mounted Shank Accelerometer.” *Journal of Applied Biomechanics* 29(1):118–22.
Sipp, A. R., J. T. Gwin, S. Makeig, and D. P. Ferris. 2013. “Loss of Balance during Balance Beam Walking Elicits a Multifocal Theta Band Electrocortical Response.” *Journal of Neurophysiology* 110(9):2050–60.
Slobounov, Semyon, Cheng Cao, Niharika Jaiswal, and Karl M. Newell. 2009. “Neural Basis of Postural Instability Identified by VTC and EEG.” *Experimental Brain Research* 199(1):1–16.
Steptoe, A. et al. 2002. “Stress Responsivity and Socioeconomic Status A Mechanism for Increased Cardiovascular Disease Risk?” *European Heart Journal* 23:1757–63.
Sutton, S., M. Braren, J. Zubin, and E. R. John. 1965. “Evoked-Potential Correlates of Stimulus Uncertainty.” *Science (New York, N.Y.)* 150(3700):1187–88.
Suzuki, Mitsuo et al. 2004. “Prefrontal and Premotor Cortices Are Involved in Adapting Walking and Running Speed on the Treadmill: An Optical Imaging Study.” *NeuroImage* 23(3):1020–26.
Taelman, J., S. Vandeput, A. Spaepen, and S. Van Huffel. 2008. “Influence of Mental Stress on Heart Rate and Heart Rate Variability.” *4th European Conference of the International Federation for Medical and Biological Engineering (IFMBE)* 1366–69.
Tarvainen, Mika P., J. P. Niskanen, J. A. Lipponen, P. O. Ranta-aho, and P. A. Karjalainen. 2009. “Kubios HRV — A Software for Advanced Heart Rate Variability Analysis.” Pp. 1022–25 in. Springer, Berlin, Heidelberg.
Thayer, Julian F., Fredrik Åhs, Mats Fredrikson, John J. Sollers, and Tor D. Wager. 2012. “A Meta-Analysis of Heart Rate Variability and Neuroimaging Studies: Implications for Heart Rate Variability as a Marker of Stress and Health.” *Neuroscience and Biobehavioral Reviews* 36(2):747–56.
Thickbroom, G. .. and F. .. Mastaglia. 1985. “Cerebral Events Preceding Self-Paced and Visually Triggered Saccades. A Study of Presaccadic Potentials.” *Electroencephalography and Clinical Neurophysiology/Evoked Potentials Section* 62(4):277–89.
Thickbroom, G. W., W. Knezevicˇ, W. M. Carroll, and F. L. Mastaglia. 1991. “Saccade Onset and Offset Lambda Waves: Relation to Pattern Movement Visually Evoked Potentials.”

Brain Research 551(1–2):150–56.
Treisman, Anne M. and Garry Gelade. 1980. “A Feature-Integration Theory of Attention.” *Cognitive Psychology* 12(1):97–136.
Tromp, Johanne, David Peeters, Antje S. Meyer, and Peter Hagoort. 2018. “The Combined Use of Virtual Reality and EEG to Study Language Processing in Naturalistic Environments.” *Behavior Research Methods* 50(2):862–69.
Tsigos, Constantine and George P. Chrousos. 2002. “Hypothalamic–pituitary–adrenal Axis, Neuroendocrine Factors and Stress.” *Journal of Psychosomatic Research* 53(4):865–71.
Vazquez, Alejandro, Matthew A. Statton, Stefanie A. Busgang, and Amy J. Bastian. 2015. “Split-Belt Walking Adaptation Recalibrates Sensorimotor Estimates of Leg Speed but Not Position or Force.” *Journal of Neurophysiology* 114(6):3255–67.
Wagner, J., S. Makeig, M. Gola, C. Neuper, and G. Muller-Putz. 2016. “Distinct Band Oscillatory Networks Subserving Motor and Cognitive Control during Gait Adaptation.” *Journal of Neuroscience* 36(7):2212–26.
Wagner, Johanna et al. 2012. “Level of Participation in Robotic-Assisted Treadmill Walking Modulates Midline Sensorimotor EEG Rhythms in Able-Bodied Subjects.” *NeuroImage* 63(3):1203–11.
Widajewicz, W., B. Kably, and T. Drew. 1994. “Motor Cortical Activity during Voluntary Gait Modifications in the Cat. II. Cells Related to the Hindlimbs.” *Journal of Neurophysiology* 72(5):2070–89.
Wieser, M. et al. 2010. “Temporal and Spatial Patterns of Cortical Activation during Assisted Lower Limb Movement.” *Experimental Brain Research* 203(1):181–91.
WU, ZHAOHUA and NORDEN E. HUANG. 2009. “ENSEMBLE EMPIRICAL MODE DECOMPOSITION: A NOISE-ASSISTED DATA ANALYSIS METHOD.” *Advances in Adaptive Data Analysis* 01(01):1–41.
Yanagihara, Dai, Masao Udo, Ikio Kondo, and Takayoshi Yoshida. 1993. “A New Learning Paradigm: Adaptive Changes in Interlimb Coordination during Perturbed Locomotion in Decerebrate Cats.” *Neuroscience Research* 18(3):241–44.
Yang, Yea-Ru, Meng-Pin Tsai, Tien-Yow Chuang, Wen-Hsu Sung, and Ray-Yau Wang. n.d. “Virtual Reality-Based Training Improves Community Ambulation in Individuals with Stroke: A Randomized Controlled Trial.”
Zeni, J. A., J. G. Richards, and J. S. Higginson. 2008. “Two Simple Methods for Determining Gait Events during Treadmill and Overground Walking Using Kinematic Data.” *Gait & Posture* 27(4):710–14.
Zink, Rob, Borbála Hunyadi, Sabine Van Huffel, and Maarten De Vos. 2016. “Mobile EEG on the Bike: Disentangling Attentional and Physical Contributions to Auditory Attention Tasks.” *Journal of Neural Engineering* 13(4):046017.